Seton Hall University
eRepository @ Seton Hall

Seton Hall University Dissertations and Theses (ETDs)

Seton Hall University Dissertations and Theses

Fall 2012

Real-time Reaction Monitoring and Flash Separation as a Process Analytical Technology Tool and HPLC Method Development for Melamine in Infant Formula

Gopalakrishnan Venkatasami
Seton Hall University

Follow this and additional works at: https://scholarship.shu.edu/dissertations

 Part of the Chemistry Commons

Recommended Citation
Venkatasami, Gopalakrishnan, "Real-time Reaction Monitoring and Flash Separation as a Process Analytical Technology Tool and HPLC Method Development for Melamine in Infant Formula" (2012). *Seton Hall University Dissertations and Theses (ETDs)*. 1819.
https://scholarship.shu.edu/dissertations/1819

Real-time Reaction Monitoring and Flash Separation as a Process Analytical Technology Tool and HPLC Method Development for Melamine in Infant Formula

by

Gopalakrishnan Venkatasami

Ph.D. DISSERTATION

Submitted in partial fulfillment of the requirements for the degree of Doctor of Philosophy in the Department of Chemistry and Biochemistry of Seton Hall University

December, 2012

South Orange, New Jersey

We certify that we have read this thesis and that in our opinion it is sufficient in scientific scope and quality as a dissertation for the degree of Doctor of Philosophy

APPROVED

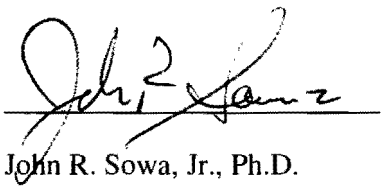

12/3/12

John R. Sowa, Jr., Ph.D.

Mentor, Member of Dissertation Committee, Seton Hall University

12/3/12

Cecilia Marzabadi, Ph.D.

Member of Dissertation Committee, Seton Hall University

12/3/12

David Sabatino, Ph.D.

Member of Dissertation Committee, Seton Hall University

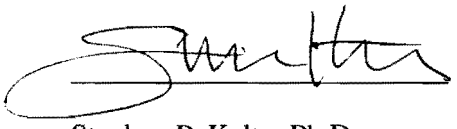

12/3/12

Stephen P. Kelty, Ph.D.

Chair, Department of Chemistry and Biochemistry, Seton Hall University

Dedicated to my Parents, Wife and my Kids

Table of Contents

List of Figures

List of Schemes

List of tables

List of abbreviations

ATR	Attenuated Total Reflection
ATR-IR	Attenuated Total Reflection-Infrared Spectroscopy
FDA	Food and Drug Administration
HPLC	High Performance Liquid Chromatography
IR	Infrared Spectroscopy
FTIR	Fourier Transform Infrared Spectroscopy
LOD	Limit of Detection
LOQ	Limit of Quantitation
RPM	Revolutions per Minute
TFA	Trifluoroacetic acid
UV	Ultra-Violet
PAT	Process analytical technology
CQA	Critical Quality Attribute
CPP	Critical Process Parameters
MCT	Mercury Cadmium telluride
FlashIR	Flash chromatography monitored by Infrared Spectroscopy
TLC	Thin Layer Chromatography
BTBE	Benzyl tert-Butyl Ether
NMR	Nuclear Magnetic Resonance
CMR	Continuous Microwave Reactor

Abstract

Real-time Reaction Monitoring and Separation as a Process Analytical Technology Tool and HPLC Method Development for Melamine in Infant Formula

Process analytical technology (PAT) is a technique for the analysis and control of chemical processes to assure the production of acceptable quality of the end-product. In this thesis, the application of mid-IR (1900 – 650 cm^{-1}) spectroscopy as a real-time monitoring technique for reaction and purification is illustrated. A technique using *in-situ* ATR-IR spectroscopy to monitor a real-time reaction followed by purification of the product by flash chromatography is developed in this study. The application of mid-IR spectroscopy was focused in etherification, acetylation and isomerization reactions which demonstrate the value of PAT. This study also focusses on the development of flash chromatographic purification conducted with *in-situ* ATR-IR spectroscopy detection. The results obtained indicated that this technique can be successfully used as an alternative to the traditional UV-Vis detection with the advantage of being able to characterize the eluent via *in-situ* ATR-IR as a real-time technique. In addition to the methods described above (synthesis and purification), a real-time on-column synthesis is successfully described.

Overall, this work presents the use of ATR-IR as a technique for monitoring chemical reactions and purification in real-time. The use of ATR-IR as a detection technique for flash chromatography is demonstrated to be an orthogonal detection technique to off-line HPLC-UV analysis.

Another project within this thesis is development of a simple, precise, accurate and validated, acetonitrile-free, reverse phase high performance liquid chromatography (HPLC) method for the determination of melamine in dry and liquid infant formula. The separation

was performed on a Kromasil C18 column (150 mm×3.2 mm I.D., 5 μm particle size) at 25° C. The mobile phase (0.1 % TFA/methanol 90:10) was pumped at a flow rate of 0.3 $mLmin^{-1}$ with detection at 240 nm. Melamine elutes at 3.7 min. A linear response ($r > 0.999$) is observed for samples ranging from 1.0 to 80 μgmL^{-1}. The method provides recoveries of 97.2–101. 2% in the concentration range of 5–40 μgmL^{-1}, intra- and inter-day variation in <1.0 % R.S.D. The limit of detection (LOD) and limit of quantification (LOQ) values are 0.1 μgmL^{-1} and 0.2 μgmL^{-1}, respectively.

Motivation

In practice of flash chromatography for purification of a reaction mixture, UV detection and thin layer chromatography (TLC) are the traditional and historic detection methods.[1] Although, direct analysis can be performed on collected fractions of the separated components by various methods, present demand motivated us to apply the coupled techniques of on-line real-time analysis of the fractions. Until now, the IR as a detection tool for the flash separation has not been documented. IR has been documented for monitoring HPLC separations[2] although similar because it is IR detection coupled with chromatography, HPLC and flash chromatography are fundamentally different separation techniques that are used in different environments; therefore, we consider that our method is indeed novel. We decided to explore the *in-situ* ATR-IR technique as a detection tool to analyze eluent fractions in real-time. In order to obtain better understanding of the separation process, we successfully integrated real-time IR monitoring of chemical reactions with real-time monitoring of separations by IR. By doing so we are able to understand the reaction and separation in real-time simultaneously by one means of detection. Since IR detection provides detailed chemical information the *in-situ* ATR-IR technique can be used to understand the real-time changes of the reactants during the chemical reaction and with the background information that is obtained it can facilitate the flash separation process.

[1] Still, W.C.; Kahn, S. W.; Mitra, M. *J. Org. Chem.* **1978**, *43*, 2923–2925.
[2] Edelmann, A.; Diewok, J.; Baena, J. R.; Lendl, B. *Anal.Bioanal.Chem.* **2003** *376*, 92–97.

Aim of the Thesis

Real-time reaction monitoring has turned out to be highly valuable for the efficient control of chemical processes and is a key tool in process analytical technology (PAT). For obtaining real-time information on chemical composition, mid-IR spectroscopy has proven to be highly versatile, especially when performed with the attenuated total reflectance (ATR) technique. Without the need for optical transmission paths, integration into existing experimental setups is easily achieved and not restricted by optical density. The kinetic information obtained from such studies allows improved monitoring and control of reactions during routine production and also facilitates the design of robust processes and the understanding of reaction mechanisms. By eliminating the need for manual sampling and off-line analysis, on-line analysis greatly reduces the labor required to perform a synthetic reaction. The technique is especially useful in situations where some of the reaction components are labile or where the reaction conditions may be hazardous to the operator.

Traditionally organic syntheses and organic processes have been conducted by using batch protocols due to their flexibility and versatility for cost-effective manufacture of small quantities of chemicals with short product lifetimes. Batch reactions are carried out in the laboratory, by means of small glass flasks (mL), while on the industrial scale in glass-lined stirred tank reactors (ranging from few milliliters up to several liters). The batch production of chemicals involves several intermediate reactions. This inherent character of the syntheses leads to time-consuming and costly production processes. Moreover, off-line analytical techniques such as chromatography and spectroscopy are employed for reaction monitoring and quality control of such processes which prove to be a bottleneck for timely production of quality product. Therefore, the Process Analytical Technology (PAT) initiative cannot be easily implemented in the traditional batch production processes. The pharmaceutical and fine chemical industry is continuously placing emphasis on the research and development of

more efficient and economical technology, in order to maintain their competitive edge in the growing global health care market. A continuous production process shares several intrinsic advantages over the batch processes which include higher productivity, improved safety, reduced manufacturing costs, and reduction or elimination of inventories instead of batch production. Furthermore, continuous production also contributes to product quality by reducing opportunities for human error. Due to the highly automated nature of the operation, people could directly carry out fewer steps in this type of production. This minimizes the opportunity for quality to be compromised by errors such as contamination, damage due to improper handling, etc.

During recent years flow chemistry has been adopted for use in organic synthesis and organic processes. Thus, continuous flow reactors have come to be an important means for performing organic synthesis, being both present in the academic laboratory as well as in the organic process environment for the production of various fine and pharmaceutical chemicals.

By keeping in mind the demands, this thesis is aimed at the following topics:

1. To explore the possibility of *in-situ* ATR-IR novel detection tool for flash chromatographic separation.
2. Monitor real-time reactions for background information for flash separation.
3. Explore the proposed technique to monitor on-column synthesis.

Acknowledgments

I would like to offer my heartfelt thanks and gratitude to my mentor, Prof. John R. Sowa, Jr., for his continuous guidance and support, without which I would not have been able to complete this project. The key characteristics of a successful scientist: strength, perseverance, and optimistic curiosity were bestowed upon me by him.

I would like to give special appreciation to Dr. Marzabadi and Dr. Sabatino for encouraging, motivating and supporting me throughout my research work. I would like to acknowledge Dr. Kazakevich and Dr. Wei for their support.

Next, I would like to acknowledge Dr. Sowa's research group as well as the faculty members of the Department of Chemistry and Biochemistry and all my friends at Seton Hall University.

I offer my acknowledgement to my parents for their unequivocal support throughout my study.

I would like to thank my wife Aruna for her personal support and great patience for standing with me throughout the work. It is due to her help and continuous prayers which provided me the strength to accomplish this goal.

Last but not the least; I would like to thank my sons Harsha and Prashanth for their support and understanding.

1. Introduction and Literature Overview

1.1. Process analytical technology (PAT)

Process analytical technology (PAT) is a method for analysis and control of manufacturing processes that measures critical quality parameters and performance attributes of raw and in-process materials.[3] It enables in-process data to be used for assessing the quality of a batch during manufacture, significantly reducing the need for finished product testing, and, as a result, improves lead times.

The main objectives[4] of PAT are: a) to assist in understanding a chemical process ; b) increasing the yield of the product during a reaction; c) decreasing the production cycle time with the help of control and on-line measurements; d) reduce the cost due to the decrease in the consumption of energy; e) observing the reaction products in real-time. The whole process of implementation of PAT can be classified into three steps design, analyze and control as shown in Figure 1-1.

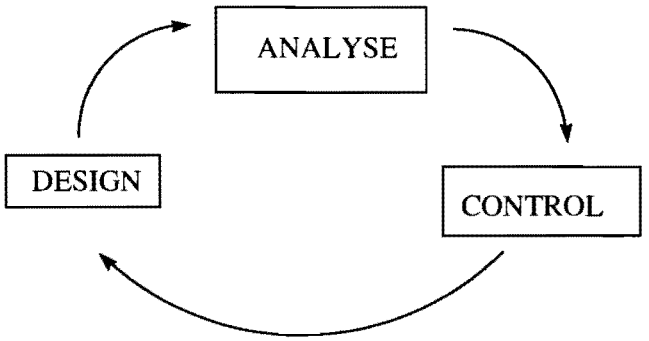

Figure 1-1. Steps for PAT implementation.[3]

[3] Rathore, A. S. *Trends. Biotechnol.* **2009**, *27(12)*, 698–705; (b) Scott, B.; Wilcock, A. *J. Pharm. Sci. Technol.* **2006**, *60(1)*, 17–53.

[4] (a) Rathore, A. S.; Gerhardt, A. S.; Montgomery, S. H.; Tyler, S. M. *Biopharm. Int.* **2009**, *22(1)*, 36–44; (b) Read, E. K.; Park, J. T.; Shah, R. B.; Riley, B. S.; Brorson, K. A.; Rathore, A. S. *Biotechnol. Bioeng.* **2009**, *105(2)*, 276–284.

The design phase starts during the design of the unit operation with the critical quality attributes (CQA) which are defined as a chemical properties or characteristics that must be controlled directly or indirectly to ensure the product meets its intended safety, efficacy, stability and performance. The critical process parameter (CPP) such as reaction times, temperatures, reactant ratios and concentrations, pressures, pH, and impurity levels which affects the CQA are also determined in this phase. In the analysis phase, an analyzer is suitably chosen to monitor the CQA and CPP. The PAT application is said to be on-line when the sample is analyzed without being removed from the process stream with respect to off-line analysis when the sample is removed and analyzed away from the process stream. However, the results should be obtained within a short time frame in order to facilitate real-time decision making. A control scheme is designed in the control phase which helps in understanding the process. The data is analyzed and used for making a real-time process decision which may finally help obtain a product of desirable quality.

The literature documents the applications of PAT in the pharmaceutical and chemical industry for quality drug and chemical development and manufacturing.[5] The analytical instrumentation used in this field include near-infrared (NIR) spectroscopy, acoustic sensing, nuclear magnetic resonance (NMR), Raman and Fourier transform infrared spectroscopy (FTIR). The productivity and the quality of the product are standardized along with the reaction conditions. Any deviation in the system would be brought back to control by the real-time adjustments.

[5] (a) Freund, H.; Sundmacher, K. *Chem. Eng. Process* **2008**, *47*, 2051–2060; (b) Koch, M. V. *Anal. Bioanal. Chem.* **2006**, *384*, 1049–1053; (c) *Process Analytical Technology: Spectroscopic Tools and Implementation Strategies for the Chemical and Pharmaceutical Industries,* Bakeev, K. A., Ed.; Blackwell: Oxford, 2005, 5-12.

1.2. Attentuated Total Reflectance–Infrared (ATR-IR) spectroscopy

Attenuated Total Reflectance-Infrared (ATR-IR) spectroscopy is one of the popular sampling techniques using FTIR instrumentation. ATR generally allows qualitative or quantitative analysis of samples with little or no sample preparation which greatly improves the rate of analysis. The main benefit of ATR sampling comes from the very thin sampling path length or depth of penetration of the IR beam into the sample. This is in contrast to traditional FTIR sampling by transmission where the sample must be diluted with an IR transparent salt (e.g., KBr), pressed into a pellet or pressed to a thin film, prior to analysis to minimize absorption and reflection by the sample.

In ATR a beam of infrared light is allowed to interact with the sample and the beam gets internally reflected as it bounces through a crystal. Changes relative to a background signal are recorded by the instrument. A crystal with high refractive index is used and the infrared beam is allowed to impact at a certain angle. An evanescent wave is formed due to the internal reflectance which penetrates out of the crystal and passes through the sample which is in contact with the crystal as shown in Figure 1-2. However, the evanescent wave moves only 0.5 μm to 5 μm out of the crystal making it mandatory for the sample to be in very good contact with the crystal. The evanescent wave is altered in the regions where the sample absorbs energy and the altered wave is reflected back to the IR beam. The beam passes through the crystal and is sent to the detector of the spectrometer which ultimately gives an IR spectrum after processing.

The following experimental factors affect the quality of final spectrum:

- Refractive indices of the ATR crystal or internal reflectance element (IRE) and the Sample
- Angle of incidence of the IR beam
- Critical angle
- Depth of penetration

- Wavelength of the IR beam
- Number of reflections
- Quality of the sample contact with ATR crystal
- ATR crystal characteristics

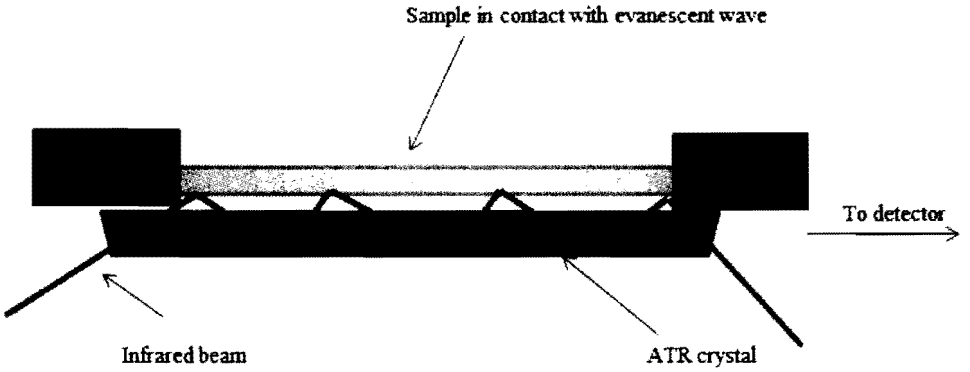

Figure 1-2. A schematic representation of a multiple reflection ATR system.[6]

The radiation moving through an optically dense medium of refractive index (n_1), on reaching the interface of an adjacent medium having less optical density (n_2) will suffer total internal reflection which is the basis of internal reflection spectroscopy. Additionally, the beam undergoes total internal reflection only when the incident angle is more than the critical angle (Θ_c) as shown in the Figure 1-3.

[5]FT-IR spectroscopy, PerkinElmer, application note.
http://shop.perkinelmer.com/content/technicalinfo/tch_ftiratr.pdf (accessed September 19, 2012)

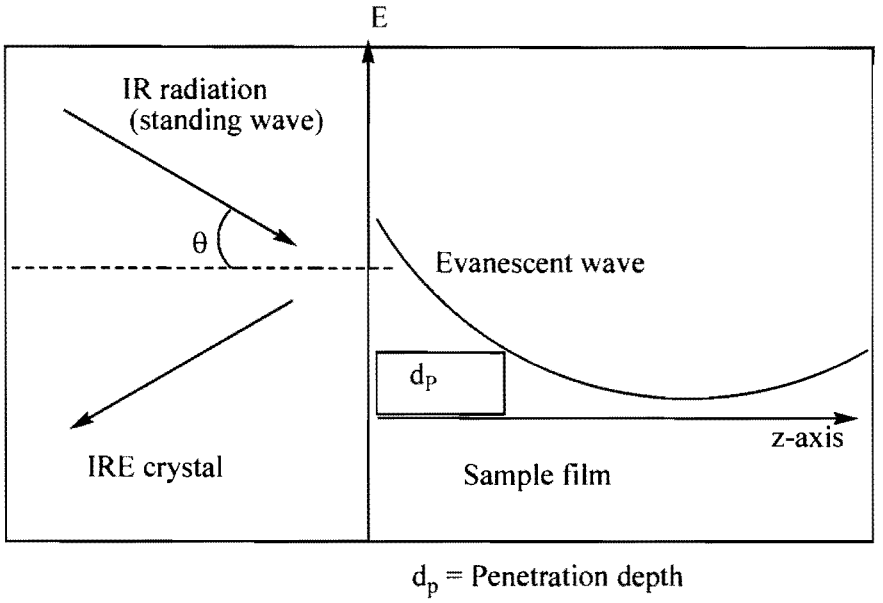

Figure 1-3. Schematic representation of the evanescent wave formed due to internal reflection.[7]

The critical angle (Θ_c) is given by:

$$\sin(\Theta_c) = \frac{n1}{n2} \qquad 1$$

In the medium of the lower refractive index, the field intensity of the evanescent wave is more than zero. However, the energy flow is instantaneous and the time average is taken as zero which leads to no loss of energy and the radiation in the denser medium will undergo total internal reflection. Additionally the evanescent wave possesses the property of non-transverse wave which means exponentially decaying wave having electric vector components in all spatial orientation and thus, can move in any direction after being reflected. The field is present near the surface as the intensity of the field decreases with the increase in the distance into the medium. Again, due to the Goos-Hanchen shift (which is an optical

[7] Skourlis, T. P.; McCullough, R. L. *J. Appl. Pol. Sci.* **1994**, *52*, 1241-1248.

phenomenon in which linearly polarized light undergoes a small shift when totally internally reflected[8]) there is a displacement of the incident and the reflected wave as a result of the flow of nonzero energy parallel to the interface.

The parameter penetration depth (d_P) was proposed by Harrick and du Pre[9] It is defined as the distance required for the electric field amplitude to fall to e^{-1} of its value at the surface and is further defined by the following equation 2:

$$d_p = \frac{\lambda}{2\pi(n_1^2 \sin^2\theta - n_2^2)^{1/2}} \qquad 2$$

Where λ is the wavelength of light and θ is the angle of incidence of the IR beam relative to a perpendicular from the surface of the crystal typical depth of penetration in ATR ranges from 0.5 μm up to 5 μm.

[8] a) Renard, R. H. *J. Optic. Soc. Am.* **1964**, *54*, 1190-1193; (b) Hirschfield, T. *Appl. Spectros.* **1977**, *31*, 243-246.

[9] Harrick, N. J.; du Pre, F. K. *Appl. Optics.* **1966**, *5*, 1739-1742.

The infrared region of the electromagnetic spectrum can be subdivided into far-IR, mid-IR and near-IR regions as shown in Figure 1-4.

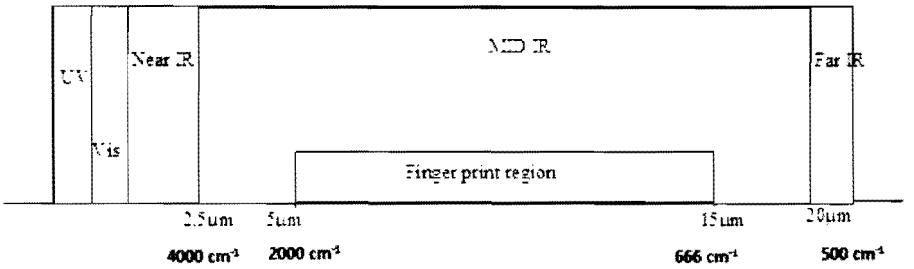

Figure 1-4. The infrared region of the electromagnetic spectrum.[9]

The spectral range within 400 – 4000 cm^{-1} has been assigned as the mid-infrared spectral region which is used for both quantitative and qualitative analysis as major molecular vibrations, overtones and also combination frequencies occur in this region. The spectral fingerprint region present within this area provides structural information and assists in the identification of the components in a complex mixture.[10] The spectral information can be processed by chemometric methods which makes the mid-IR spectroscopy an important device for the investigation of dynamic process such as phase transitions, chemical reactions, sedimentation, etc. This instrument also assists in the identification of the interaction of the investigated molecule with the surrounding molecules.[11]

1.3. The optical fiber probes used in mid-infrared analysis

The fiber optics plays a versatile role in the arena of vibrational spectroscopy and is important in Raman as well as near-infrared spectroscopy. Presently, optical transparent fibers have also been applied in the technology of mid-IR[12] which places the fiber optic probe

[10] Melling, P. J.; Thomson, M., Fiber-optic Probes for Mid-infrared Spectrometry, In: *Handbook of Vibrational Spectroscopy,* John Wiley & Sons, **2002**.
[11] Raichlin, Y.; Katzir, A. *Appl. Spectros.* **2008**, *62(2),* 55A-72A.
[12] Lendl, B.; Mizaikoff, B. Optical Fibers for Mid-infrared Spectrometry, In: *Handbook of Vibrational Spectroscopy,* John Wiley & Sons, 2002, 75-85.

directly within the reaction medium.[9] Mid-IR spectroscopy provides detailed physical and chemical information and the technology to monitor the samples in all the three phases of gas, liquid and solid enables it to become a very significant tool in the field of spectroscopy. Moreover the ATR mid-IR fiber optic probes have been used extensively within different reaction media[13] and in biotechnological process.[14]

The mid-IR fibers should possess certain characteristic physical properties such as mechanical and thermal stability, flexibility as well as transparency over the required spectral range. The optical transparency is based on the various loss mechanisms such as

- Extrinsic loss
- Fresnel loss
- Bending loss

Extrinsic loss means losses that are specific to the geometry and handling of the fibers and are not functions of the fiber material itself and intrinsic loss is caused by interaction with one or more major components of the glass. Fresnel loss is due to reflections at the entrance aperture. Bending loss is distortion of the fiber from the ideal straight-line configuration.

Silica fibers cannot be used in mid-IR as the transmission is limited to 2.5 μm. The spectra recorded from a mid-IR fiber made of silica shows interference from the reflection of glass in the mid-IR region even under transmission spectroscopy.[15] Glass remains opaque in the mid-IR region due to the strong absorption bands for the silicon oxygen bonds.

---

[13] Brancaleon, L.; Bamberg, M. P.; Kollias, N. *Appl. Spectros.* **2000**, *54(8)*, 1175-1182.
[14] Mazarevica, G.; Diewok, J.; Baena, J. R.; Rosenberg, E.; Lendl, B. *Appl. Spectros.* **2004**, *58(7)*, 804-810.
[15] Nishio, N.; Ikuto, N.; Okabayashi, H.; Hannah, R. W. *Appl. Spectros.* **1990**, *44*, 614 – 617.

The initial IR transparent fibers were made of chalcogenide glasses which is a glass containing one or more chalcogenide elements in group 16 in the Periodic Table.[16] Some of the materials used for the construction of IR fibers are shown in Table 1-1.

Table1-1. Materials used to construct the IR fibers[15]

Category	Sub-category	Example
Glass	Heavy metal fluoride, Germanate, Chalcogenide	ZrF_4-BaF_2-LaF_3-AlF_3-NAF GeO_2-PbO AsS_3 and AsGeTeSe
Crystal	Polycrystalline Single crystal	AgBrCl Sapphire
Hollow waveguide	Metal or dielectric film Refractive index< 1	Hollow glass wavelength Hollow sapphire at 10.6 μm

1.4. Advantage of mid-IR over near-IR

Near-infrared (NIR) spectroscopy (4000 – 12000 cm^{-1}) has been applied widely in pharmaceutical industries[17] and mainly used to analyze intact and blister packed tablets. [18,19] NIR is used to monitor the compounds in a general manner while the mid-IR analyses the compounds specifically. NIR spectroscopy is based on molecular overtone and combination vibrations. Such transitions are forbidden by the selection rules of quantum mechanics. As a result, the molar absorptivity in the near IR region is typically quite small. One advantage is

[16] Minnich, C. B.; Buskens, P.; Steffens, H. C.; Bauerlein, P. S.; Butvina, L. N.; Kupper, L.; Leitner, W.; Liauw, M. A.; Greiner, L. *Org. Proc. Res. Develop.* **2007**, *11(1)*, 94-97.

[17] Schirmer, R. E. *Modern Methods of Pharmaceutical Analysis*, 2nd ed.; CRC Press: Boca Raton, FL, 1991; Ch. 3, p. 127-170.

[18] Lodder, R. A.; Hieftje, G. *Appl. Spectroc.* **1988**, *42*, 556-558.

[19] Aldridge, P. K.; Mushinsky, R. F.; Andino, M. M.; Evans, C. L. *Appl. Spectrosc.* **1994,** *48* (10), 1272-1276.

that NIR can typically penetrate much farther into a sample than mid infrared radiation. Near-infrared spectroscopy is, therefore, not a particularly sensitive technique, but it can be very useful in probing bulk material with little or no sample preparation. NIR also is a non-invasive detection method of conjugated compounds. The properties and effects of phthalocyanines are diverse and cover many important hi-tech applications, including photodynamic therapy, optical data storage, reverse saturable absorbers and solar screens and the biodetection of phthalocyanines was explored by NIR.[20] The molecular overtone and combination bands seen in the near IR are typically very broad, leading to complex spectra; it can be difficult to assign specific features to specific chemical components. Multivariate (multiple variables) calibration techniques (e.g., principal components analysis, partial least squares, or artificial neural networks) are often employed to extract the desired chemical information. Careful development of a set of calibration samples and application of multivariate calibration techniques is essential for near-infrared analytical methods.[21]

The mid-IR analysis has more advantage over the near-IR analysis since it can detect the functional groups more specifically in the solid, gas and liquid phase and spectral overlap is decreased due to the narrow absorption bands. Moreover, chemical species can be monitored simultaneously. Near-IR can well analyze samples with sizes greater than 50 micrometer. The particle size of the sample has a significant effect on the NIR spectrum. If the particle size changes it causes a change in the amount of radiation scattered by the sample. When the particles are large, the direction of radiation does not change as often as with small particles, so more radiation is absorbed. This results in a higher absorbance, and

---

[20] Minnes, R.; Weitman, H.; Lee, J.H.; Gorun, S.M.; Ehrenberg, B. *Photochemistry and Photobiology*. **2006**, *82(2)*, 593-599.

[21] Vidrine, D. W.; Mattson, D. R. *Appl. Spectrosc.* **1978**, *32*, 502-506.

thereby has an additive effect on the spectra. Particle size has also a multiplicative effect as the strong absorbers show more change with particle size.

If the particles generally do not aggregate during the processing step those with a particle size smaller than 10 microns can be detected by mid-IR spectroscopy. In the ATR technique, the incident beam has to pass through a medium of high refractive index; the beam can penetrate only for 0.5 to 5 micrometers. Thus, better clarity of the image can be obtained with mid-IR as compared to near-IR due to these factors. Good resolutions of particles up to the size of 5 micrometers have been observed with mid-IR-ATR technology.

ATR spectrometry is used extensively in clinical assays, medical diagnostics, and laboratory testing. Since the depth of penetration for the evanescent wave in ATR spectrometry is shallow, there is a low incidence of Fresnel Reflection. Thus, reliable spectral analysis of murky, semisolid, turbid, and optically dense solutions is possible with ATR spectroscopy. Moreover, the ATR crystal is a relatively chemically resistant Zn-Se crystal that can be coated with an additional chemically resistant material which enables IR spectroscopy to be performed in aqueous solution. Therefore, *in situ* ATR-IR spectroscopy has the unique potential to simultaneously address problems associated with manual sampling followed by off-line analysis.

The major disadvantage of the ATR crystal is wavenumber range. Since diamond absorbs between 2200 and 200 cm^{-1} the current system has the limitation of scanning range is 1900 to 650 cm^{-1} which potentially not possible to scan the major absorption due to OH and NH_2 functional groups.

1.5. ReactIR techniques

The fiber-optic probes for reaction monitoring and spectroscopy have been used as an important device in research.[22] The flexible fiber optical probes and spectroscopic software have enhanced the development of real-time applications. The operation parameters are determined by reaction monitoring, which are mainly based on off-line techniques. However, recently, on-line methodologies have been are used for obtaining accurate data during the reaction.[23] The reaction can be monitored *in-situ* and the formation of intermediates can be detected which provides an insight to the reaction mechanism.[24]

The monitoring is specifically significant for studying polymerization reaction as it can be invariably conducted in solution.[25] The on-line technique of reaction monitoring constitutes both *in-situ* and real-time monitoring which is carried out within the reaction thereby overcoming the problem of sample alteration during the analysis. There may be a change in the reaction conditions which may lead to results that are misleading. Additionally, the reactions carried out at low temperatures are widely affected as the bypass and standard approaches are not possible under constant thermal conditions. However, the frequencies and band shape in the mid-IR changes due to factors such as hydrogen bonding and temperature which tend to make the spectra complicated. The chemical composition of gas, liquid or solid phase samples can be obtained by real-time information with the help of mid-IR-ATR spectroscopy.[26] The spectral features are well resolved and the reaction can be monitored under drastic conditions by the mid-IR probes. The data interpretation is simplified in commercially available on-line FTIR as the instrument is equipped with chemometric

---

[22] a) Shaw, M. J.; Geiger W.E. *Organometallics.* **1996**, *15*, 13; b) Michel, A. J.; Puskas, J. E.; Tzaras, E. *Macromolecules*, **2000**, *33*, 3518.

[23] *Process Analytical Technology - Spectroscopic Tools and Implementation Strategies for the Chemical and Pharmaceutical Industries*, Bakeev, K. A. Ed. Blackwell, 2005, Oxford/UK.

[24] Minnich, C. B.; Buskens, P.; Steffens, H. C.; Bauerlein, P. S.; Butvina, L. N.; Küpper, L.; Leitner, W.; Liauw, M. A.;Greiner, L. *Org. Process Res. Dev.* **2007**, 11 (1), 94-97.

[25] Thomson, M. A.; Melling, P. J.; Slepski, A. M. *Polym. Prepr*, **2001**, *42*, 310 – 311.

[26] Grunwaldt, J. D.; Baiker, A. *Phys. Chem. Chem. Phys*, **2005**, *7(20)*, 3526-3539.

software. The presence of multiple components can also be easily monitored by the user. The spectra of authentic compounds can be fed into the software which helps in the detection of the required compound specifically. The relative changes in the FTIR signals can be calibrated against the detected absolute changes in the concentration at certain times which leads to the quantification of the data. A fiber optic FTIR probe made of diamond has been reported which is a versatile tool for flow chemistry in research and process environments.[27] The diamond probe attached to a ReactIR 45m instrument can be converted to an improved on-line monitoring flow cell as shown in the Figure 1-5 has inlet to the detector and outlet to the reaction vessel for continuous flow of the reaction mixture.

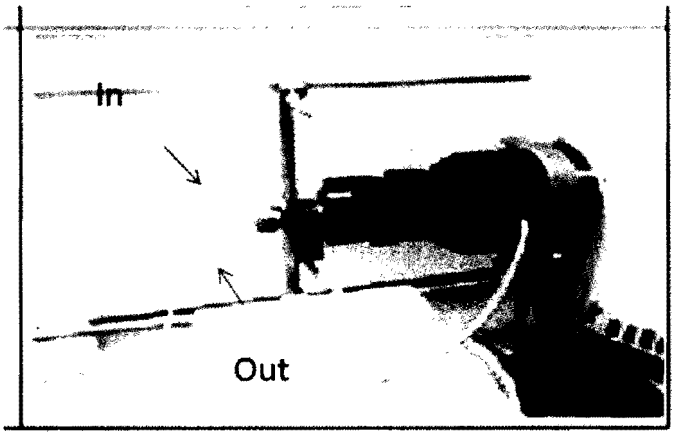

Figure 1-5. ReactIR 45m with the attachment of the flow cell.[28]

The on-line IR flow cell can be introduced at any point during the reaction. The flow cell produces better results if attached to a back-pressure regulator. The spectra of a slurry can be conveniently recorded as only the constituents of the liquid will be detected.

---

[27] Carter, C. F.; Baxendale, I. R.; OBrien, M.; Pavey, J. B. J.; Ley, S. V. *Org. Biomol. Chem.* **2009**, *7*, 4594–4597.

[28] Carter, C. F.; Lange, H.; Ley, S. V.; Baxendale, I. R.; Wittkamp, B.; Goode, J. G.; Gaunt, N. L. *Org. Proc. Res. Dev.* **2010**, *14(2)*, 393-404.

The ReactIR technology assists in the field of flow and continuous chemistry with the help of real-time reaction monitoring.[29] This technology has been widely used to monitor organic reactions. Among the various analytical processes, FTIR is more advantageous as it is non-destructive unlike mass spectroscopy, cheaper than NMR, and can record both solid and liquid samples similar to Raman spectroscopy. Kappler *et al.*[30] used ReactIR based on ATR-FTIR technique to study the co-polymerization of ethylene and 1-hexene. A detailed study on the activity of catalyst such as activation and deactivation time along with the polymerization kinetics, parameters of co-polymerization and the degree of homogeneity was reported. Additionally, the study was carried out accurately for a co-polymerization reaction in solution using the ReactIR set up shown in Figure 1-6.

[29] Bernstein, M. A. *Spectrosc. Eur.* **2007**, *19*, 11–13.

[30] Kappler, B.; Tuchbreiter, A.; Faller, D.; Liebratraut, P.; Horbelt, W.; Timmer, J.; Honerkamp, J.; Mulhaupt, R. *Polymer*, **2003**, *44*, 6179 – 6186.

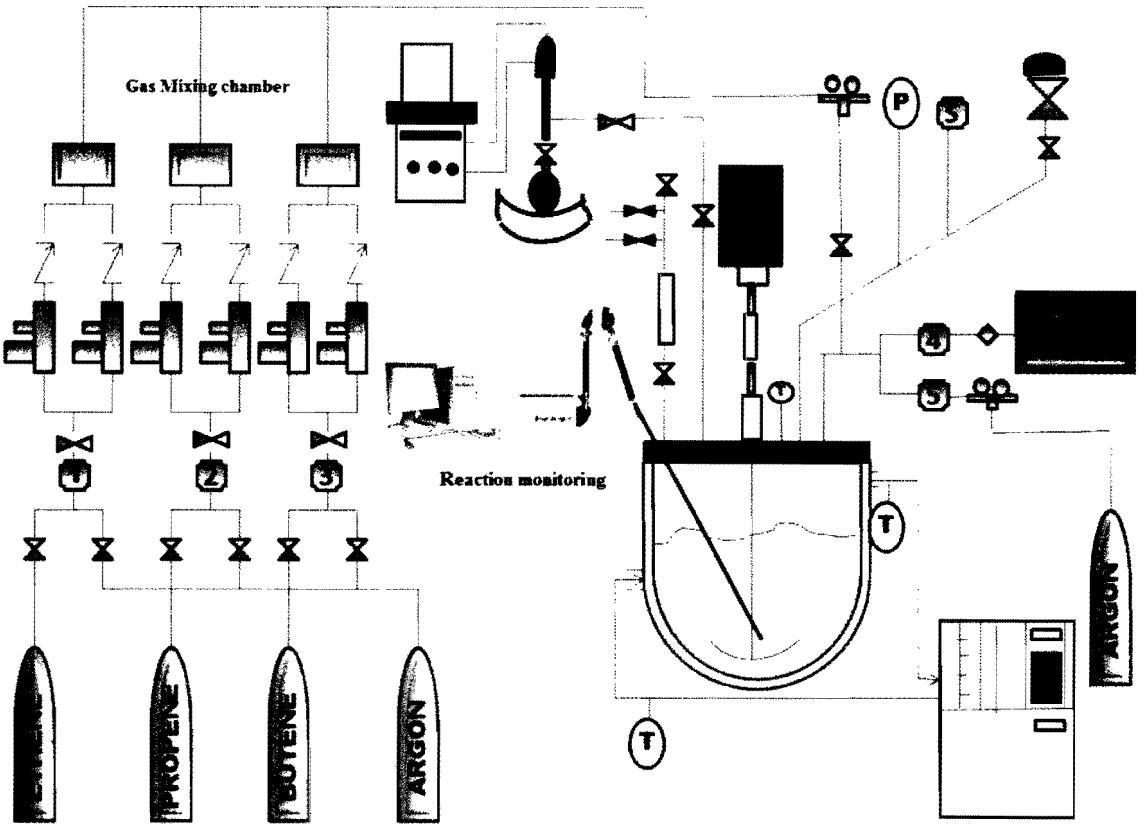

Figure 1-6. A schematic representation of polymerization reactor equipped with ReactIR. Figure is modified from prior publication.[27]

The major requirements for an IR cell reactor for studying polymerization reactions as shown in the Figure 1-6 are that it should have the capability of recording the IR spectra under all reaction conditions. Additionally, the volume of the chamber should allow proper mixing of the gases for proper conversion. The gases should have the arrangement for flowing in and out continuously. The IR cell used in flow chemistry can operate in batch mode both in vacuum and at high pressure where the reactors can monitor covering a large IR frequency range. Temperature programming and concentration programming are two different types of operation carried out during the studies. In the temperature programming method, the IR absorbance is recorded as a function of temperature or time with a linear increase in the reaction temperature. However, in the concentration programming method, the

flow rate of the reactants can be changed linearly in order to determine the concentration of the gases in the reactor. Nevertheless, the optical fiber technology is a novel tool for *in-situ* reaction monitoring.

1.6. Flash chromatography

Flash chromatography is an important technique made popular by Clark Still of Columbia University.[1] This technique is also known as medium pressure liquid chromatography is comparable to gravity chromatography. The silica gel required in the flash chromatography has a smaller particle size of 250 – 400 mesh. The movement of the solvent is hindered due to the small particle size and hence gas is used to pressurize the column in order to facilitate elution. It is a technology used to purify compounds to high purity in preparative scale quantities.

Some important characteristics of flash chromatography are: a) when the quantity of analyte is increased, the resolution decreases;[31] b) the geometry and the silica quality determines the optimal flow rate;[32] c) as the packing of the homogeneous stationary phase is improved better separation results are obtained with good reproducibility;[33] d) the stationary phase should have a smaller particle size which gives more surface area for improved separation.

Two types of solvent mixtures used in flash chromatography are isocratic solvent and gradient solvent mixtures. The isocratic solvent system separates the compounds using the same eluent conditions throughout the run, while the gradient solvent system separates the complex mixture using different solvent compositions during the elution.

---

[31] Cox, G. B.; Snyder, L. R. *J. Chromatogr.* **1989**, *483*, 95–110.
[32] McGuffin, V. L. *J. Chromatogr.* **2004**, *15*, 441–449.
[33] *A Practical Handbook of Preparative HPLC*, Wellings, D. A., Elsevier, Oxford, 2006, 180-190.

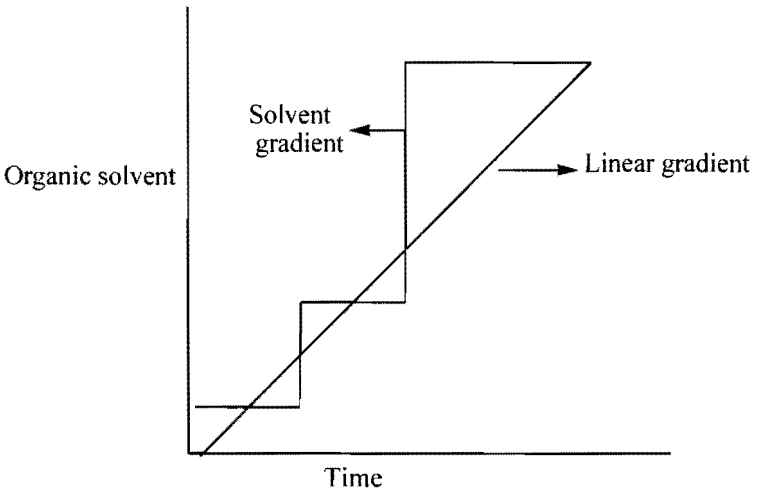

Figure 1-7. Schematic representation of solvent and linear gradient.[29]

There are two types of gradient solvent systems: a) a linear gradient system where the composition of the polar solvent is gradually increased until the complete elution of all the compounds in the mixture and b) the step gradient system, in which the composition of the solvent system is changed in large steps as shown in the Figure 1-7.

1.7. Detectors used in flash chromatography

The fractions obtained from flash chromatography are commonly analyzed by TLC which is time consuming. In order to skip this step, techniques have been developed to detect the fraction containing the desired compounds at the end of the column. Automated flash chromatography systems can be compared with HPLC systems. They are equipped with sample injection ports, gradient pumps, collectors to collect the eluent and a UV/Vis-detector. The fraction containing the target compound can be collected after being detected by the light in the UV/Vis-region. The normal phase chromatography is carried out with unmodified silica, while the reverse phase can be done with modified silica.[34]

[34] Roge, A. B.; Firke, S. N.; Kawade, R. M.; Sarje, S. K.; Vadvalkar, S. M. *Int. J. Pharm. Sci. Res.* **2011**, *2(8)*, 1930– 1937.

Another method of detection is to record the change in refractive index in a particular the region of illumination as the analyte passes through it.[35] The non-absorbing materials can become transparent when the refractive index of the analyte is similar to that of the particles. The light beam will be scattered if the refractive index of the analyte becomes different from that of the particles. This principle is used in the detection of the compound present in the fraction in the column itself as shown in the Figure 1-8.

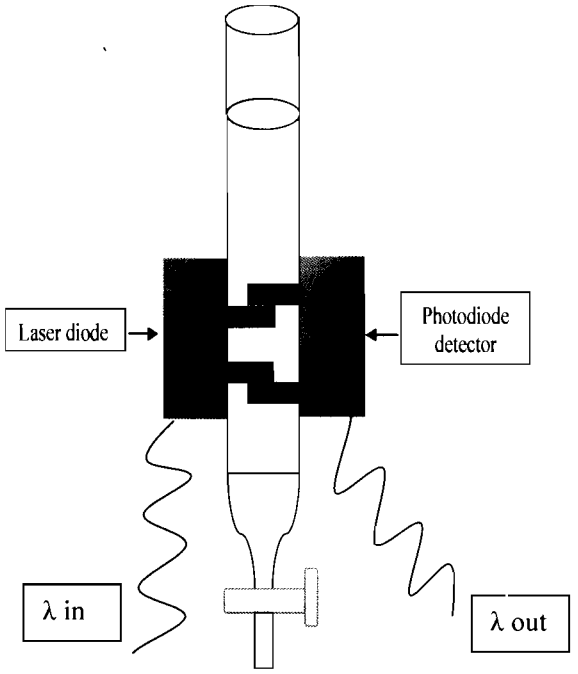

Figure 1-8. Flash chromatography on column refractive index detector.[37]

FlashLC is another method for detection of the compounds during flash chromatography which is used in both laboratory and pilot plant scales. The solvent system has to be properly selected and optimized to obtain the best results for normal phase-FlashLC

[35] Westerbuhr, S. G.; Rowlen, K. L. *J. Chromatogr.* **2000**, *886*, 9–18.

as the particle size of the packing materials is small generally on the order of 50 μm.[36] The selectivity for the reverse phase FlashLC is obtained either by the proper choice of the organic modifier or pH.[37]

To date, there have been no literature reports of using IR spectroscopy as a tool for detecting the compounds in the column while performing flash chromatography. As the IR enables detection of vibration of bonds in the compounds, it can be effectively used to detect the functional groups in the molecule which is difficult to obtain using classical UV or Refractive index detection The fractions having the desired compound as indicated by the IR spectra can be directly collected avoiding further analysis and purification steps, and accelerating the sample characterization process.

1.8. Reaction carried out by on column synthesis

The flow reactions carried out in presence of transition metal catalyst generally use a fixed-bed which is heated inductively. The catalysts can be homogeneous, or, more commonly, heterogeneous. The silica particles are impregnated with palladium nanoparticles which act as the catalyst in carbon–carbon coupling reactions. Transition metals are also used for solid phase oxidations by blending chromium oxide and nickel oxide with the silica shell of Magsilica which is silica coated maghemite/magnetite particles and belongs to family of iron oxides (Scheme 1-1).[38]

---

[36] (a) Snyder, L. R.; Glajch, J. L.; Kirkland J. J. *J. Chromatogr.* **1981**, *218*, 299; (b) Glajch, J. L.; Kirkland, J. J.; Snyder, L. R. *J. Chromatogr.* **1982**, *238*, 269.

[37] Dubant, S.; Mathews, B. *Chromatogr. Today* **2009**, 10 -12.

[38] Wegner, J.; Ceylan, S.; Friese, C.; Kirschning, A. *Eur. J. Org. Chem.* **2010**, *23*, 4372–4375.

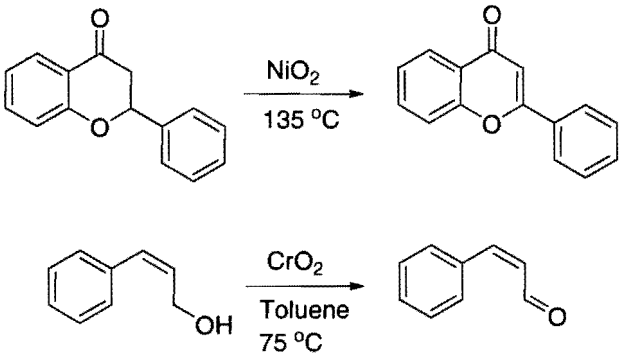

Scheme1-1. Solid phase oxidation using transition metals.

Hafez *et al.*[39] reported the asymmetric synthesis of β-lactams by packing the column with an asymmetric catalyst. The reagents were added to the gravity or pressure fed column which catalyzed the reaction to produce an enantiopure product (62% yields with 90% ee) which was eluted at the bottom (Figure 1-9). The column was reused for 20 times with no significant loss of selectivity.[40]

[39] Hafez, A. M.; Taggi, A. E.; Wack, H.; Drury III, W. J.; Lectka, T. *Org. Lett.*, **2000**, *2*, 3963 – 3965.

[40] Annis, D. A.; Jacobsen, E. N. *J. Am. Chem. Soc.* **1999**, *121*, 4147- 4154. (b) Kamahori, K.; Ito, K.; Itsuno, S. *J. Org Chem.* **1996**, *61*, 8321- 8324.

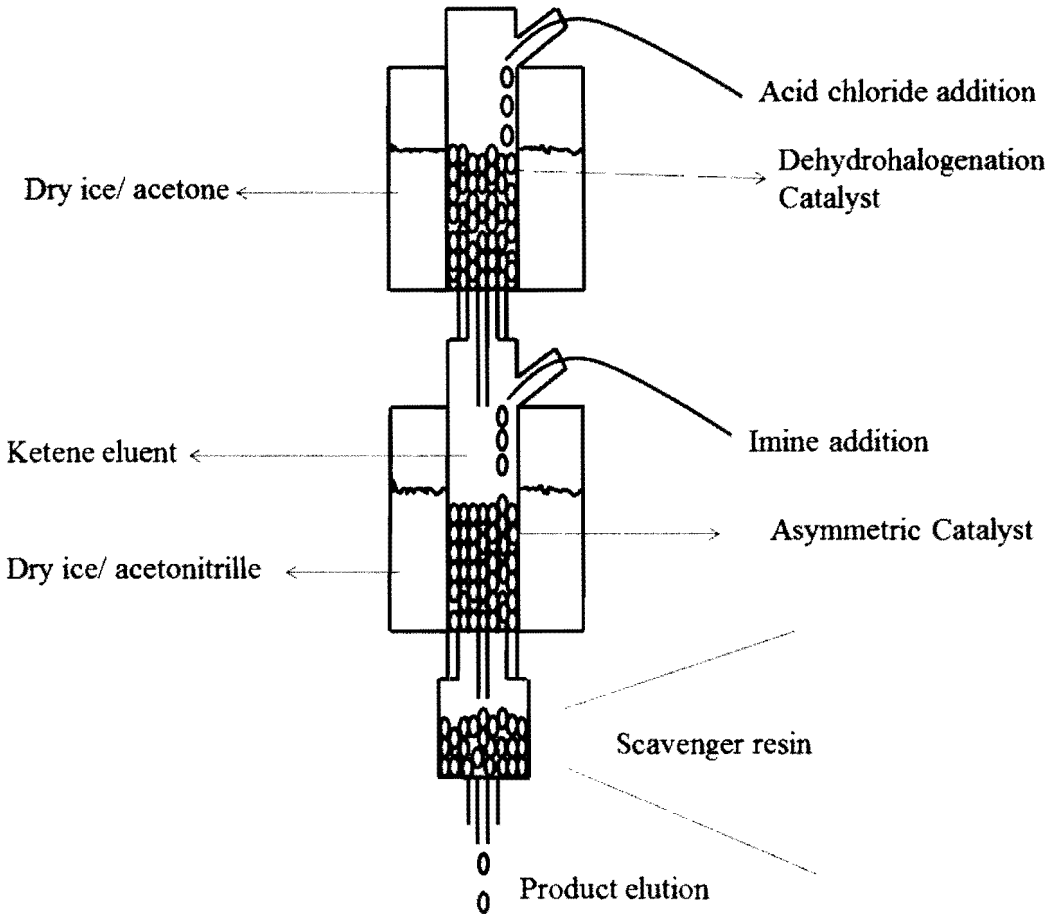

Figure 1-9. The column used for asymmetric synthesis.[38]

1.9. Flow chemistry

Flow cell reactors are used to scale up for production scale manufacturing and are a significant tool for synthetic chemists.[41] Moreover a wide range of reaction conditions can be analyzed and optimized within a very short time. The pump flow rate for each reaction can be altered to change the reaction stoichiometry. Continuous flow reactors allow good control over reaction conditions including heat transfer, time and mixing. The residence time of the reagents in the reactor (i.e., the amount of time that the reaction is heated or cooled) is calculated from the volume of the reactor and the flow rate through it.

---

41. Wiles, C.; Watts, P. *Eur. J. Org. Chem.* **2008**, *34*, 1655-1671.

Residence time = Reactor Volume / Flow Rate

Therefore, to achieve a longer residence time, reagents can be pumped more slowly and/or a larger volume reactor used. Production rates can vary from nanoliters to liters per minute

The reactions carried out in a conventional apparatus in the laboratory are called batch reactions; however, continuous flow reactions are those in which a chemical reaction is run in a continuously flowing stream rather than in a batch production. In other words, pumps move fluid into a tube, and where tubes join one another, the fluids contact one another. If these fluids are reactive, a reaction takes place.[42]

The distinction between flow and batch reaction is as follows:

- Reaction stoichiometry: In batch production this is defined by the concentration of chemical reagents and their volumetric ratio. In flow this is defined by the concentration of reagents and the ratio of their flow rate.

- Residence time: In batch production this is determined by how long a vessel is held at a given temperature. In flow this is determined by the volume of the reactor, and the bulk flow rate.

The flow reaction has the following advantages over batch reactions:

- Mixing can be achieved within seconds at the smaller scales used in flow chemistry.

- The thermal mass of the fluid is typically far lower than the thermal mass of the system (and orders of magnitude less than with batch chemistry). This makes

[42] (a) Muller, G.; Gaupp, T.; Wahl, F.; Wille, G. *Chimia*, **2006**, *60*, 618–622. (b) Klemm, E.; Dçring, H.; Geibelemann, A.; Schirrmeister, S. *Chem. Ing. Tech.* **2007**, *79*, 697–706.

controlling the temperature of the media both faster and easier ensuring that exothermic and endothermic process can be conducted without safety consequences.

- Because reagents come rapidly to temperature in a flow reactor, reaction time (especially for fast reactions) can be very precisely controlled.
- Multi-step reactions can be arranged in a continuous sequence. This can be especially beneficial if intermediate compounds are unstable, toxic, or sensitive to air, since they will exist only momentarily and in very small quantities.
- Position along the flowing stream and reaction time point are directly related to one another. This means that it is possible to arrange the system such that further reagents can be introduced into the flowing reaction stream at precisely the time point in the reaction that is desired.
- It is possible to arrange a flowing system such that purification is coupled with the reaction. There are three primary techniques that are used:
    - Solid phase scavenging
    - Chromatographic separation
    - Liquid/Liquid Extraction
- Flow reactions can be automated in a manner that is far less expensive than batch reactions, so a flow reactor system paired with a fraction collector can perform a series of reactions unattended.
- By coupling the output of the reactor to a detector system, it is possible to go further and create an automated system which can sequentially investigate a range of possible reaction parameters (varying stoichiometry, residence time and temperature) and therefore optimize reactions with little or no intervention.
- Multi-phase liquid reactions (e.g., phase transfer catalysis) can be performed in a straightforward way with high reproducibility over a range of scales and conditions.

The most acceptable real-time reaction optimization process is on-line monitoring of the chemical reaction which is done by UV,[43] NMR,[44] MS,[45] Raman[46] and FTIR[47] spectroscopy.

The flow cell apparatus has three individually controlled reagent streams as shown in the Figure 1-10. The three streams meet at a four point union system. The forward flow of various streams of reagents is facilitated by the front-end pressure regulators. The reactor is made of a coil of steel tubes and constant pressure drop in the reactor is maintained by a back-end pressure regulator. The eluent stream is monitored by on-line FT-IR to record the various changes in the chemical reaction.

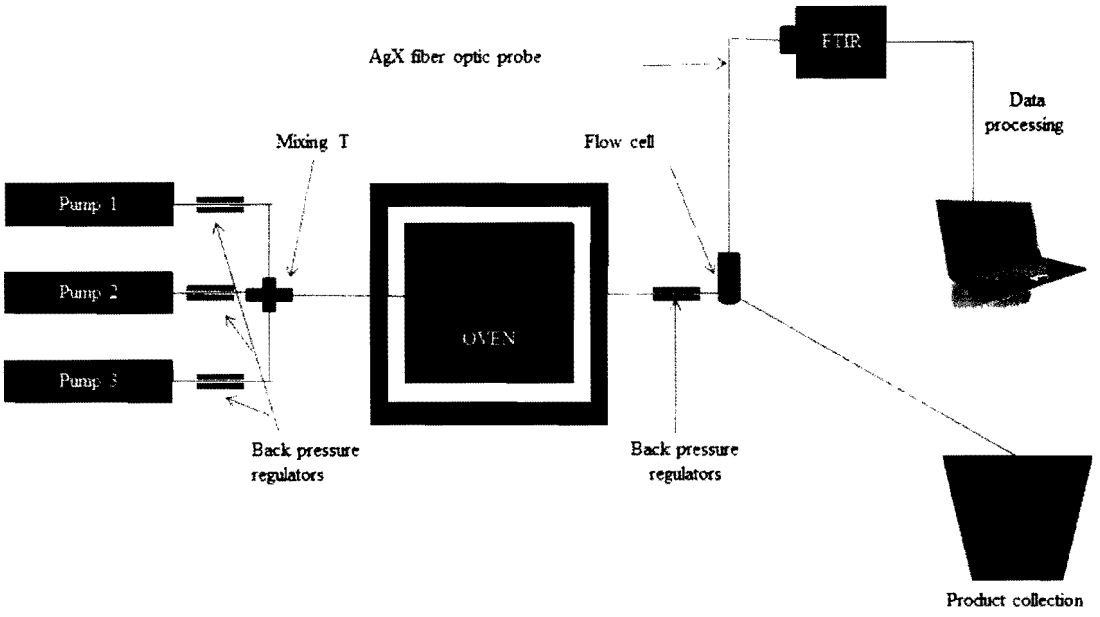

Figure 1-10. Schematic representation of a flow cell.[48]

[43] Jackman, R. J.; Floyd, T. M.; Schmidt, M. A.; Jenson, K. F. *Micro Total Analysis Systems 2000, Proceedings of the TAS Symposium, 4th, Enschede, Netherlands, May 14-18*, **2000**,*1*, 155-159.

[44] Bart, J.; Kolkman, A. J.; Oosthoek-de Vries, A. J.; Koch, K.; Nieuwland, P. J.; Janssen, H. J. W. G.; van Bentum, J. P. J. M.; Ampt, K. A. M.; Rutjes, F. P. J. T.; Wijmenga, S. S.; Gardeniers, H. J. G. E.; Kentgens, A. P. M. *J. Am. Chem. Soc.* **2009**, *131*, 5014-5018.

[45] Martha, C. T.; Elders, N.; Krabbe, J. G.; Kool, J.; Niessen, W. M. A.; Orru, R. V. A.; Irth, H. *Anal. Chem.***2008**, *80*, 7121-7126.

[46] Leung, S.; Winkle, R.; Wootton, R.; deMello, A. Analyst.**2005**, *130*, 46-50.

[47] Hubner, S.; Bentrup, U.; Budde, U.; Lovis, K.; Dietrich, T.; Freitag, A.; Kupper, L.; Jahnisch, K. *Org. Process. Res. Dev.* **2009**, *13*, 952-959.

1.10. Reactions in flow chemistry

The first applications of synthetic chemistry in the flow mode were reported with the dehydration reaction of diethylcarbinol and heterogeneous catalyst. [49] Although no experimental details were given it was reported that acidic silica gel was heated at high temperature for catalyzing the dehydration reaction. This synthesis opened the doors for the solid phase organic synthesis (SPOS) and polymer assisted solution synthesis (PASS). Flow chemistry was carried out in a similar manner as flash chromatography in the solution phase synthesis in the initial stages of its development.[50] The sulfoxide derivative of penicillin was obtained by passing penicillin through a peroxy resin packed column in 10 min at 40 °C (Scheme 1-2).[51]

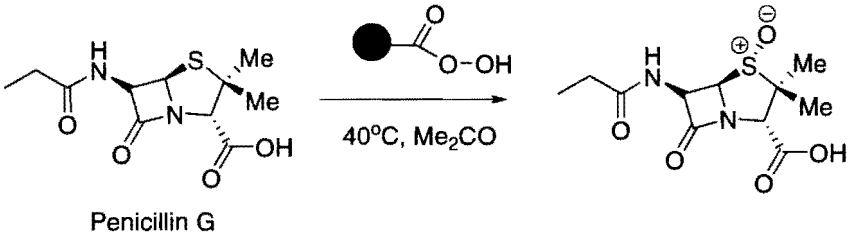

Scheme 1- 2. Flow oxidation of penicillin G.

Accordingly, a Knoevenagel reaction was carried out by allowing the substrates to pass through a gravity fed column packed with an alkylamine tethered silica which acts as the basic catalyst and can also be reused (Scheme 1-3).[52]

---

[48] Mattrey, F.T.; Dolman, S.; Nyrop J.; Skrdla P.J. *Am. Pharm. Rev.* **2012**,
[49] Karnatz, F. A.; Whitmore, F. A. *J. Am. Chem. Soc.* **1932**, *54*, 3461.
[50] Hodge, P. *Chem. Soc. Rev.* **1997**, *26*, 417 – 424.
[51] Harrison, C. R.; Hodge, P. *J. Chem. Soc., Perkin Trans.* **1976**, *1*, 2252 - 2254
[52] Angelleti, E.; Canepa, C.; Martinetti, G.; Venturello, P. *Tetrahedron Lett.* **1988**, *29*, 2261 – 2264.

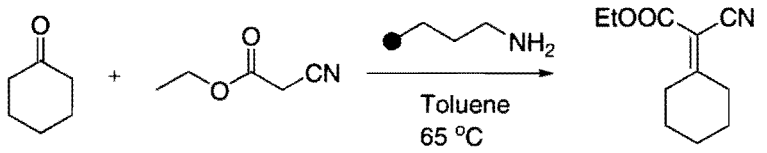

Scheme 1-3. Flow synthesis of Knoevenagel product.

The first enantioselective reaction by flow chemistry was reported by Itsuno *et al.*[53] where valerophenone was reduced by borane in the presence of an amino alcohol supported on a polymer which acts as the asymmetric catalyst. In this process substrates were added to the bottom of the column and the products flowed out from the top. The yield was 39% with 94% ee (Scheme 1-4).In this case the support bound asymmetric catalyst favors the formation of a chiral Schiff base with substrate, directing the reduction reaction stereoselectively.

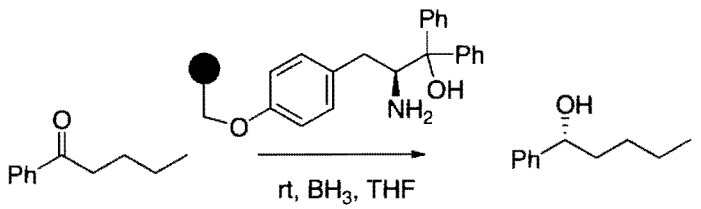

Scheme 1-4. Enantioselective reduction of ketone by flow chemistry.

The enantioselective Diels-Alder reaction was also carried out by packing the column with a catalyst (chiral oxazoborolidine) attached to the polymers. These catalysts are synthesized by copolymerisation reaction of a sulphonamide modified styrene monomer. The column is packed with the polymer at -30 °C and a mixture of methylacrolein and cyclopentadiene in the ratio of 1:1.5 was allowed to flow through the column which furnished the desired product enantioselectively in yields of 82% with 92% ee (Scheme 1-5).

[53] Itsunu, S.; Ito, K.; Maruyama, T.; Kanda, N.; Hirao, A.; Nakahama, S. *Bull. Chem. Soc. Jpn.* **1986**, *59*, 3329 – 3331.

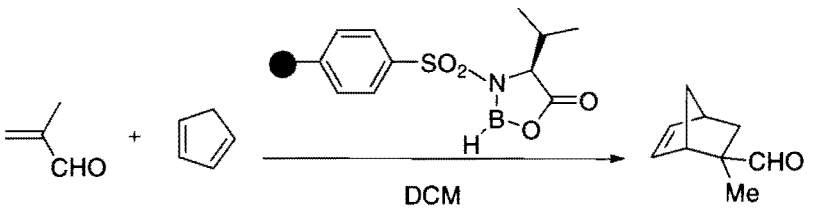

Scheme1-5. Diels-Alder reaction by flow chemistry.

Flow chemistry has been a powerful contribution in various fields of chemistry. The syntheses of drugs are accompanied in packed reactors as well as tube-like hollow reactors. The fixed-bed in these reactors is functionalized with a heterogeneous catalyst.[54] Further development prompted the use of homogeneous catalysts as well as reagents in the flow cell by immobilizing them on solid support. Inorganic supports are also used as scavengers. The fixed-bed is mainly made of monolithic materials as they possess a large surface area.[55] The fluid while passing through can have maximum contact with the reagent or catalyst.[56] Micro reactors equipped with functionalized monolithic polymer and composite materials were used for the reaction of steroids. Testosterone was converted to amino-functionalized steroid in the micro reactor (Scheme 1-6).[57]

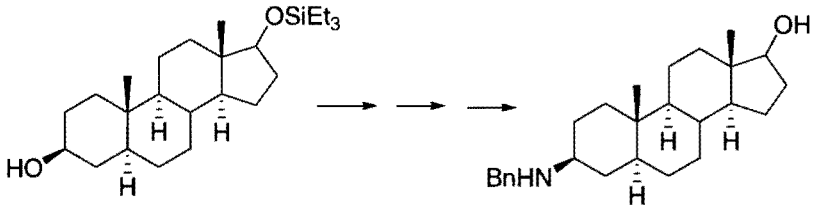

Scheme1- 6: Conversion of testosterone to amino-functionalized derivative.

---

[54] C. D. Keith, Apparatus for purifying exhaust gases of an internal combustion engine, U.S. Patent 3,441,381, April 29,1969.

[55] Svec, F.; Frechet, J. M. J. *Science*, **1996**, *273*, 205-207; (b) Hickman, D. A.; Schmidt, L. D. *Science*, **1993**, *259*, 343-346.

[56] Kirschning, A.; Jas, U.; Kunz, G. Chemistry in flow—new continuous flow reactors in organic synthesis, Innovation and Perspectives, in Solid Phase Synthesis and Combinatorial Libraries, R. Epton, Ed., MPG Book Ltd., Kingswindford, UK, **2004**; (b) Svec, F.; Huber, C. G. *Anal. Chem.* **2006**, *78*, 2100-2103

[57] Kirschning, A.; Altwicker, C.; Drager, G.; Harders, J.; Hoffmann, N.; Hoffmann, U.; Schonfeld, H.; Solodenko, W.; Kunz, U. *Angew. Chem. Int. Ed.* **2001**, *40*, 3995-3999.

Flow chemistry combined with photochemistry has been applied for the Barton reaction of steroidal derivatives.[58] Large scale photochemical reactions are more effective in flow processes as many micro reactors are assembled in parallel and irradiated simultaneously. The entire reaction mixture is uniformly irradiated as the micro reactors are small and maximum penetration is possible.

The continuous microwave reactor (CMR) is a device in which the two techniques of microwave heating and the synthesis with flow reactors have been blended together. The initial reports performed Michael addition, Williamson ether synthesis, esterification, Baeyer-Hillmann reaction and Mannich reactions.[59] The reactors are heated under flow conditions by irradiating with microwave. Heat can be applied directly at positions where the interaction between the two phases takes place within the reactor. The early CMR device was a microwave which was designed with monitor, meter, and control switches for maintaining the parameters such as temperature and pressure. Berlan *et al.* used a microwave reactor equipped with 66 mL quartz cylinder to conduct heterogeneous and homogeneous reactions.[60]

Thus, flow chemistry is an enabling technology which will assist in speeding up the reaction along with the simplification of the purification procedure in near future.

1.11. Conclusion

As discussed in the introduction section, the advantages of the real-time process monitoring is emphasized as data for the reaction is obtained instantaneously as the reaction is proceeding. This saves time, materials and allows the scientist or engineers to make

---

[58] Sugimoto, A.; Fukuyama, T.; Sumino, Y.; Takagi, M.; Ryu, I. *Tetrahedron* **2009**, *65*, 1593-1595.

[59] Strauss, C. R. *Chem. Aust.* **1990**, *57*, 186-189; (b) Cablewski, T.; Faux, A. F.; Strauss, C. R. *J. Org. Chem.* **1994**, *59*, 3408–3412; (c) Chen, S. T.; Chiou, S, H.; Wang, K. T. *J. Chem. Soc. Chem. Commun.* **1990**, 807–809.

[60] Chemat, F.; Poux, M.; Martino, J. L.; Berlan, *J. Chem. Eng. Technol.* **1996**, *19*, 420–424.

adjustments in the reaction conditions more efficiently. The work in this thesis is designed to explore the connection between real-time reaction monitoring and monitoring separations in real-time under batch and flow reaction conditions. The experimental sections and results and discussion sections in the following chapters present the details of the design of the combined real-time reaction monitoring and separation system and the successful outcomes.

Another project within this thesis is development of a simple, precise, accurate and validated, acetonitrile-free, reverse phase high performance liquid chromatography (HPLC) method for the determination of melamine in dry and liquid infant formula. The experimental outcomes were published in Analytica Chimica Acta journal.

The published article is cited in 35 different publications as tabulated in Table-1-2 and comparison in Figure 1-11.

Table.1-2 Citations report

S.No	Title	Authors	Source/Year
1.	Efficient Fluorescence Energy Transfer System between CdTe-Doped Silica Nanoparticles and Gold Nanoparticles for Turn-On Fluorescence Detection of Melamine.	Gao, Feng.; Ye, Qingqing.; Cui, Peng.; Zhang, Lu.	Journal of Agricultural and Food Chemistry (2012), 60, 4550-4558.
2.	Determination of melamine concentrations in dairy samples.	Feng, Wei.; Lv, Changyin.; Yang, Liping.; Cheng, Jianlin.; Yan, Chengyan.	Food Science and Technology (2012), 47, 147-153.
3.	Determination of melamine and its analogues in food.	Zhao, Ting Kai.; Liu, Le Hao.; Li, Guang Ming.; Li, Tie Hu.	Advanced Materials Research (2012).403-408, 2675-2678.
4.	The Importance of Acetonitrile in the Pharmaceutical Industry and Opportunities for its Recovery from Waste.	McConvey, Ian F.; Woods, Dean.; Lewis, Moira; Gan, Quan.; Nancarrow, Paul.	Organic Process Research & Development (2012), 16,612-624
5.	Determination of melamine in milk and dairy products by high performance liquid chromatography	Filazi, A.; Sireli, U. T.; Ekici, H.; Can, H. Y.; Karagoz, A.	Journal of Dairy Science (2012), 95(2), 602-608.
6.	Identification and Determination of Melamine in Milk by High Performance Liquid Chromatography – UV Detector	Mahmood, S.; El-Sayed S.; Mohamed S. A.; Lubna S. M. T.; Salih .A. B.	Der Pharma Chemica, (2012), 4(2), 737-748.
7.	Electrochemical Determination of Melamine with a Glassy Carbon Electrode Coated with a Multi-Wall Carbon Nanotube/Chitosan Composite	Tingkai, Z.; Lehao, L.; Guangming, L.; Alei, D.; Tiehu ,L.	Journal of Electrochemical. Society, (2012), 159(5), 141-145.

S.No	Title	Authors	Source/Year
8.	Determination of cyromazine and melamine in chicken eggs using Quick, Easy, Cheap, Effective, Rugged and Safe (QuEChERS) extraction coupled with liquid chromatography tandem mass spectrometry	Pei-Cheng, W.; Ren-Jye, L.; Chung-Yu, C.; Chi-Chung, C.; Maw-Rong, L.	Analytica Chimica Acta, (2012). In press.
9.	Flow-injection chemiluminescence determination of melamine in urine and plasma.	Xiaoshuang, T.; Xiyan, S.; Yuhai, T.; Zhongjin, Y.; Qiqi, H.	Journal of biological and chemical Luminescence,(2012), 27(3),229-233.
10	The application of Near-Infrared Reflectance Spectroscopy (NIRS) to detect melamine adulteration of soya bean meal.	Simon, A. H.; Stewart ,F. G.; Emmanuelle C.; Christopher, T. E.	Food Chemistry,(2012) Article in press.
11.	A 100% Water Mobile Phase HPLC-PDA Analysis of Melamine and Related Analogues	Naoto, F.	American Journal of Analytical Chemistry, (2012), 3, 295-299.
12.	Colorimetric Determination of Melamine by Pyridine-3-Boronic Acid Modified Gold Nanoparticles	Wu, Z.; Zhao, H.; Xue, Y.; He, Y.; Li, X.; Yuan, Z.	Journal of Nanoscience and Nanotechnology,(2012), 12(3), 2412-2416.
13.	Green" HPLC with 100% Water Eluent for Analysing Melamine in Milk.	Naoto, F.; Eriko, T.	LCGC, Europe, (June,2012).
14.	Detection of melamine in infant formula and grain powder by surface-assisted laser desorption/ionization mass spectrometry	Yi-Ting, H.; Wen-Tsen , C.; Iva, T.; Jan, P.; Huan-Tsung, C.	Rapid Communications in Mass Spectrometry, (2012). 26(12), 1393-1398.
15.	A sensitive, acetonitrile-free, HPLC method for determination of alibendol in dog plasma and its application to pharmacokinetic studies	Jae Kuk Ryu.	Journal of Pharmaceutical Investigation, (2012), 42(4), 185-190.

S.No	Title	Authors	Source/Year
16.	Determination of Melamine in Liquid Milk and Milk Powder by Titania-Based Ligand-Exchange Hydrophilic Interaction Liquid Chromatography	Jin, T.; Rong, L.; Zi-Tao, J.	Food Analytical Methods, (2012), 5(5), 1062-1069.
17.	Recent developments in the detection of melamine.	Yuan, L.; Ewen, E. D.T.; Qiang, Z.; Jiang-rong, S.; Xian-jin, L.	Journal of Zhejiang University - Science B,(2012),13(7),525-532.
18.	Application of Tandem Mass Spectrometry for Analyzing Melamine.	Wei-Chih, C.; I-Jen, Wang.	Tandem Mass Spectrometry, Application and principles (2012).373-388 Edited by Dr Jeevan Prasain.
19.	Visual detection of melamine in raw milk by label-free silver nanoparticles	Hong, P.; Minwei, Z.; Hongkun, L.; Shugui, L.; Quansi, C.; Chunyan, S.;' Tiehua, Z.	Food Control, (2012), 23, 191-197.
20.	Development of gold nanoparticle-based rapid detection kit for melamine in milk products.	Zhou, Q.; Liu, N.; Qie, Z.; Wang, Y.; Ning, B.; Gao, Z.	Journal of Agricultural and Food Chemistry, (2011), 59(22), 12006-12011.
21.	One-step synthesis of silver/dopamine nanoparticles and visual detection of melamine in raw milk.	Ma, Y.; Niu, H.; Zhang, X.; Cai, Y.	Analyst, (2011), 136, 4192-4196.
22.	Characterization of the Disposition of Melamine in Female Sprague-Dawley Rats Using Ultra-Performance Liquid Chromatography-Tandem Mass Spectrometry.	Wu, D.; Liu, J.; Zhao, Q.; Xu, X.; Yang, L.; Huang, H.; Yuan, J.; Zhou, L.; Zhuang, Z.	Journal of Analytical Toxicology, (2011), 35, 551-557.
23.	Synthesis of [^{15}N3]melamine and [^{13}C3]cyanuric acid.	Yong, L.; Liya, Z.; Weicheng Y.; Weixia L.; Weijing, L.; Meihua L.	Journal of Labelled Compounds and Radiopharmaceuticals, (2011), 54(4),171-172.

S.No	Title	Authors	Source/Year
24.	A Highly Sensitive Aptamer-Nanogold Catalytic Resonance Scattering Spectral Assay for Melamine.	Aihui, L.; Lianping, Z.;Huimin Q.; Yi Z.; Huixiang, O.;Zhiliang J.	Journal of Fluorescence, (2011), 21(5), 1907-1912.
25.	A Simple and Sensitive Resonance Scattering Spectral Assay for Detection of Melamine Using Aptamer-Modified Nanosilver Probe.	Aihui, L.; Lianping, Z.; Zhiliang J.	Plasmonics, (2011), 6(2), 387-392.
26.	Determination of Melamine in Dairy Products and Melamine Tableware by Inhibition Electrochemiluminescent Method.	Wei, J.; huiyuan L.; Xiaojing L.; Xiaofen, J.; Minshi, C.; Ming, L. Xi T.; Caiming, X.; Jinquan, C.	Chinese Journal of Chemistry, (2011), 29(8), 1601-1605.
27.	Melamine detection by mid- and near-infrared (MIR/NIR) spectroscopy: A quick and sensitive method for dairy products analysis including liquid milk, infant formula, and milk powder	Roman M. B.; Sergey V. S.	Talanta,(2011), 85(1), 562-568.
28.	Sensitive turn-on fluorescent detection of melamine based on fluorescence resonance energy transfer	Liangqia G.; Jianhai Z.; Jinmei ,W.; FengFu, F.; Guonan C.; Yongxuan, C.; Xiaoyan, Z.;Song, L.	Analyst, (2011), 136(8),1659-1663.
20.	Determination of melamine by flow injection analysis based on chemiluminescence system.	Hua-jin, Z.;, Ran, Y.; Qing-wen, W.; Jian-jun, L.; Ling-bo, Q.	Food chemistry, (2011), 127(2), 842-846.
30.	Determination of melamine based on electrochemiluminescence of $Ru(bpy)_3^{2+}$ at bare and single-wall carbon nanotube modified glassy carbon electrodes	Fengyu, L.; Xue, Y.; Shiguo, S.	Analyst, (2011), 136, 374-378.

S.No	Title	Authors	Source/Year
31.	Development of an Optical Biosensor Based Immunoassay to Screen Infant Formula Milk Samples for Adulteration with Melamine.	Terence, L. F.; Colin, S. T. Imelda, M. T.; Simon, A. H. D. G.K.; Steven R. H. C.	Analytical chemistry, (2011), 83(12), 5012-5016.
32.	Resonance scattering detection of trace melamine using aptamer-modified nanosilver probe as catalyst without separation of its aggregations.	Zhiliang, J.; Lianping, Z.; Aihui, L.	Chemical communications, (2011), 47, 3162-3164.
33.	Development of an Immunochromatographic Strip Test for Rapid Detection of Melamine in Raw Milk, Milk Products and Animal Feed	Xiangmei, L.; Pengjie, L.; Shusheng, T.; Ross, C. B.; Xiaoping, W.; Lili, Y.; Yanwei, L.; Xilong, X.	Journal of Agriculture and Food Chemistry, (2011), 59(11), 6064-6070.
34.	One-step synthesis of silver/dopamine nanoparticles and visual detection of melamine in raw milk	Yurong, M.; Hongyun, N.; Xiaole, Z.; Yaqi, C.	Analyst, (2011), 136(20), 4192-4196.
35.	Visual detection of melamine in milk products by label-free gold nanoparticles.	Liangqia, G.; Jianhai Z.; Jinmei, W.; FengFu, F.; Guonan, C., Xiaoyan, Z.; Song, L.	Talanta, (2010), 82(5), 1654-1658.

Figure. 1-11.Citations in each year comparison

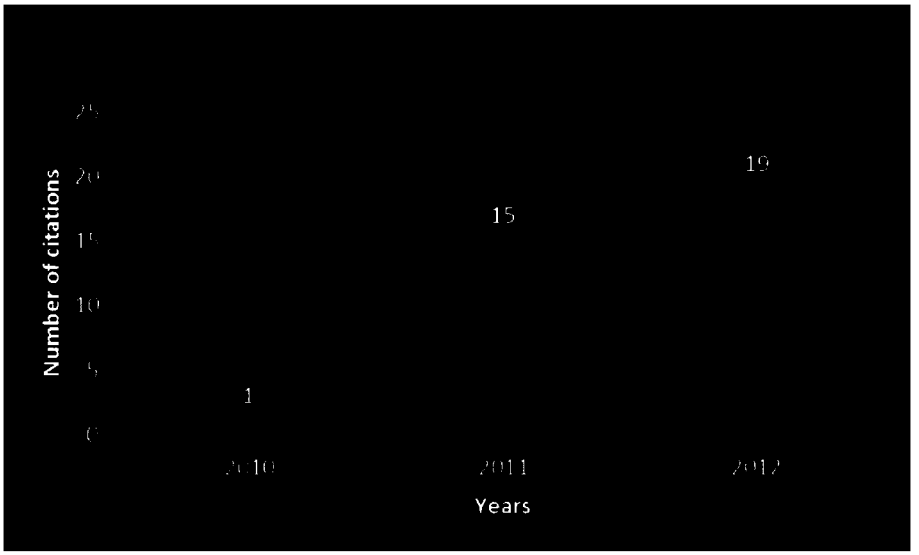

2. Experimental Section

2.1. Instrumentation for real-time reaction monitoring

The objective of this study was to monitor known reactions and separations in real-time by ReactIR instrument. The chemical changes during the reactions was monitored by ReactIR and the separation of the components was monitored by FlashIR system that we designed. The IR analysis of the real-time reaction provided detailed chemical information which was used to guide the flash separation.

The organic reaction processes were conducted in a Mettler-Toledo EasyMax™ instrument (Figure 2-1) with FT-IR monitoring using a ReactIR iC10 (Figure 2-2) instrument. The EasyMax™ is a synthesis workstation consisting of a single, self-contained unit with built-in solid state thermostats. Two vessels are hosted that operate independently of each other. The powerful and self-sufficient solid state heating and cooling system controls the temperature of the reaction mixture accurately. The thermostat provides the necessary performance to grant outstanding heating and cooling rates over a wide temperature range. The reactions monitored were controlled with assistance from Mettler Toledo's iC10 version 3.0 and 4.0 software.

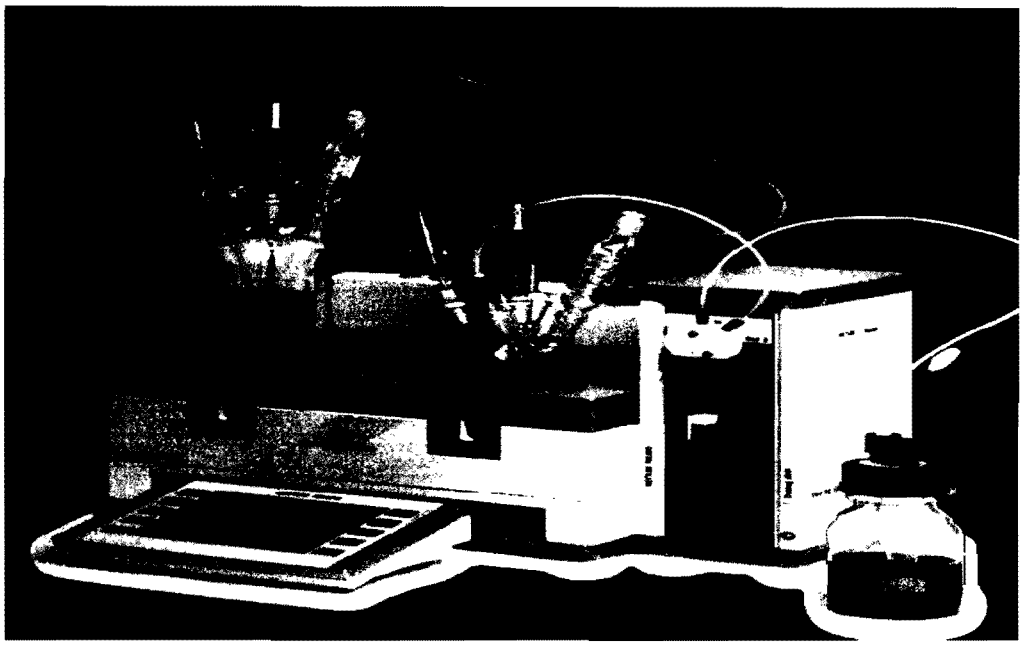

Figure 2-1. EasyMax System (MettlerToledo®).

The reactions were monitored for real-time changes by the ReactIR iC10 FT-IR instrument from Mettler Toledo which has a Mercury Cadmium Telluride (MCT) detector (liquid nitrogen cooled) and a Fiber Conduit™ as shown in the Figure 2-2. The Fiber Conduit™ is comprised of flexible IR transparent silver chloride/silver bromide optical fibers. The fiber optic probe interface (AgX 9.5 mm × 1.5 m fiber (silver halide)) contains a 1 mm diamond tip (DiComp) ATR crystal and the resolution was set to 8 wavenumbers. The optical range used by the system is: 1900 – 650 cm^{-1}. The system uses compressed air (house air, filtered and dehumidified) to purge the optics. This spectrometer operates according to the Fourier transform method and utilizes the ATR principle (Attenuated Total Reflection). contact with a sample. The ATR-IR system was configured to collect spectra every 2-3 minutes.

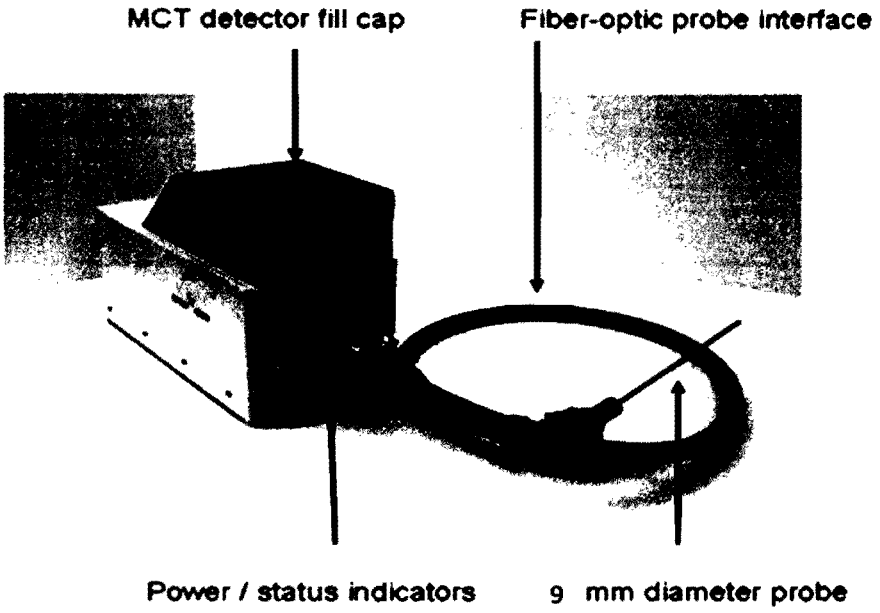

Figure 2-2. React-IR system (Mettler Toledo).

2.1.2. Instrumentation for Separation

The purification of the reaction mixture was done without doing much post synthetic work-up procedure to accelerate the purification process. The separation of the reaction mixture was carried out by the flash chromatographic method and the fractions were monitored by the ReactIR system. The flash separation was conducted using a commercially available pre packed flash column called SNAP cartridge as shown in the Figure 2-3 which is designed with universal fit into all flash systems with Luer-Lok fitting. The fittings are securely joined by means of a tabbed hub on the female fitting which screws into threads in a sleeve on the male fitting. The usage of SNAP cartridge avoided errors in manual packing the silica gel in the column. The cartridges were obtained from Biotage™ which were made using polypropylene and polyethylene containing silica gel ranges from 2

g to 40 kg with particle size of 30 μm. The column packed with 25 g of silica gel with 30 μm particle size was used for all the experiments.

Figure 2-3. SNAP Cartridge.

A flow cell was designed with an inlet for eluent from the column, outlet for the fraction collection and the ReactIR probe which was placed in such a way that the eluent from the column was directly monitored to identify the compound to be purified which can be observed in the fractions as shown in the Figure 2-4. The flow cell was designed from an isolated flow cell from a non-operating HPLC.

Figure 2-4. Retrofitted Flow Cell.

The block diagram of the designed system which is named as FlashIR is shown in the Figure 2-5. It has a flash pump, flash column, flow cell and fraction monitoring *in-situ* ATR-IR system and the fractions collected manually with approximately 5 mL in each test tube.

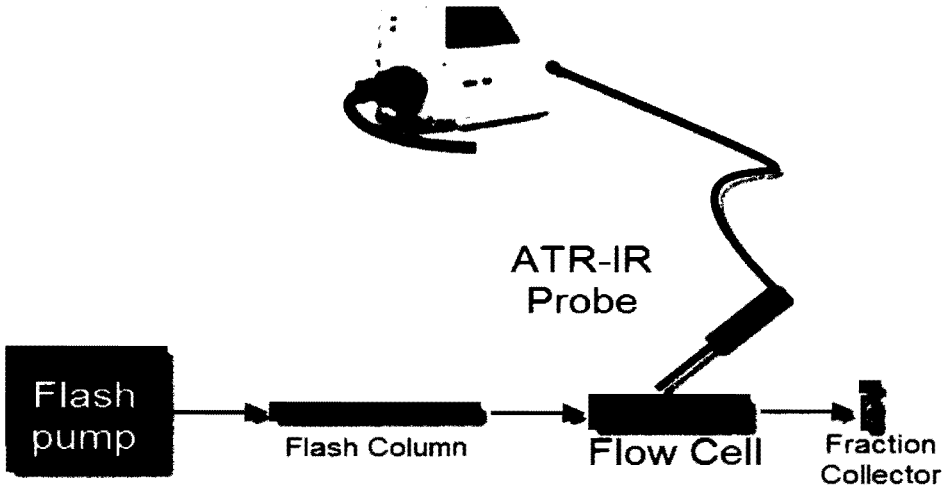

Figure 2-5. Block diagram of FlashIR.

The pre-weighed reaction mixture intended for separation was dissolved in the solvent combination chosen by thin layer chromatographic analysis and was placed on top of the

column using a syringe. The mobile phase was pumped from the reservoir using a HP 1050 HPLC pump at 5 mL per minute to the head of the column. The eluents come off the column and go through the flow cell. The fractions were monitored in a real-time using the *in-situ* ATR-IR system during several collections. The collected fraction was used for off-line analysis by HPLC for comparison purpose. The assembled instrument which is a FlashIR as discussed is shown in Figure 2-6.

Figure 2-6. Design of FlashIR.

The separation was monitored based on the background knowledge gained during the real-time reaction monitoring. Approximately 1.0 g of reaction mixture was used for purification based on the loading capacity recommended for the SNAP cartridges by the manufacturer.

2.2. Synthesis of benzyl tert-butyl ether (Williamson ether synthesis)

In our first attempt, the Williamson ether synthesis reaction was used to prepare benzyl *tert*-butyl ether. The overall strategy was to follow the reaction in real-time by IR; assess when the reaction is complete and then purify the reaction while monitoring the eluents in real-time by IR.

The Williamson ether synthesis is a nucleophilic substitution reaction between an alkyl halide and an alkoxide to furnish an ether derivative as a product. Ethers are important solvents and precursors of cosmetics, fragrances and dyes. The synthesis is important to produce both symmetrical and unsymmetrical ethers. [61,62,63]

Benzyl *tert*-butyl ether (13). Potassium *tert*-butoxide **11** (1.1 g, 10 mmol) was added to THF (25 mL) in an inert atmosphere and the mixture was heated at 50 °C with simultaneous stirring at 200 rpm . 1.2 equivalent of benzyl bromide **12** (1.5 g, 12 mmol) was then added. The reaction was conducted under nitrogen atmosphere. The completion of the reaction was identified by TLC analysis using the hexane: dichloromethane in ratio of 80:20. The R_f values of benzyl bromide and benzyl *tert*-butyl ether (BTBE) are 0.76 and 0.23 respectively The reaction mixture was directly used after removal of excess solvents and without the post synthetic preparation steps. Purification of the crude material by flash separation monitored by IR was yielded 0.65 g (65%) colorless liquid.

The analysis of the fractions was also carried out using HPLC with UV detection. This off-line analysis is an orthogonal detection method to IR. The HPLC conditions: HP 1050 HPLC, Phenomenex, C18, Hypersil column 100 X 4.6 mm length and diameter with 5 μm particle size, and mobile phase was 50:50 (water:acetonitrile) was pumped at flow rate of

[61] Williamson, A. W. *J. Chem. Soc.* **1852,** *4,* 229-231.
[62] Zerbe, C.; Jage, F. *Brennstoff-Chemie* **1935**, *16*, 88-92.
[63] Chapman. J. J.; Reid, J. R. *J. Org. Chem.* **1989**, *54*, 3757-3759.

0.5 mL/min in isocratic mode. The injection volume was 10 µL and UV detector was set at 254 nm. The retention time of benzyl bromide and BTBE are 8.3 and 12.8 minutes respectively as shown in Figure 2-7.

Figure 2-7. HPLC analysis of Williamson reaction mixture.

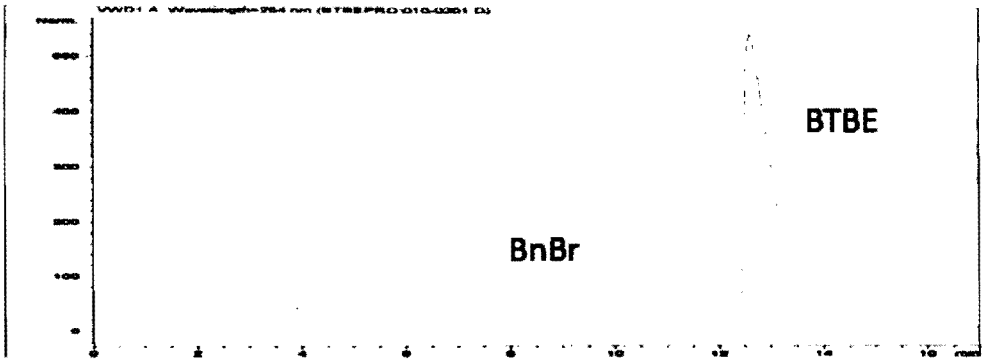

The pure product was isolated by combining the chosen fractions and removing the solvents using a rotary evaporator. The isolated yield was 65% (0.65 g). The structure identification was established by NMR. ^{1}H NMR (200 MHz, $CDCl_3$) δ 7.38 – 7.32 (m, 5H), 4.44 (s, 2H), 1.28 (s, 9H).

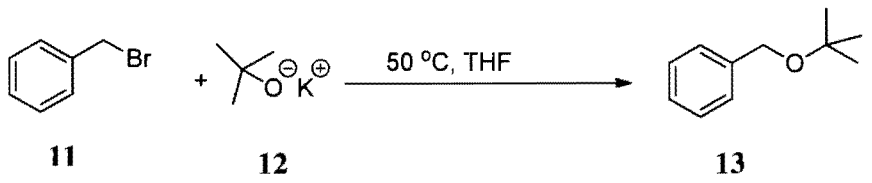

Scheme 2-1.Williamson ether synthesis. [64]

[64] Hurd, C. D.; Raterink, H. R. *J. Am. Chem. Soc.***1933**, 55, 1541-1544.

2.3. Reaction monitoring of conversion of cholesterol to cholesteryl acetate (acetylation).

Our next attempt was to study an acetylation reaction in a steroid molecule since it has weak UV chromophore containing functional groups that are non-sensitive to UV-light.[65] The cholesterol was chosen as the model substrate to perform the acylation reaction.

Cholesterol serves as a precursor for the biosynthesis of steroid hormones, bile acids, and vitamin D, etc. The molecule can be transformed to a variety of products either by oxidation of the hydroxyl group or by degradation of the side chain.[66] Traditionally, cholesteryl acetate can be obtained from cholesterol by an acetylation reaction with an excess of acetic anhydride as both catalyst and solvent.[67,68]

The IR has been an efficient tool to provide detailed chemical information and as an alternative for the detection of certain compounds such as carbohydrates and alkyl alcohols which cannot easily be detected under UV-light.

The acylation of the hydroxyl group is a reaction involving the replacement of the hydrogen atom of a hydroxyl group with an acetyl group (CH_3CO) yielding the methyl ester. The hydroxyl group can be easily protected by acetylation which has stability in acidic conditions and can easily be removed under mild alkaline conditions.[69] The acetylation of

---

[65]Edelmann, A.; Baena, J. D. J. R.; Lendl, B. *Anal. Bioanal. Chem.* **2003**, *376*, 92–97.
[66]Butenandt, A.; Dannenbaum, H.; Kudszus, H. *Z. Physiol. Chem.* **1935**, 57, 237-240; (b) Cook, R. P., "*Cholesterol*," Academic Press, New York, **1958**, 58-65.
[67]Hudson, C. S.; Dale, J. K. *J. Am. Chem. Soc.* **1915**, *37*, 1264-1268; (b) Wolfrom, M. L.; Thompson, A. *Methods Carbohydr. Chem.* **1963**, *2*, 211-215.
[68]Hofle, G.; Steglich, W.; Vorbruggen, H. *Angew. Chem., Int. Ed. Engl.* **1978**, *17*, 569-573; (b) Scriven, E. F. V. *Chem. Soc. Rev.* **1983**, *12*, 129-134.
[69] Green, W.; Wuts, P. G. M. *Groups in Organic Synthesis*, 3rd ed.; Wiley: New York, 1999; pp. 150–160; (b) Pearson, A. L.; Roush, W. J. *Handbook of Reagents for Organic Synthesis: Activating Agents and Protecting Groups*; John Wiley and Sons: UK, 1999; pp. 9–16.

alcohol is carried out in presence of acetic anhydride as the acetylating reagent and a basic catalyst mainly pyridine.[70]

Acetic anhydride exhibits an IR absorption peak at 1850 cm^{-1} which is assigned to the carbon-oxygen stretching (C=O) frequency. The consumption of the acetic anhydride over time during the progress of the reaction as acetylating reagent was considered rather than the characteristic IR bands in cholesterol. The formation of the cholesterol acetate as product could be identified by observing a distinct peak at 1735 cm^{-1} which is assigned to the carbonyl (C=O) stretching frequency present in the acetate group.

The experimental procedure that was followed to conduct the acetylation of cholesterol to cholesteryl acetate was as follows: **Cholesteryl acetate (23).** Cholesterol **21** (3.0 g, 10 mmol) was added to THF (25 mL) and the mixture was heated at 45 °C with simultaneous stirring at 200 rpm. A 10 mmol equivalent of acetic anhydride **22** (3.0 mL) was added after 30 minutes. The completion of the reaction was identified by TLC analysis using the hexane: dichloromethane in ratio of 80:20. The R_f values of cholesterol and cholesteryl acetate are 0.21 and 0.77 respectively. The reaction mixture was directly used after removal of excess solvents and without the post synthetic preparation steps. Purification of the crude material by flash separation monitored by IR was yielded 0.7 g (70%) of crystalline white solid. Melting point 108-110 °C.

The HPLC with UV detection was performed under the following HPLC conditions: HP 1050 HPLC Waters, Symmetry, C18, column 150 x 3.9 mm length and diameter with 5 μm particle size using mobile phase combination of 90/10 (IPA/water). The flow rate was 0.7 mL/min in isocratic mode and the injection volume was 10 μL. The UV detector was set

[70] Horton, D. *Organic Synthesis Collective*; Wiley: New York, 1991; Vol. V, pp. 1–6; (b) Zhdanov, R. I.; Zhenodarova, S. M. *Synthesis* **1975**, *4*, 222–245.

at 210 nm. The retention time of cholesterol and cholesteryl acetate is 5.2 and 11.6 minutes respectively as shown in Figure 2-8.

Figure 2-8. HPLC analysis of acetylation reaction mixture.

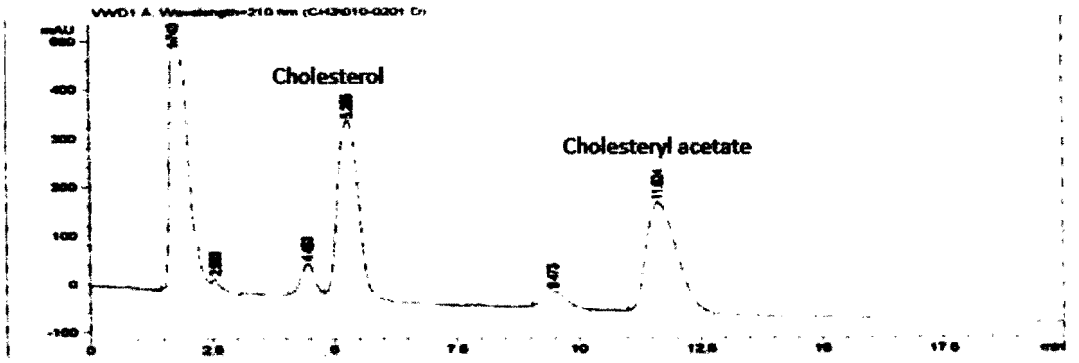

The pure product was isolated by combining the chosen fractions and removing the solvents using a rotary evaporator. The isolated yield was 70% (0.7 g). The structure identification was established by NMR. ^{1}H NMR (400 MHz, $CDCl_3$) δ 5.40-5.35 (m, 1H), 4.70-4.60 (m, 1H), 2.33-2.30 (m, 2H), 2.03 (s, 3H), 2.00-1.80 (m, 5H), 1.60-0.90 (m, 21H), 1.02 (s, 3H), 0.91 (d, 3H), 0.87 (d, 3H), 0.86 (d, 3H), 0.68 (s, 3H).

^{13}C NMR (200 MHz, $CDCl_3$) δ 170.61, 140.24, 122.87, 74.28, 57.16, 56.59, 54.93, 54.39, 53.84, 53.30, 52.76, 50.18, 42.70, 40.19, 39.91, 38.53, 37.42, 37.00, 36.60, 36.24, 32.28, 28.62, 28.44, 28.17, 24.66, 24.22, 22.98, 22.73, 21.58, 21.44, 19.52, 18.92, 12.04

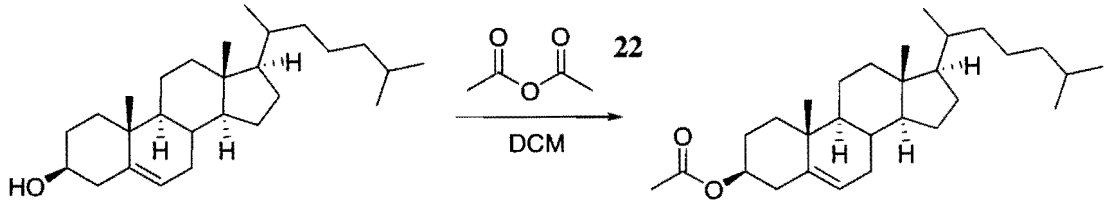

21 **23**

Scheme 2-2. Acetylation of cholesterol.

2.4. Isomerization of cyclohexen-1-ol to cyclohexanone

In our next endeavor we explored an isomerization reaction to follow by real-time monitoring and separation. The conversion of allylic alcohols to ketones and aldehydes is a significant isomerization reaction. [71,72] This process has been widely used in pharmaceutical industries to synthesize products in bulk quantity. These particular isomerization reactions have been catalyzed by different transition metals. However, in many cases the amount of catalyst required is comparatively high coupled with very harsh reaction condition, restricts the use of the transition metals as catalyst.

The isomerisation reaction of (Z)-but-2-en-1,4-diol to 4-hydroxybutyraldehyde catalysed by palladium has been reported at high temperature.[73] Another hydrogen pre-activated palladium-carbon catalysed isomerisation has been reported in the gas phase by using a flow apparatus at 180 °C.[74]

The experimental procedure to conduct the isomerization reaction was as follows: **Cyclohexanone (32).** Cyclohexen-1-ol **31** (1.0 g, 10 mmol) was added to isopropanol (25 mL) and stirred at 200 rpm. The mixture was heated at 80 °C after addition of palladium-carbon catalyst (50mg, 5 wt %) with simultaneous stirring. The completion of the reaction was identified by TLC analysis using the ethyl acetate: hexane in ratio of 90:10. The R_f values of cyclohexen-1-ol and cyclohexanone are 0.62 and 0.82 respectively. The reaction

---

[71] Cadierno,V.; Crochet, P.; Gimeno, J. *Synlett*, **2008**, *8*,1105–1124; (b) van der Drift, R. C. E.; Bouwman, R. C. E.; Drent, E. *J. Organomet. Chem.* **2002**, *650*, 1–24; (c) Trost, B. M.; Kulawiec, R. J. *Tetrahedron Lett.* **1991**, *32*, 3039–3042; (d) Trost, B. M.; Kulawiec, R. J. *J. Am. Chem. Soc.* **1993**, *115*, 2027–2036; (e) Ahlsten, N.; Bartoszewicz, A.; Martin-Matute, B. *Dalton Trans.* **2012**, *41*, 1660–1670; (f) Batuecas, M.; Esteruelas, M. A.; Garcia-Yebra, C.; Onate, E. *Organometallics* **2010**, *29*, 2166–2175.

[72] a) Masters, C. *Homogeneous Transition-Metal Catalysis;* Chapman and Hall: London, **1981**; pp 70-81; b) Davies, S. G. *Organotransition Metal Chemistry. Applications to Organic Synthesis,* Pergamon Press: Oxford, **1982**, pp 266-290.

[73] Sedding, B.; Alm, J. *J. Prakt. Chem.* **1987**, *329*, 711–716.

[74] Delaby, R. *Compt. Rend.* **1926**, *182*, 140–142; (b) Kraus, M. *Collect. Czech. Chem. Commun.* **1972**, *37*, 460–465.

mixture was directly used after removal of excess solvents and without the post synthetic preparation steps. Purification of the crude material by flash separation monitored by IR yielded 0.85 g (85%) colorless liquid.

The HPLC analysis of the collected fractions was performed on HP 1050 HPLC, using a C18 Hypersil column of 150 x 3.9 mm of length and diameter with 5 μm particle size. The mobile phase was used as acetonitrile:water in the ratio of 50:50 with a flow rate of 0.5 mL/min in the isocratic mode. The injection volume was 10 μL with the setting of the UV detector at 300 nm. The retention time of cyclohexanone peak was 7.1 minutes as shown in Figure 2-9.

Figure 2-9. HPLC analysis of isomerization reaction mixture.

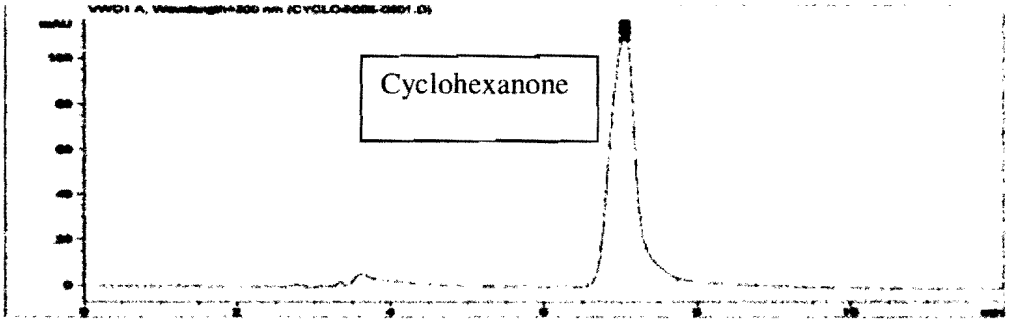

The pure product was isolated by combining the chosen fractions and removing the solvents using a rotary evaporator. The isolated yield was 85% (0.85 g). The structure identification was established by NMR. ^{1}H NMR (200 MHz, $CDCl_3$) δ 2.29 – 2.23 (t, 4H), 1.85 – 1.61 (m, 6H). ^{13}C NMR (200 MHz, $CDCl_3$) δ 212.09, 41.94, 27.00, 24.95.

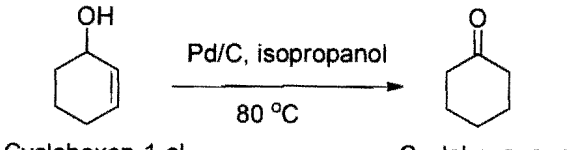

31 **32**

Scheme 2-3. Isomerization of cyclohexene-1-ol to cyclohexanone.

3.0. Results and Discussion

3.1. Synthesis of benzyl *tert*-butyl ether (Williamson ether synthesis)

Synthesis of benzyl tert-butyl ether was performed in Mettler-Toledo EasyMax^{TM} instrument with FT-IR monitoring using a ReactIR iC10 instrument as described in the Experimental Section 2-2. The progress of the reaction was monitored in real-time as the expected characteristic differences of the vibrational spectra of starting material and product. The peak at 1210 cm^{-1} was due to the stretching vibration of the ethereal carbon–oxygen bond as shown in the IR spectrum shown in the Figure 3-1 which was obtained from a published spectral database (SDBS).[75] The peak response in that region was considered for monitoring for the product.

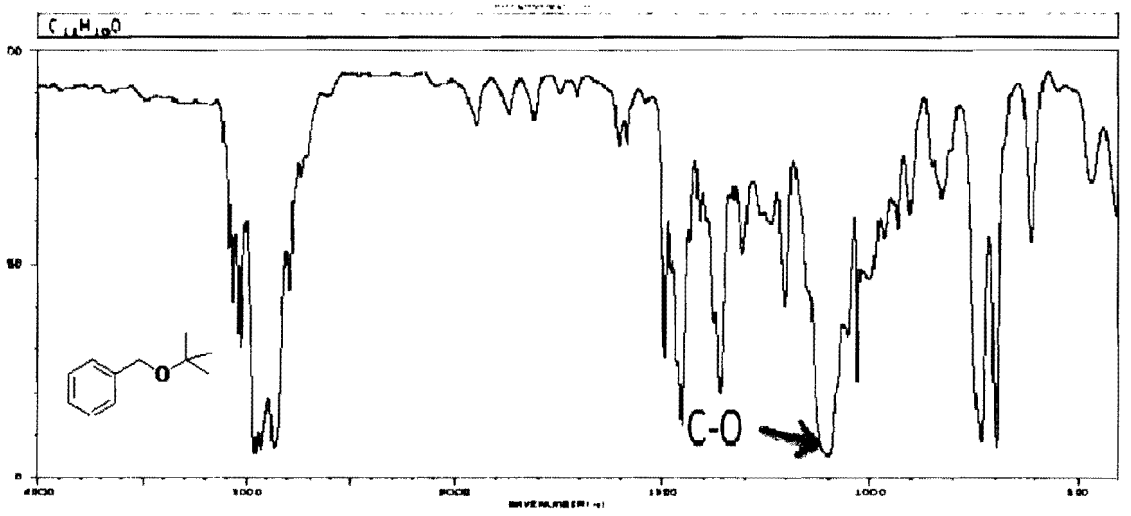

Figure 3-1. The IR spectrum of benzyl tert-butyl ether obtained from SDBS data base.[76]

Alternately the peak at 750 cm^{-1} was assigned to the carbon-bromine bond as shown in the IR spectrum in Figure 3-2 which was obtained from SDBS. The peak response at this

[75] Spectral data base system for organic compounds. http://riodb01.ibase.aist.go.jp/sdbs/cgi-bin/direct_frame_top.cgi (accessed October 7, 2012).

region was considered for benzyl bromide as reactant gradually decreases in peak response due to the cleavage of the carbon-bromine bond.

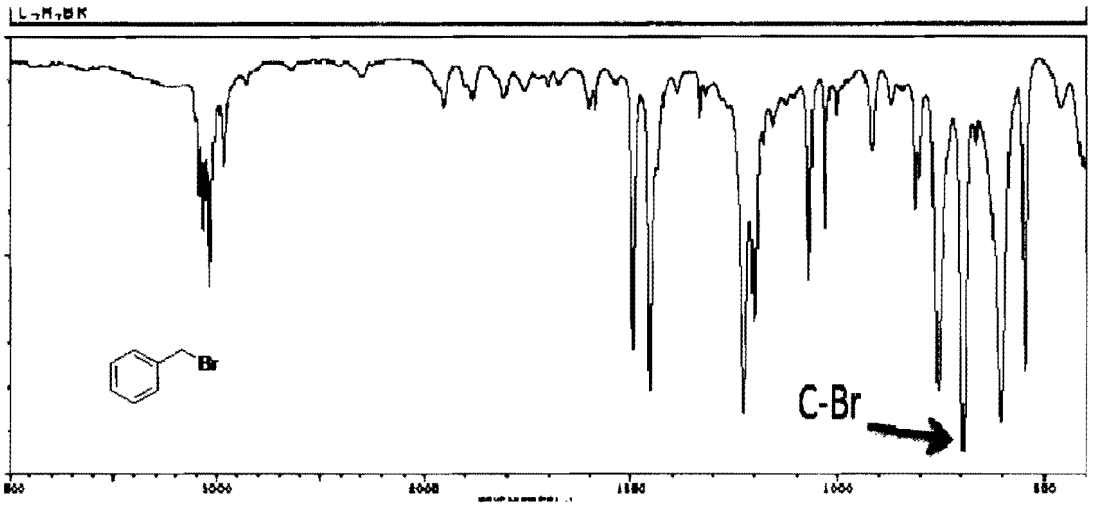

Figure 3-2. The IR spectrum of benzyl bromide obtained from SDBS database.[75]

The decreasing response of the reactant and increasing response of the product *versus* time was clearly observed from the full spectrum output from the system (Figure 3-3).

In Figure 3-3.A, section 'a' shows the full spectrum visualizing the real-time reaction showing the reactant and the product changes during the progress of the reaction. Section 'b' in the figure shows an expanded view of the spectrum in the 1210 cm^{-1} region for C-O bond formation. Section 'c' in the figure shows expanded view of the spectrum at 750 cm^{-1} region where the peak response started diminishing since the C-Br bond is breaking over time. The percentage change in peak area response collected as tabulated in Table 8-1 in Appendix 8.0 for the reactant and product was used for graphical representation of progress of the reaction (Figure 3-3.B). It clearly indicates that the increase in the peak area response due to product formation as the concentration of benzyl tert-butyl ether increases and decreasing peak area response as the concentration of benzyl bromide concentration started diminishing over time.

The blue curve shows the product changes and the red curve shows the reactant changes and the reaction completion was observed in about the 10^{th} hour.

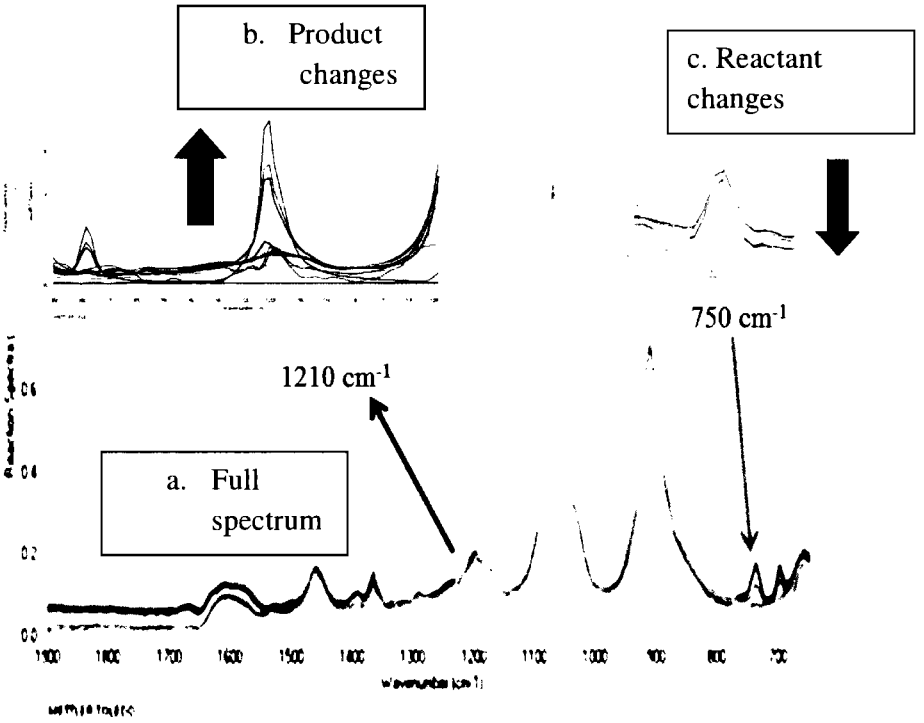

Figure 3-3.A. Change in reactant and product response in real-time reaction.

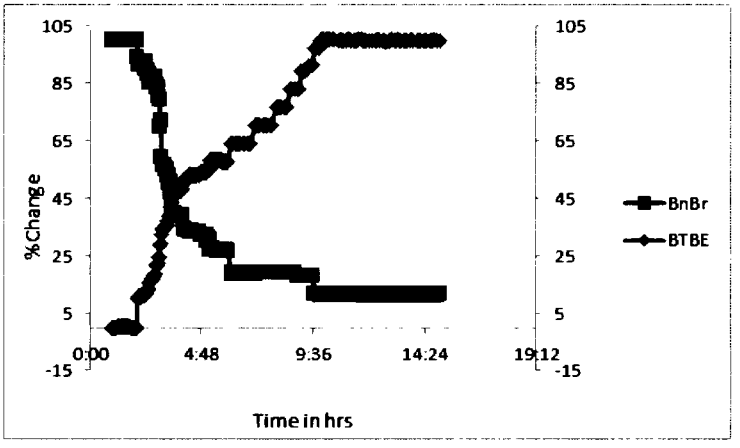

Figure 3-3.B. Graphical illustration of the reaction profile.

To verify the extent of reaction completion and to identify the best solvent combination for separation and purification of reaction mixture the TLC analysis was performed. The optimal separation was obtained using 80:20 hexane:dichloromethane. The R_f values of benzyl bromide and benzyl tert-butyl ether (BTBE) are 0.76 and 0.23 respectively. The spotted reaction mixture as BTBE shows two distinct spots and one of the spot matches with the benzyl bromide indicates that the unreacted benzyl bromide and the other spot as benzyl tert-butyl ether as shown in the Figure 3-4

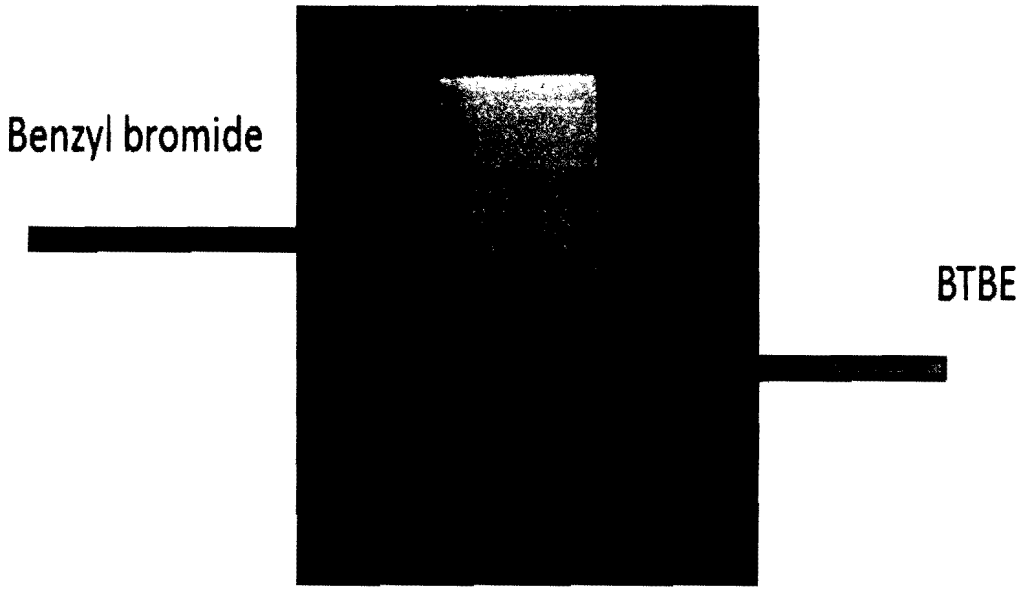

Figure 3-4. TLC analysis of the reactant and the product.

The flash separation was monitored by the FlashIR system as described in the experimental section. The elution process shown the changes as anticipated based on the changes observed during the real-time reaction. The elution of the benzyl bromide as the reactant and benzyl tert-butyl ether as the product was detected based on background information collected during the real-time reaction monitoring at the wavenumber region 750 cm^{-1} and 1210 cm^{-1} respectively.

The intensity of the eluent fractions corresponding to wavenumber 750 cm^{-1} due to carbon–bromine stretching vibration and the peak response at the frequency of 1210 cm^{-1} due to the stretching vibration of the C-O group in benzyl tert-butyl ether was shown clearly in the full spectrum of the flash separation observed (Figure 3-5).

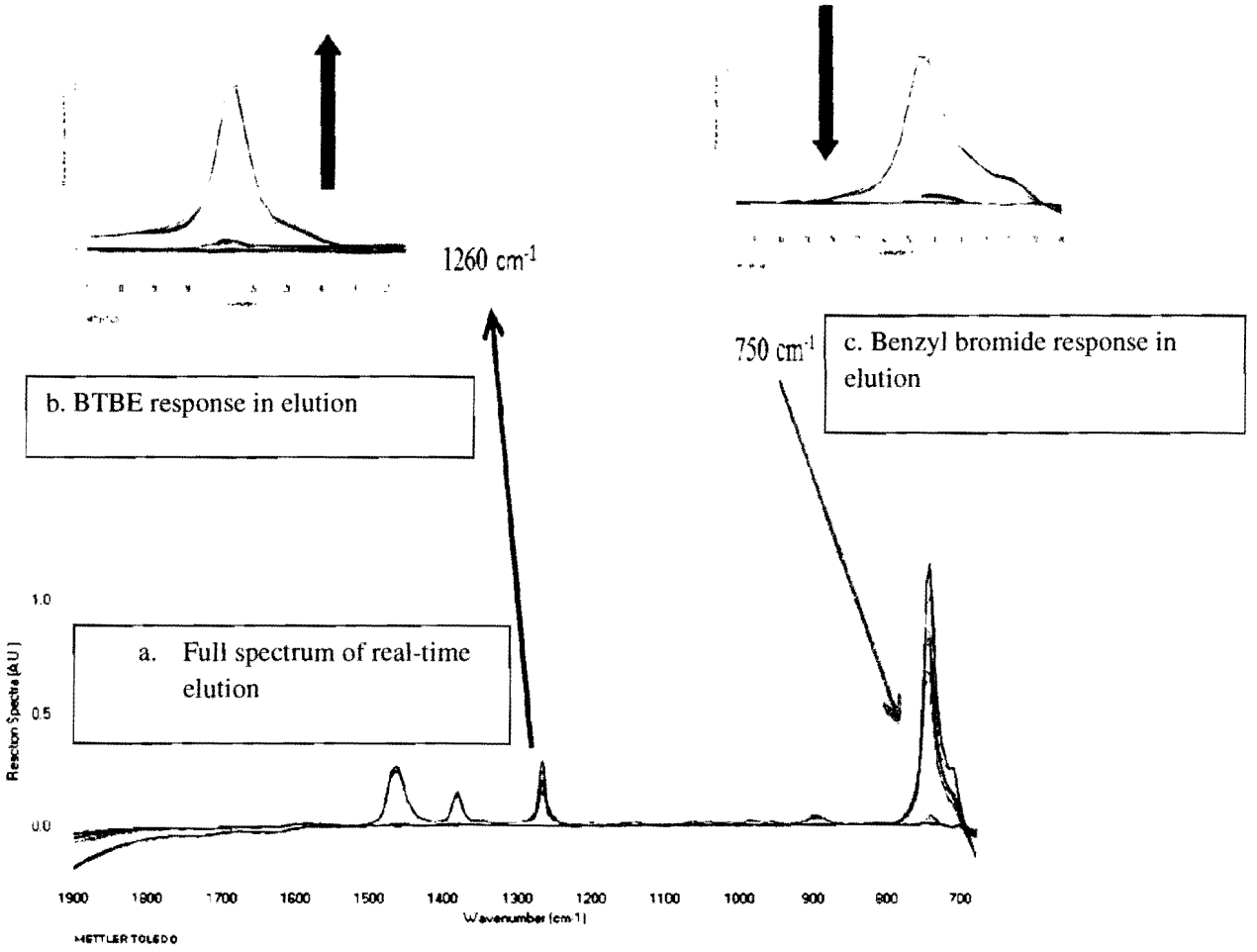

Figure 3-5. Real-time FlashIR separation of reaction mixture.

With an aim to compare the results obtained by the FlashIR, the manually collected fractions were analyzed by HPLC with an aim to confirm that IR is an alternative detection method for flash chromatography.

Fraction 1 (Figure 3-6) provides the solvent system (hexane:dichloromethane 80:20) peak response in IR and HPLC. The solvent system chosen did not interfere in the region where the reactant and product are expected to be analyzed in IR. The peak at 4.1 minutes in HPLC analysis is due to impurity in solvents and did not interfere the reactant and product retention time.

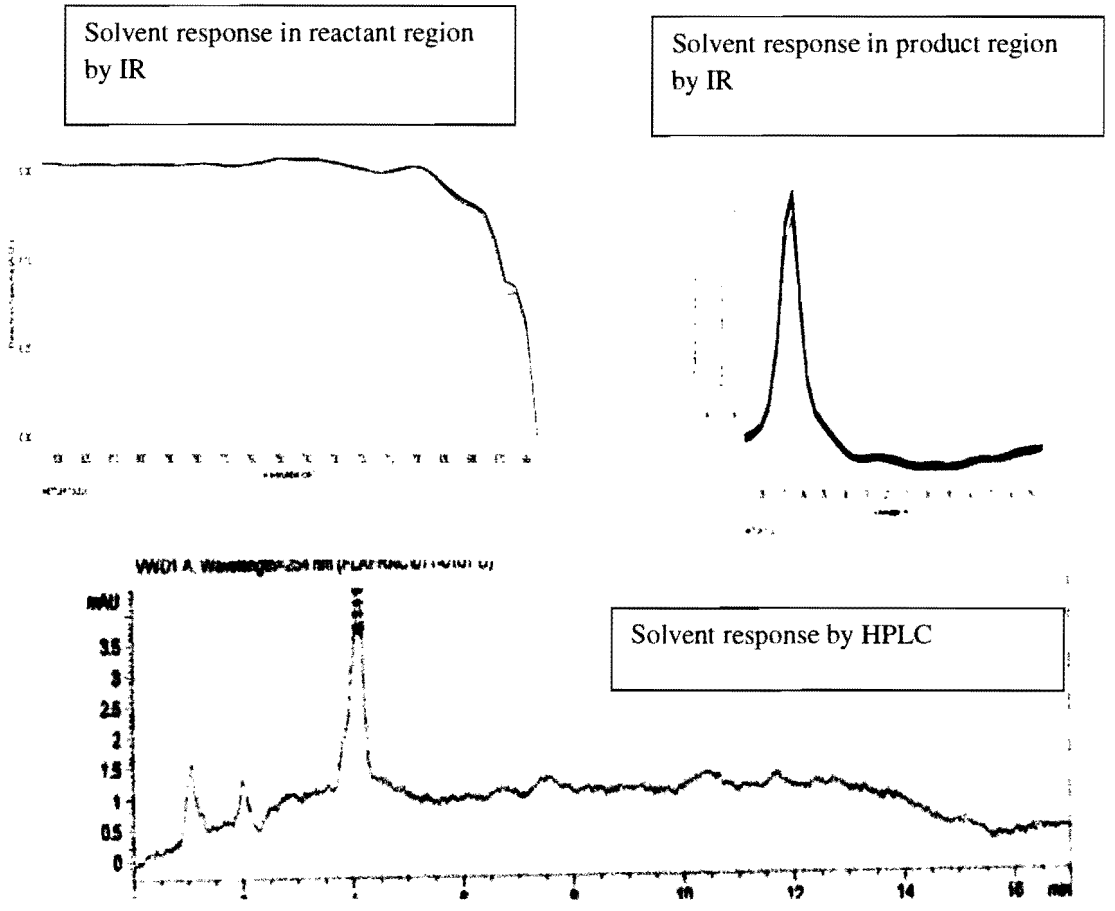

Figure 3-6. Comparison of Fraction1 FlashIR data with the HPLC data.

Based on the TLC analysis of the reaction mixture it was expected that the elution of unreacted benzyl bromide from the reaction mixture is expected in the initial few fractions and the product benzyl tert-butyl ether is expected in the later fractions. The analysis of the fractions by developed HPLC method showed the retention times of benzyl bromide and benzyl tert-butyl ether as 8.5 and 12.5 minutes, respectively.

The high peak response of benzyl bromide at 750 cm^{-1} region was shown in fraction 4 and 5 then started diminishing in the later fraction as shown in Figure 3-7. There was no peak response was observed for product at 1210 cm^{-1} which indicates that the fraction 4 and 5 is pure unreacted benzyl bromide and the elution of benzyl tert-butyl ether did not start.

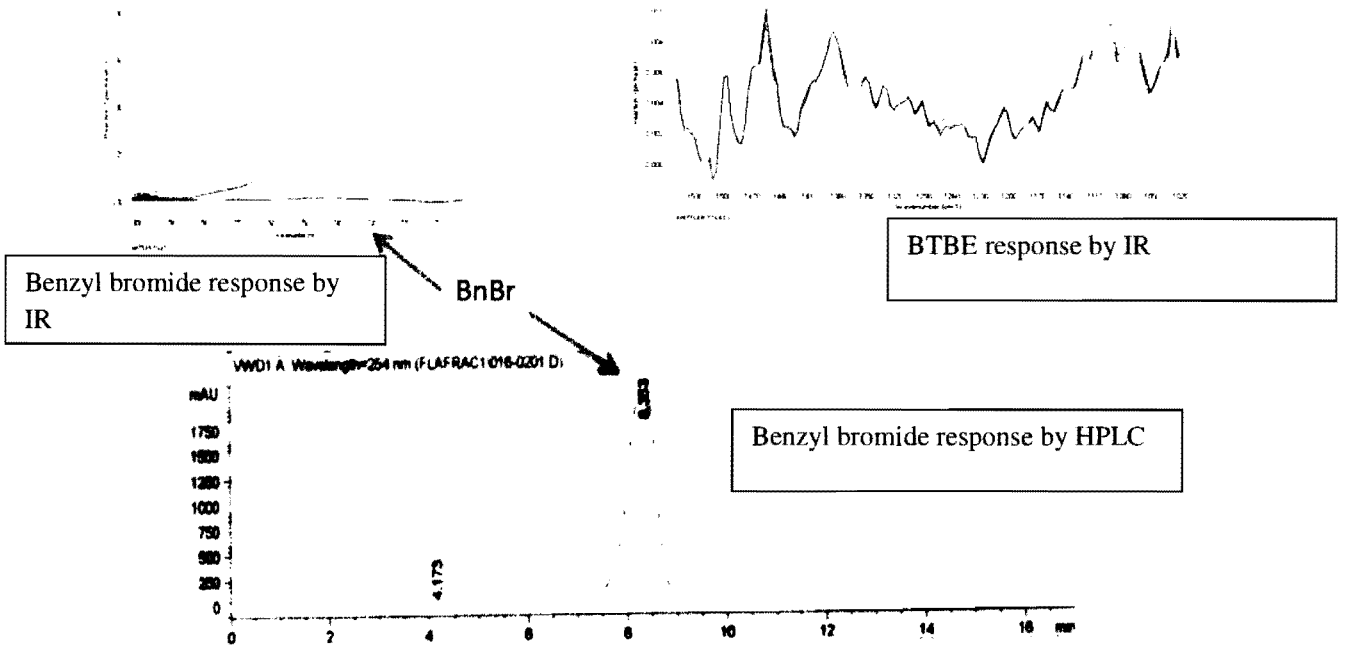

Figure 3-7. The analysis of the fourth fraction of the reaction mixture.

Fractions 6 to 8 show the combination of benzyl bromide and benzyl tert-butyl ether (Figure 3-8) which indicates that the elution of BTBE starts increasing as benzyl bromide elution starts diminishing. The peak response from reactant and the product was observed by

FlashIR as well as by HPLC analysis is comparable. The fractions 6 to 8 were not the correct fractions in isolating the pure product because the fractions are mixed with starting material.

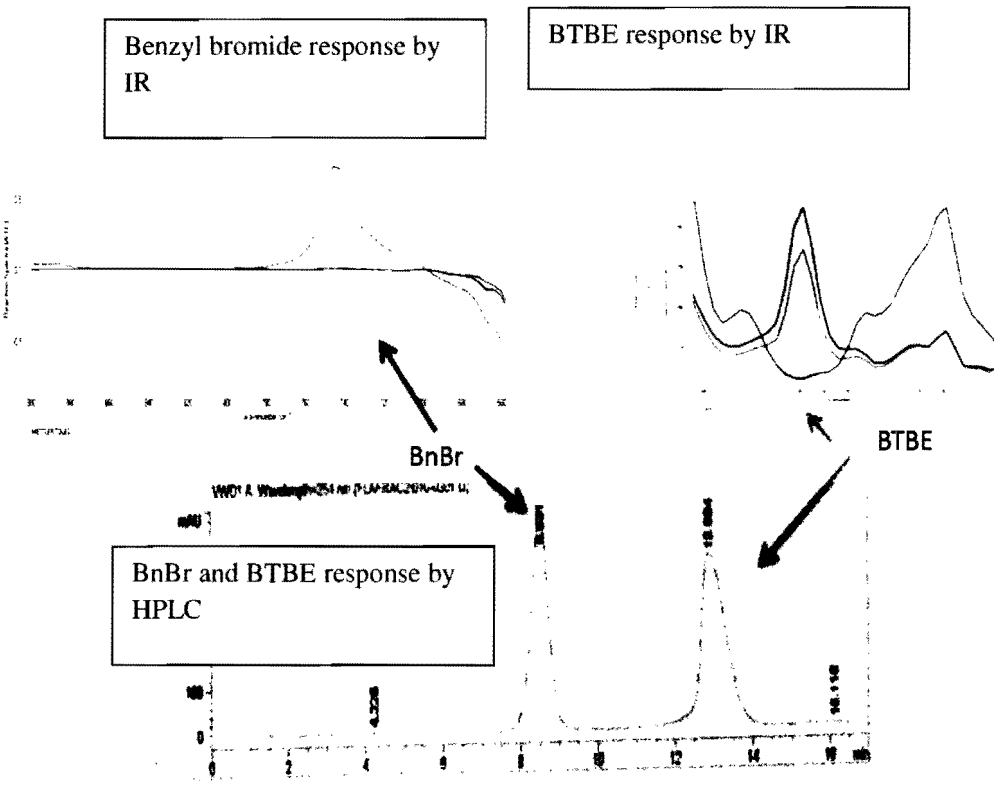

Figure 3-8. The analysis of the seventh fraction of the reaction mixture.

Fractions 9 to 14 the peak response of the product at 1210 cm^{-1} region for benzyl *tert*-butyl ether was high in the beginning and started diminishing in later fractions and at the same time there was no peak response was observed for the benzyl bromide at 750 cm^{-1} region indicates that the fractions 9 to 14 are the correct fraction for isolating the pure product. The HPLC analysis also showed the same response that was observed in FlashIR. The benzyl *tert*-butyl ether was the only peak at 12.5 minutes retention time was observed and the benzyl bromide peak was not observed at retention time at 8.5 minutes (Figure 3-9).

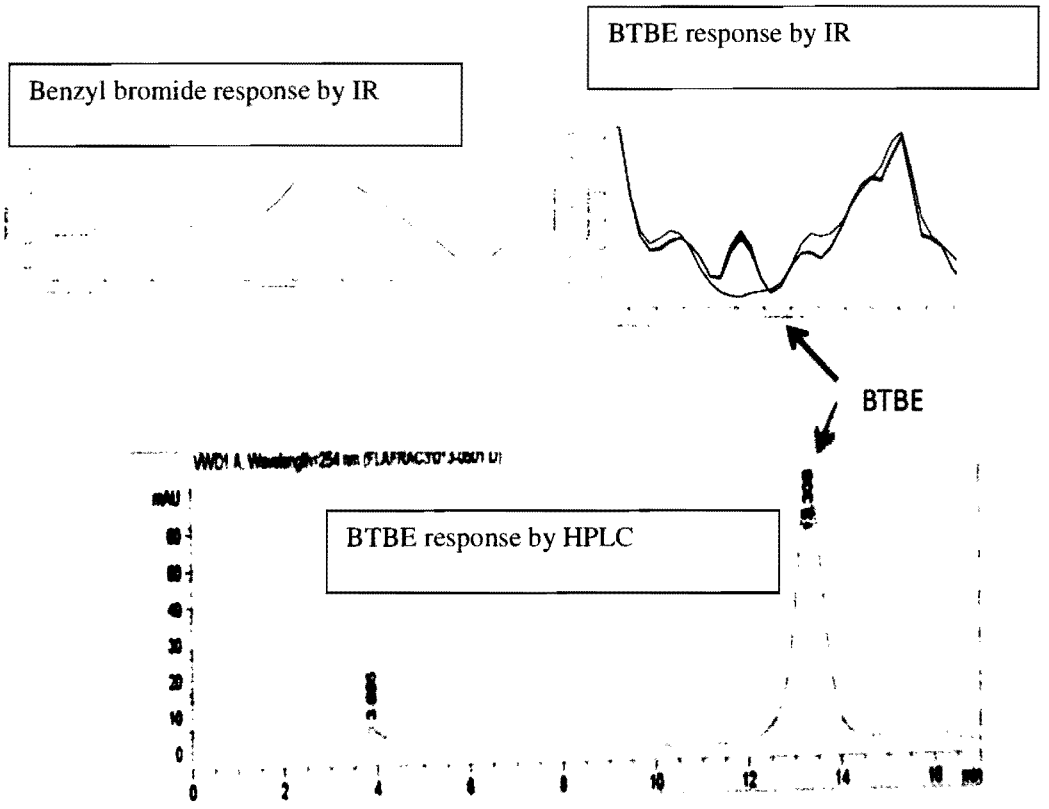

Figure 3-9. The analysis of the final fraction of the reaction mixture.

The comparison of FlashIR separation of Williamson ether reaction mixture with HPLC analysis is graphically represented in Figure 3-10 and is based on the raw data tabulated in Table 8-2 and 8-3. The data clearly indicate that the FlashIR real-time analysis and off-line HPLC analyses are comparable, therefore, validating the FlashIR method.

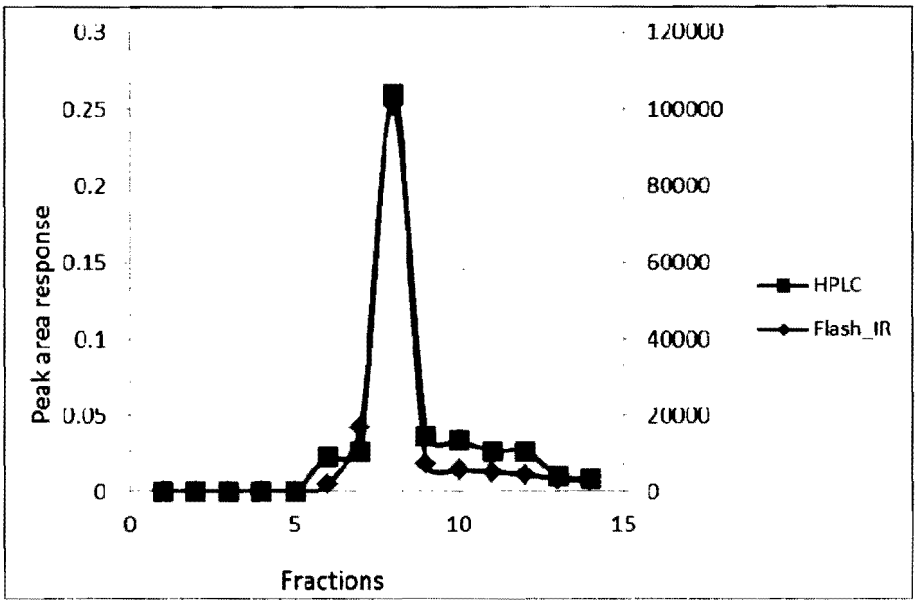

Figure 3-10. Graphical representation of comparison of Flash IR and HPLC analysis

The analysis of the fractions in the traditional way using TLC technique was also carried out for comparison. The TLC analysis of the collected fractions showed the presence of starting material and the product as shown in the Figure 3-11. Fractions 1 to 3 did not show any spots indicating that there is no reactant and product. The clearly identified spots as matched with the R_f values in comparing with the TLC analysis of the reaction mixture shown in fractions 4 to 8 indicates the presence of the benzyl bromide as reactant an as observed in the real-time FlashIR analysis. Fractions from 9 to 14 show only one spot which matches with benzyl *tert*-butyl ether and these were combined and the solvents were removed using a rotary evaporator.

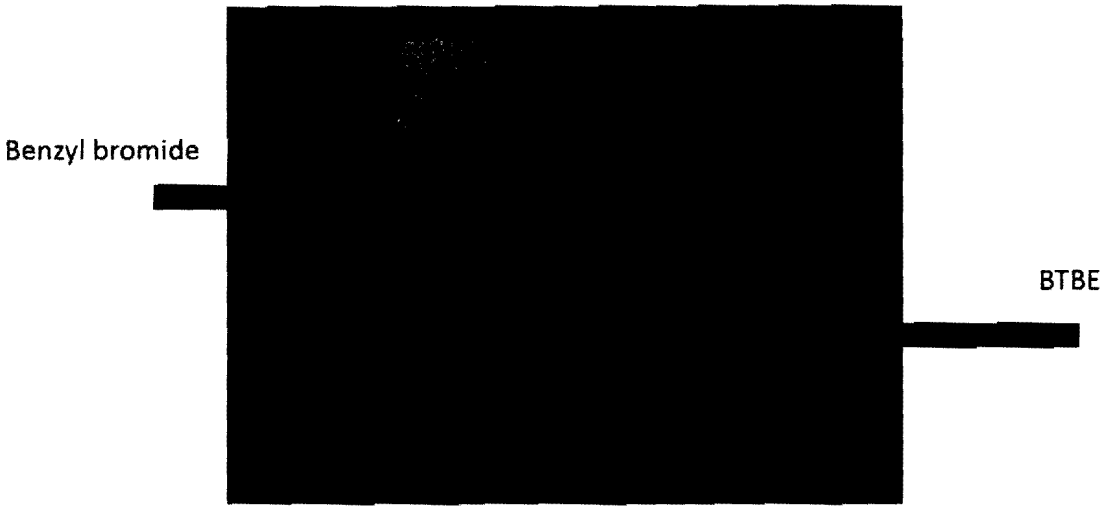

Figure 3-7. The TLC of the collected fractions.

The isolated yield for the pure product was 0.65 g (65%) and the product was further confirmed by ^{1}H NMR as shown in Figure 3-12. The singlet at 1.3 ppm was assigned to the three methyl groups present in the *t*-butyl group. The singlet at 4.5 ppm is due to the presence of two protons of the benzylic carbon attached to the aromatic ring and oxygen atom. The multiplet ranging from 7.2 to 7.4 was assigned to the aromatic protons. A small amount of residual dichloromethane is detected in the ^{1}H NMR spectrum which is from the solvent combination used for separation; however, the NMR clearly indicates a very pure product free from benzyl bromide starting material.

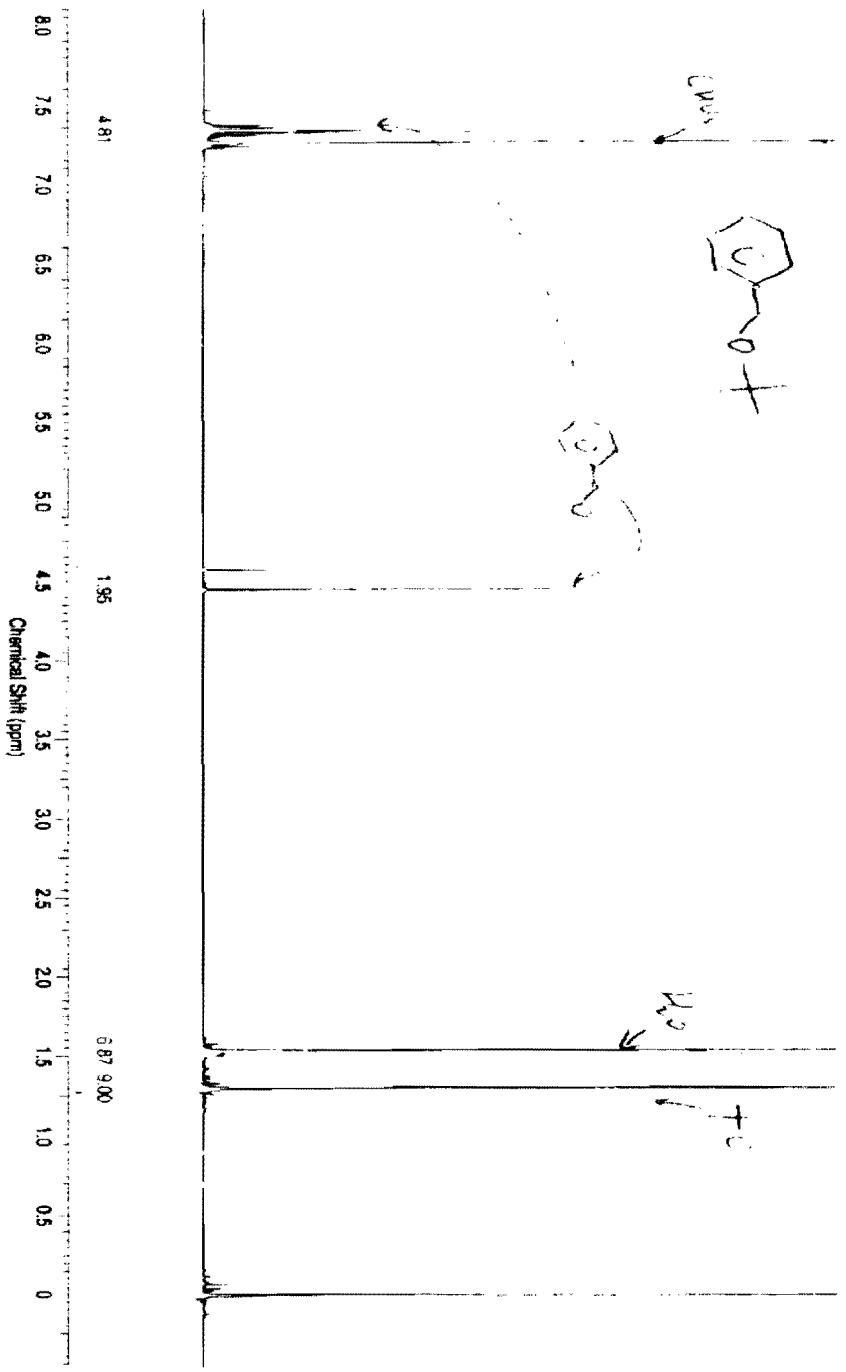

Figure 3-12. The ^{1}H NMR spectrum of benzyl tert-butyl ether.

3.2. Reaction monitoring and separation of conversion of cholesterol to cholesteryl acetate (acetylation)

In our next endeavor, the synthesis of cholesteryl acetate was performed in Mettler-Toledo EasyMax^{TM} instrument with FT-IR monitoring using a ReactIR iC10 instrument. The progress of the reaction was monitored in real-time as the characteristic changes of the vibrational spectra of the starting material and product obtained discussed below.

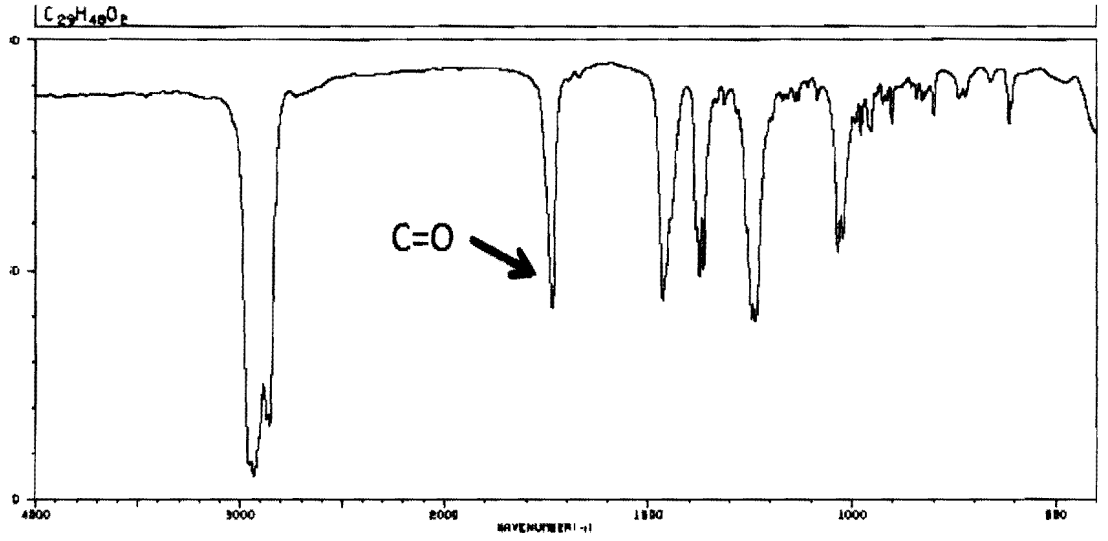

Figure 3-13. The IR spectrum of cholesteryl acetate obtained from SDBS database.[71]

The peak at 1735 cm^{-1} was due to the stretching vibration of the carbon–oxygen bond of carbonyl group of the cholesteryl acetate as shown in the IR spectrum in Figure 3-13 which was obtained from SDBS. The peak response in that region was considered for monitoring for the product.

Alternately the peak at 1850 cm^{-1} was assigned to the carbon-oxygen bond as one of the pair of anhydride peaks for acetic anhydride as shown in the IR spectrum in Figure 3-14. The peak response at this region was considered for the reagent responsible for acetylation. As the reagent is consumed over time during the reaction a decrease in the peak response is observed as discussed below.

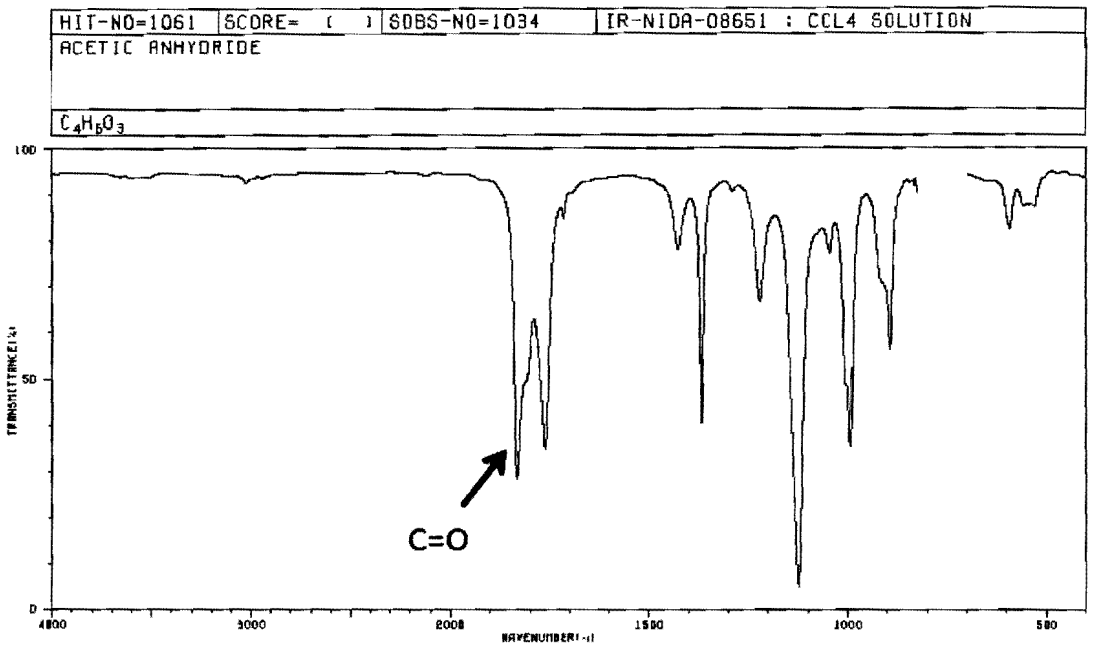

Figure 3-14. The IR spectrum of acetic anhydride obtained from SDBS database.[71]

A comparison of the IR peak response was carried out between the carbonyl group of acetic anhydride and cholesterol acetate. The results indicated that the increase in the peak response at wavenumber 1735 cm^{-1} while a gradual decrease in the peak response at wavenumber 1850 cm^{-1} for carbonyl group due to consumption of acetic anhydride. The formation of the product clearly indicated increasing peak response as the IR absorption by carbonyl group at 1735 cm^{-1}(Figure 3-15).The peak response due to C-O stretching common for cholesterol and the cholesteryl acetate was also visualized in the same figure.

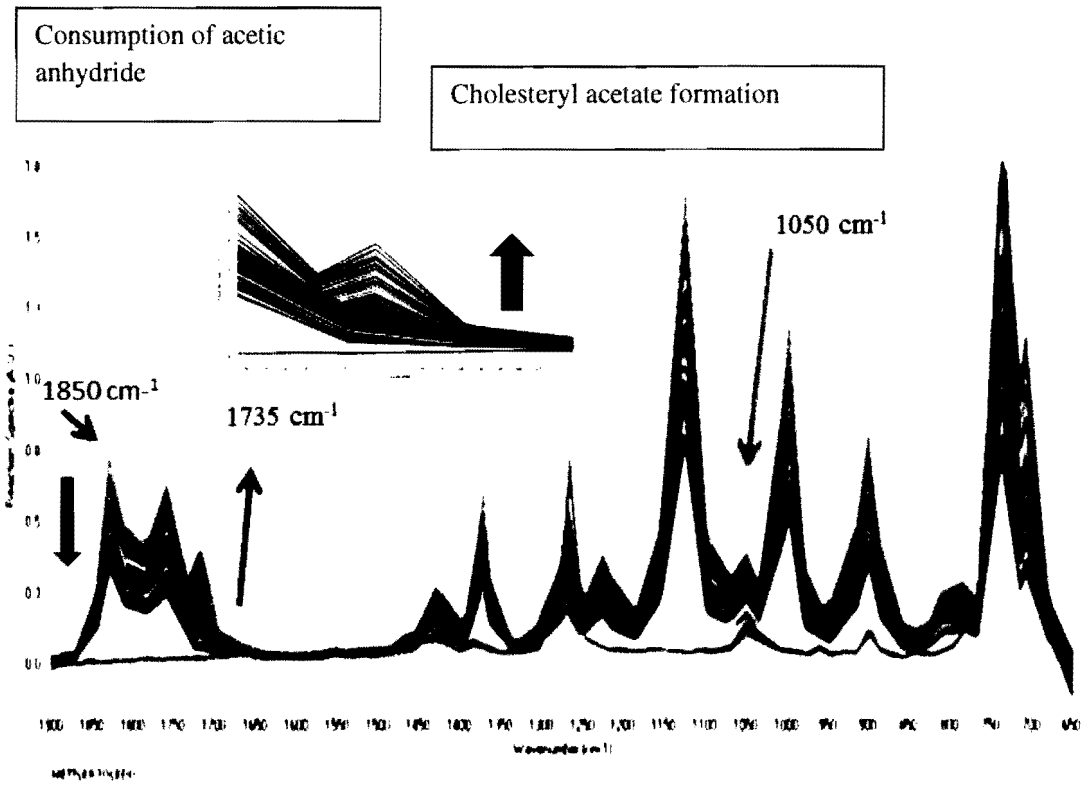

Figure 3-15. The reaction monitoring spectra for the conversion of cholesterol to cholesteryl acetate.

The solvent system for optimal separation as well as identification of completion of reaction was identified as hexane and dichloromethane in the ratio of 80:20. The solvents were chosen to avoid any strong IR absorbing properties that might interfere with sample analysis. The R_f values of cholesterol and cholesteryl acetate are 0.21 and 0.77, respectively and appear as clearly distinct spots shown in Figure 3-16. The cholesterol spot was also observed in the reaction mixture indicates that the unreacted cholesterol is present in the reaction mixture.

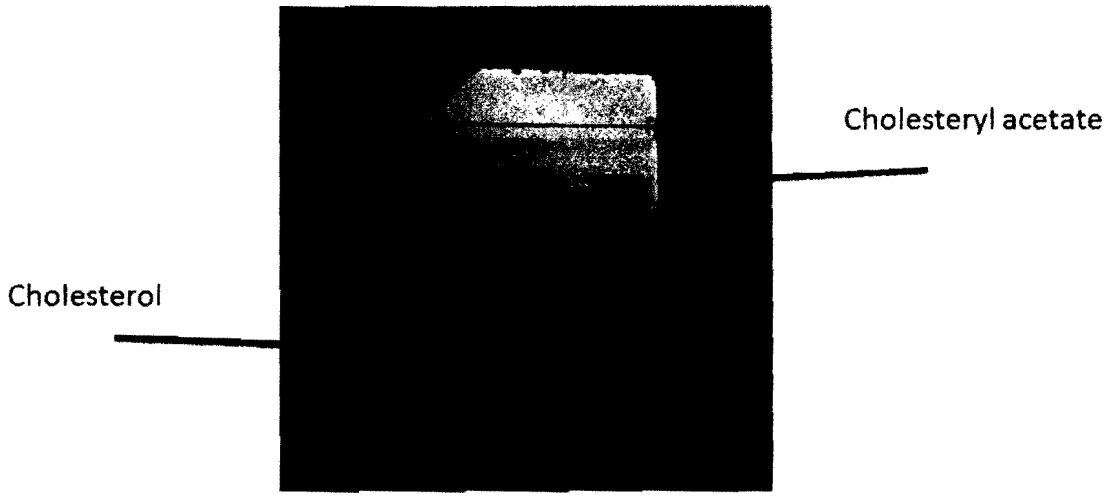

Figure 3-16. The TLC separation of the reaction mixture.

The change in concentration of the cholesteryl acetate as product and acetic anhydride as acetylating reagent over time was monitored and the result was obtained in the graphical form (Figure 3-17). The percentage change in peak area response collected at 1735 cm^{-1} for cholesteryl acetate as product and at 1850 cm^{-1} for acetic anhydride as acetylation reagent over time is used for illustration. The reaction profile of acetic anhydride is plotted in red which shows that the consumption of the reagent for the conversion of reactant to product which became stagnant after 12 h. Similarly, the formation of the cholesterol acetate increased gradually from the initial time of the reaction and completed after 12 h. It also indicates that the presence of residual acetic anhydride.

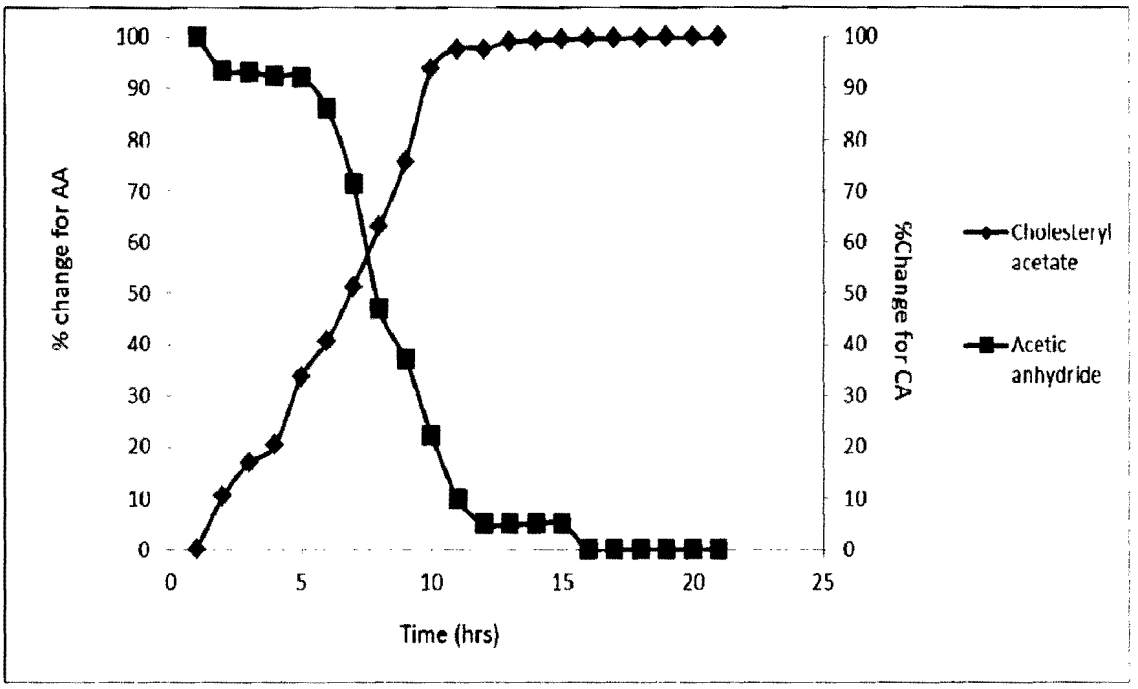

Figure 3-17. Reaction monitoring of the conversion of cholesterol to cholesteryl acetate.

The reaction mixture was purified by FlashIR and the full spectrum of the real-time separation is shown in the Figure 3-18. The peak response at wavenumber 1735 cm^{-1} was monitored for cholesteryl acetate. The fractions from 1 to 7 did not show any peak response related to the product indicating that there is no product elution. The peak response from the product started appearing from fraction 8 and the highest peak response was observed at fraction 11 and started diminishing in the later fractions. The unreacted cholesterol was not observed since it has poor elution by the solvent combination.

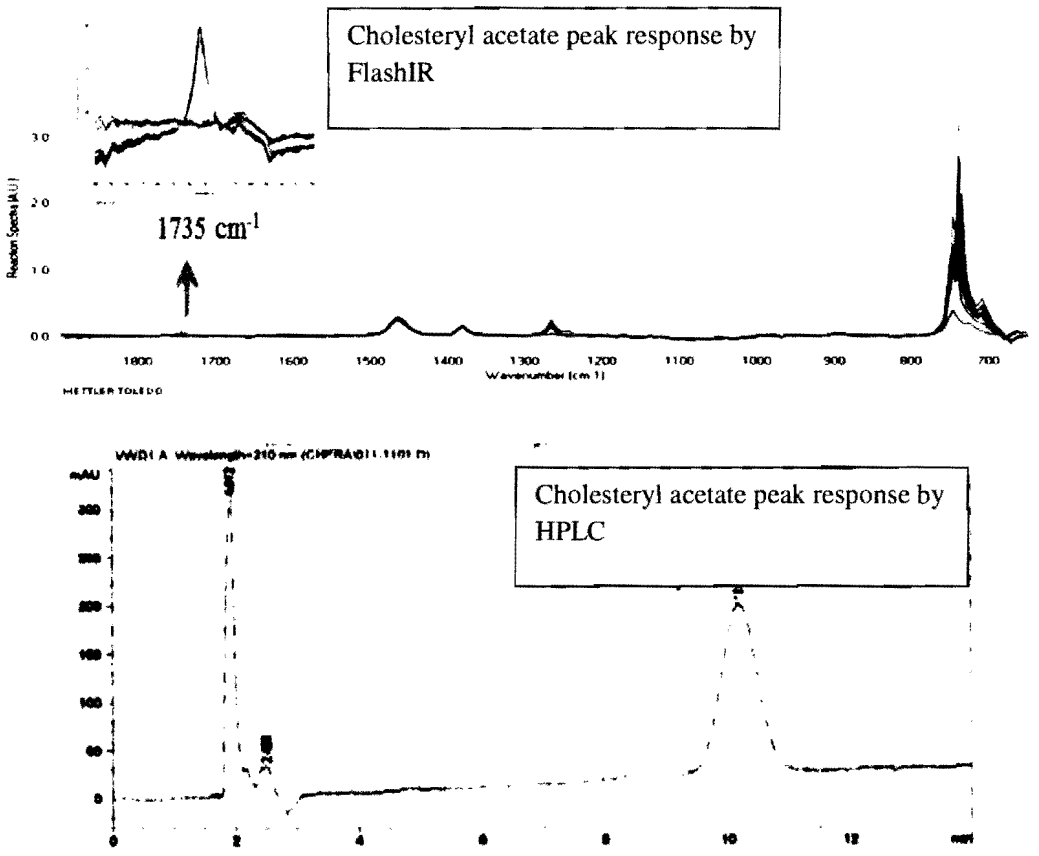

Figure 3-18. Flash-IR and HPLC analysis of comparison of fraction having cholesteryl acetate.

The collected fractions were analyzed by HPLC method. The peak area response of the product obtained from real-time on-line separation by FlashIR was compared with peak area response obtained from HPLC analysis. The graphical representation (Figure 3-19) shows both sets of experimental data nicely superimpose on each other. The blue curve corresponds to the data obtained from HPLC analysis while the red curve corresponds to the data obtained from FlashIR.

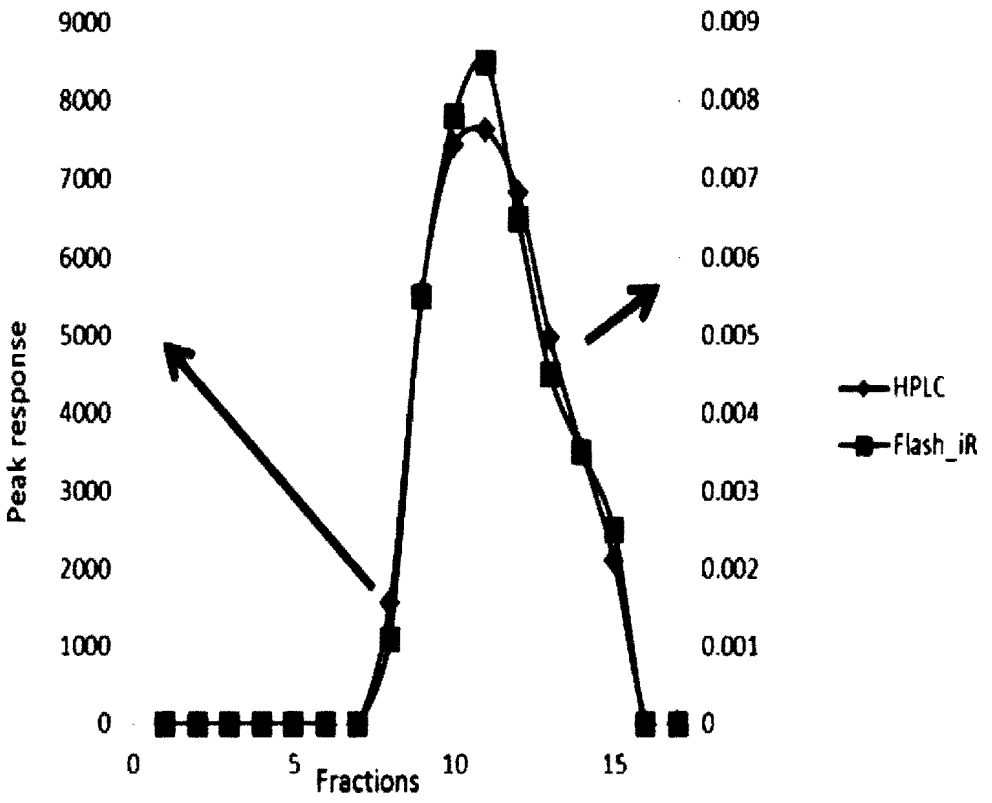

Figure 3-19. Comparison of the HPLC and Flash IR curve of cholesteryl acetate.

The fractions collected during the FlashIR separation were further analyzed by thin layer chromatography. There was no product observed from fractions 1 to 7. The product due to cholesteryl acetate with matching R_f value was compared with the TLC analysis of the reaction mixture from fractions 8 to 15 as shown in the Figure 3-20. The pure product was obtained by combining all the fractions from 8 to 15 and the solvents were removed using the rotary evaporator.

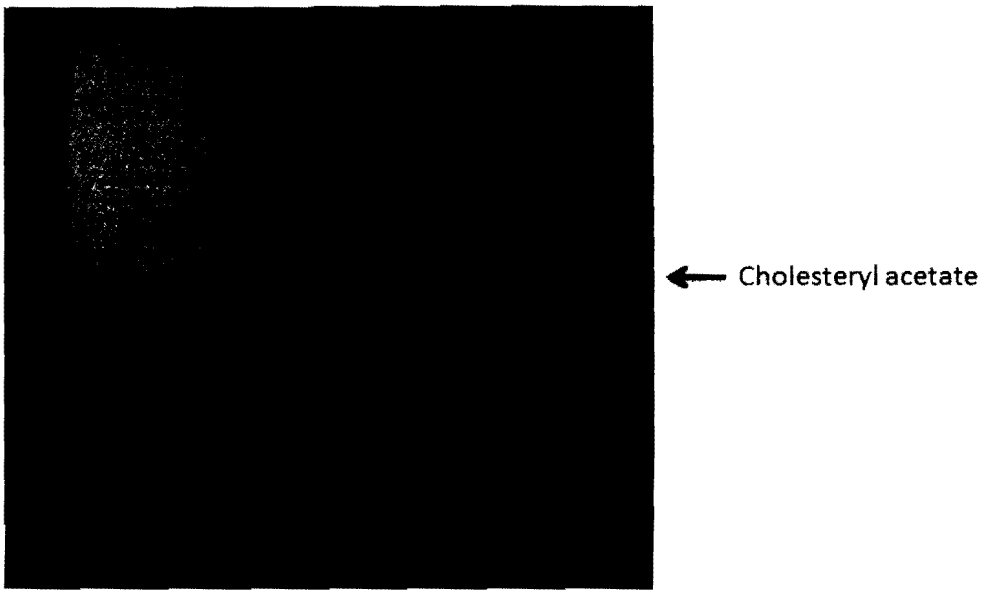

Figure 3-20. TLC of the collected fractions.

The isolated yield for the pure product was found to be 0.7 g (70%) from the combined fractions and the purity of the product finally confirmed by recording a ^{1}H NMR as shown in the Figure 3-21. The multiplets in the region of 0.8 ppm to 1.8 ppm are assigned to the protons present on the whole skeleton of the cholesterol molecule. The distinct singlet at 2.0 ppm is due to the acetate group ($COCH_3$) and another singlet at 4.5 ppm is due the proton present in carbon attached to the double bond. The purity was further confirmed by recording a ^{13}C NMR as shown in Figure 3-22. The additional carbon at signal at 28.6 ppm indicates that the acetylation reaction was successful. The signal at 170.6 ppm is due to carbon in the carbonyl/carboxyl region. The signal at 122.8 ppm indicates the presence vinyl carbon. The carbon attached with oxygen is identified by the signal at 74.2 ppm. The total number of the peaks matches with total number (29) of carbons.

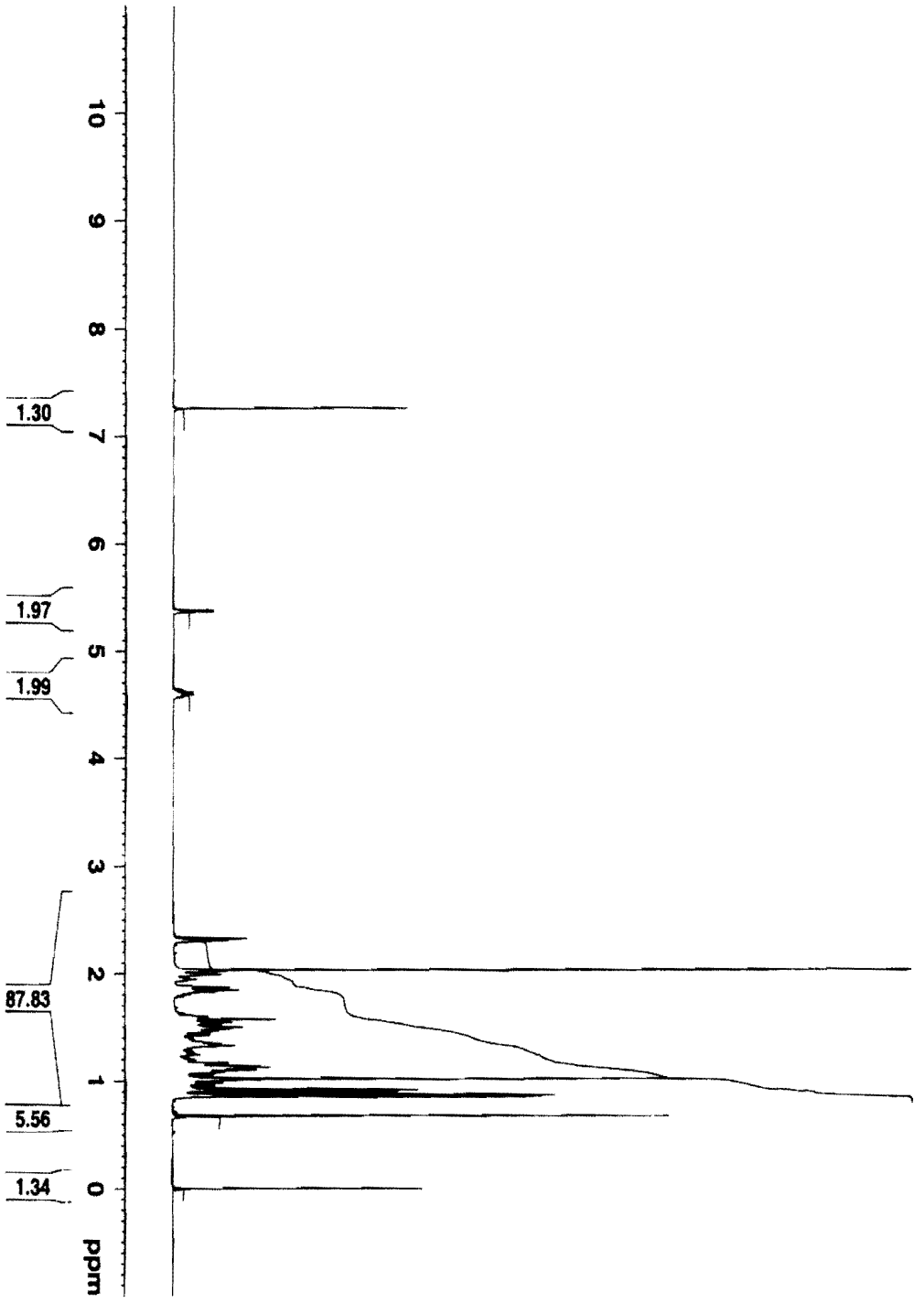

Figure 3-21.The ^{1}H NMR spectrum of cholesteryl acetate.

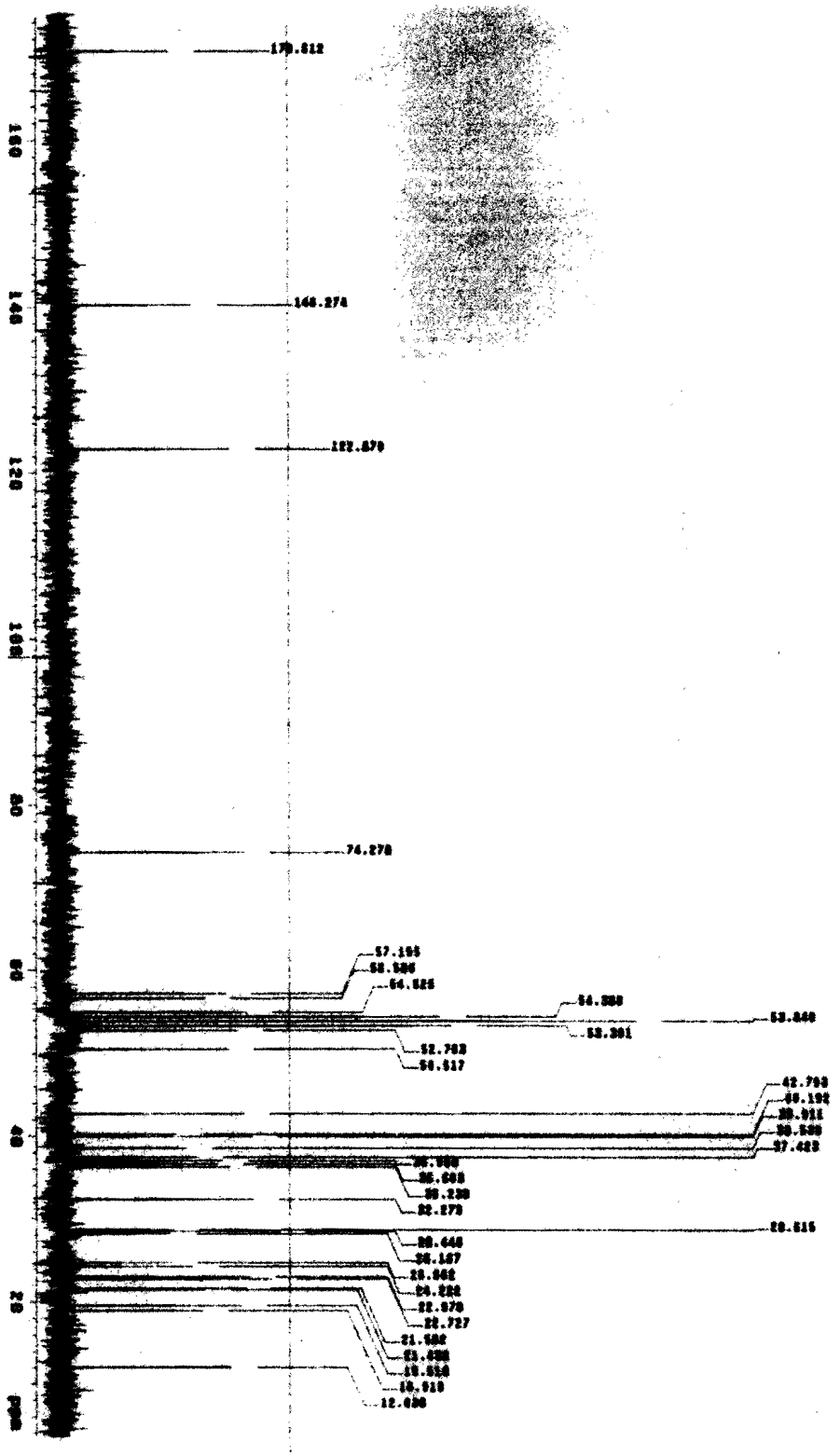

Figure 3-22. The ^{13}C NMR spectrum of cholesteryl acetate.

3.3. Reaction monitoring and separation of cyclohexen-1-ol into cyclohexanone (Isomerization)

Synthesis of cyclohexanone *via* an isomerization reaction was performed in a Mettler-Toledo EasyMax^{TM} instrument with FT-IR monitoring using a ReactIR iC10 instrument. The progress of the reaction was monitored in real-time for characteristic changes of the vibrational spectra of starting material and product was observed.

We carried out an isomerization reaction of cyclohexen-1-ol to cyclohexanone catalyzed by palladium/carbon catalyst in a batch process and monitored the reaction *in situ* by ReactIR as described in the experimental section.

The IR absorption peak observed at 1665 cm^{-1} is due to carbon–carbon double bond in cyclohexen-1-ol. At 1712 cm^{-1} due to the stretching frequency of the carbonyl group in cyclohexanone as observed in the IR spectrum obtained from SDBS (Figure 3-23).[76]

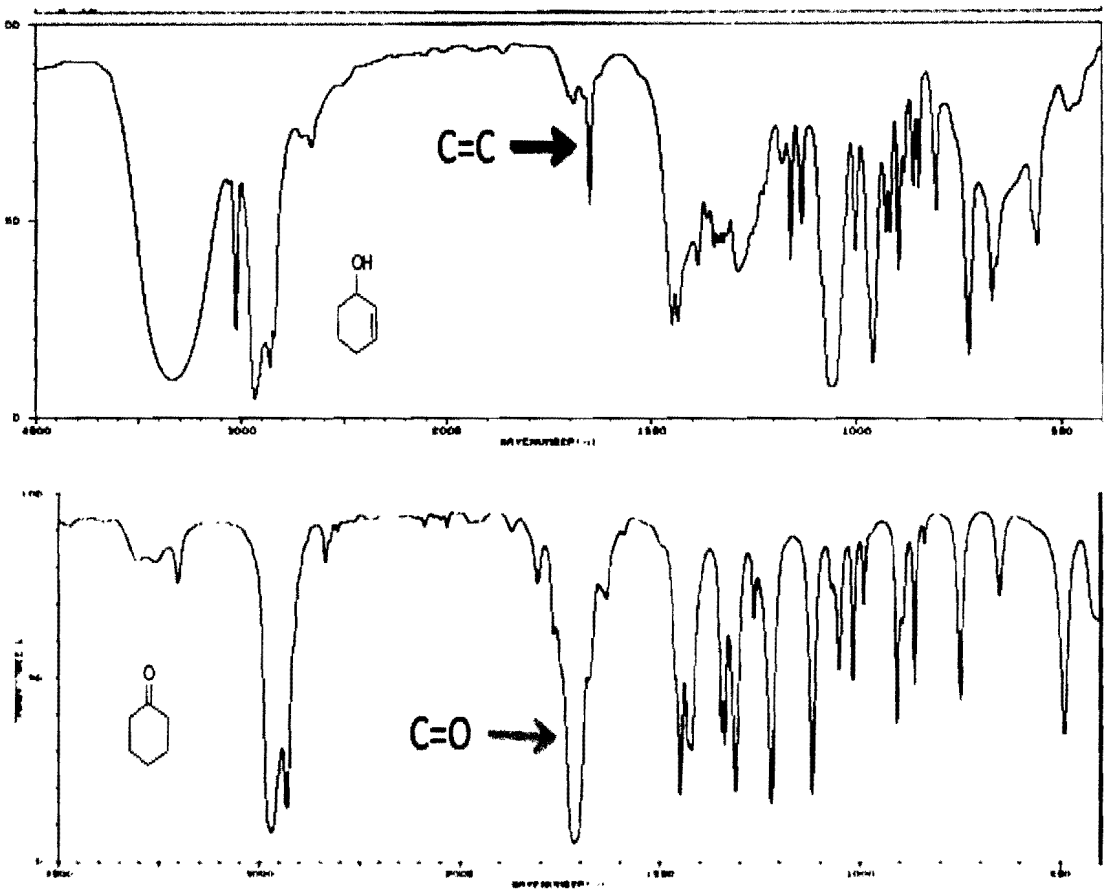

Figure 3-23. The IR spectra of cyclohexen-1-ol and cyclohexanone obtained from SDBS database.[71]

The reaction was monitored by ReactIR which reveals an increase in the peak response at wavenumber 1712 cm^{-1} indicating the formation of the product. Similarly, the peak response at wavenumber 1665 cm^{-1} is observed to decrease due to the decline in the concentration of the reactant with time (Figure 3-24).

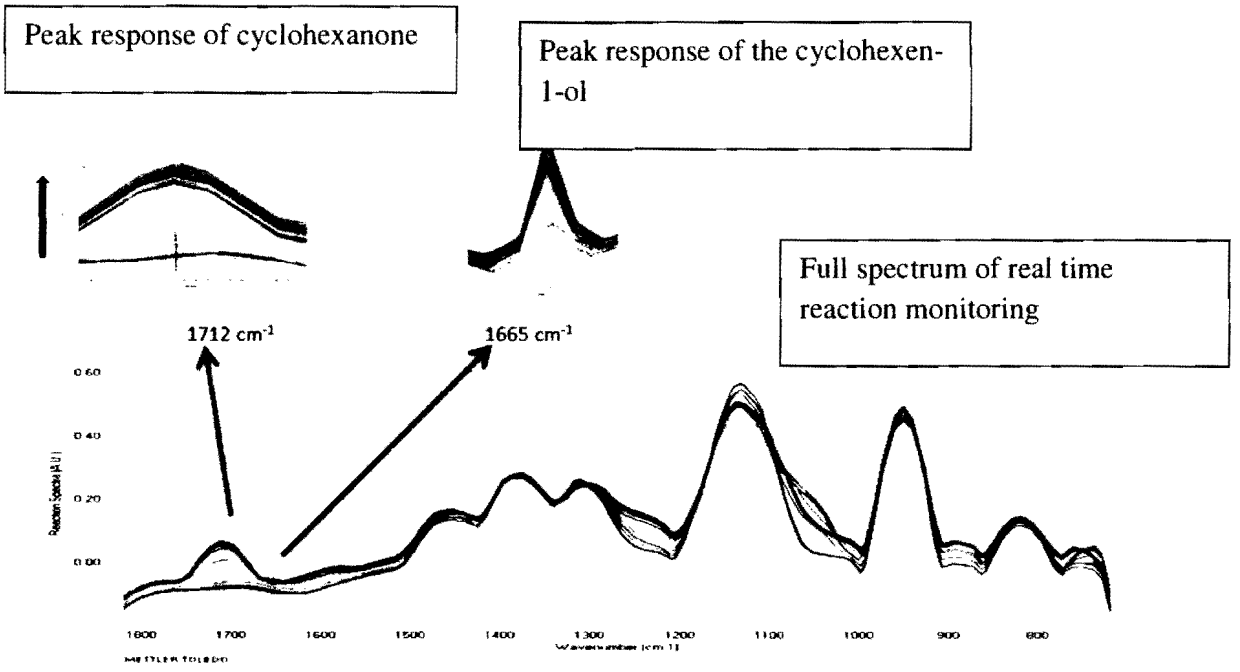

Figure 3-24. The reaction monitoring spectra for the conversion of cyclohexen-1-ol and cyclohexanone.

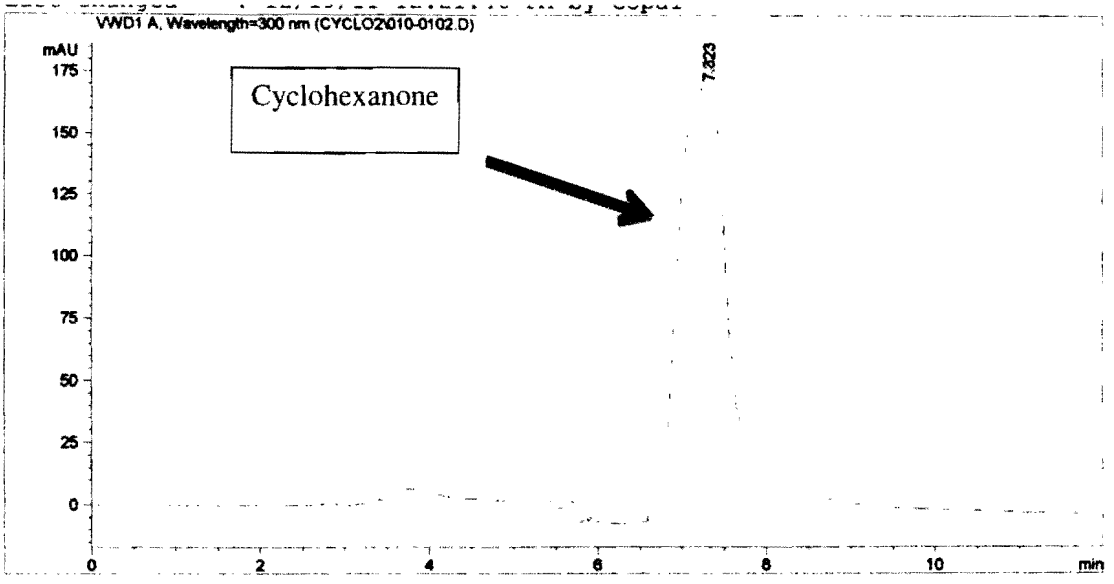

Figure 3-25. The reaction mixture analysis for completion of reaction by HPLC.

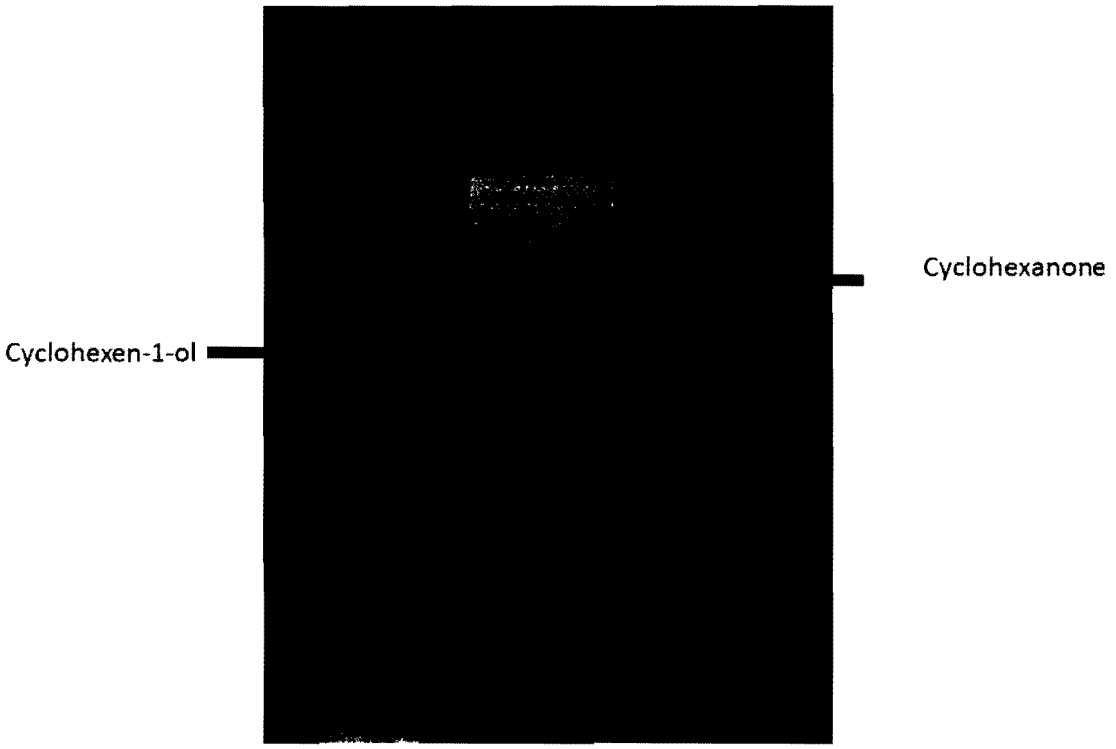

Figure 3-26. The TLC separation of the reaction mixture.

The solvent system for optimal separation and TLC monitoring the completion of reaction is ethyl acetate and hexane in the ratio of 90:10. The R_f values of cyclohexene-1-ol and cyclohexanone are 0.62 and 0.82, respectively, and clearly distinct spots are shown in Figure 3-26. At the end of the reaction there is only one spot and cyclohexene-1-ol spot is not seen which indicates that the reaction has completed. The HPLC analysis of the reaction mixture (Figure 3-25) shows only the cyclohexanone peak which further supports the observation that the reaction is complete.

The graphical representation of the reaction is obtained by plotting the concentration of the reactant and product *vs.* time as shown in Figure 3-27. The percentage change in peak response collected at 1665 cm^{-1} for cyclohexene-ol and at 1712 cm^{-1} for cyclohexanone is the basis for the graph. The red curve indicates the reaction profile of cyclohexene-1-ol, the concentration of which decreases with time. The complete conversion of the substrate takes

place after 3 h. Similarly the blue line indicates the formation of cyclohexanone and complete formation of the products are also obtained after 3 h.

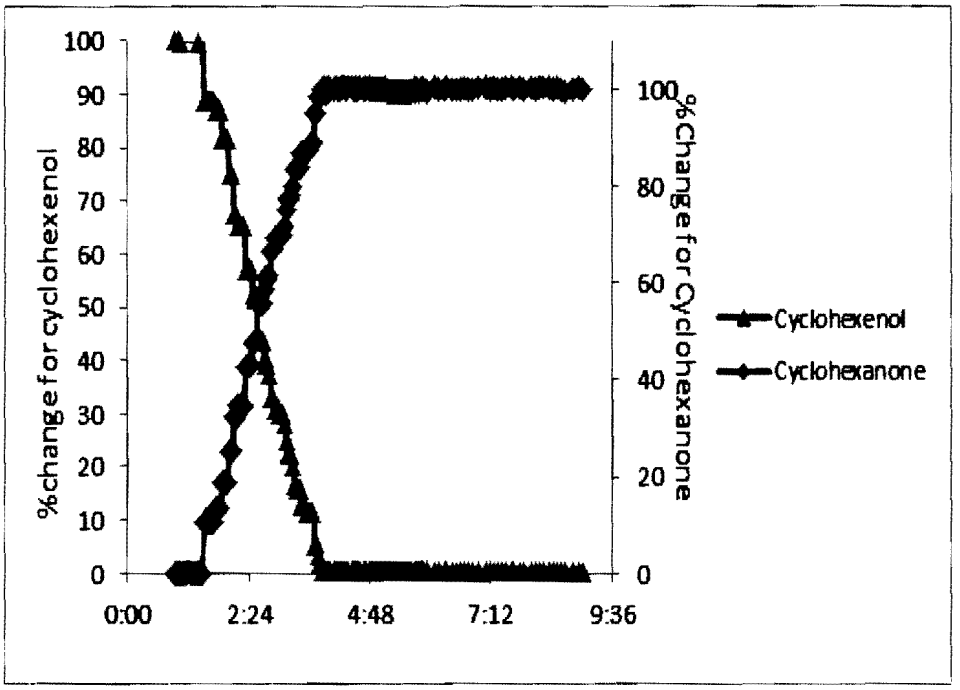

Figure 3-27. Reaction monitoring of the conversion of cyclohexene-1-ol to cyclohexanone.

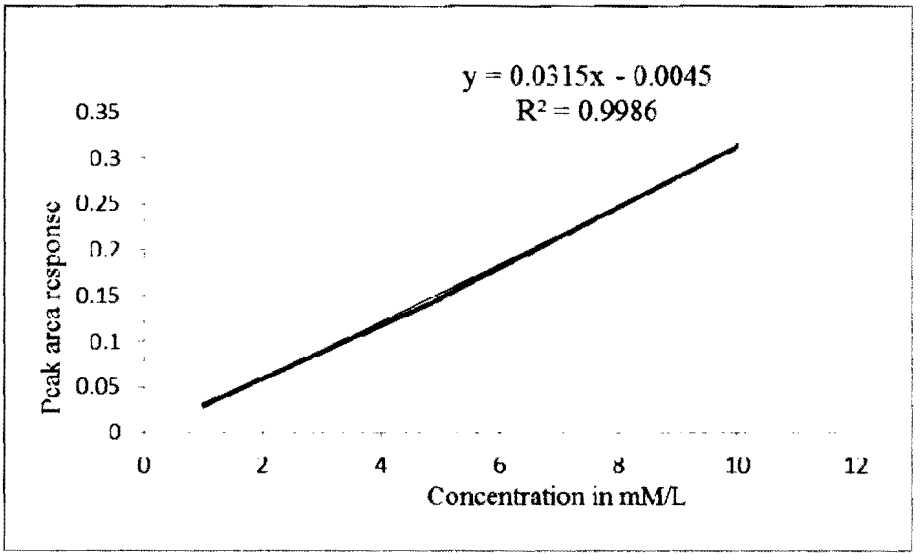

Figure 3-28. Calibration curve for cyclohexanone.

A three point calibration curve was constructed using 10, 50, and 100% of 10 millimolar concentration of the cyclohexanone as shown in Figure 3-28. By keeping the calibration curve as the background, the rate of the reaction was calculated by interpreting the concentration from the peak area of the cyclohexanone during the course of the reaction. The natural logarithm of the concentration of cyclohexanone *vs.* time was plotted. However, clearly, this is not a first order reaction as the plot is non-linear. Kinetic analysis is beyond the scope of this project; however, taking the slope gives a very rough estimate of the rate of the reaction as shown in the Figure 3-29. The initiation of the reaction is about to 30 minutes. The rate of formation of cyclohexanone was observed faster in regime_1 and slower when reaches to regime_2. In regime_3 the completion of the reaction is observed. It is estimated the rate of formation of cyclohexanone is approximately 1.2 mM/L per hour.

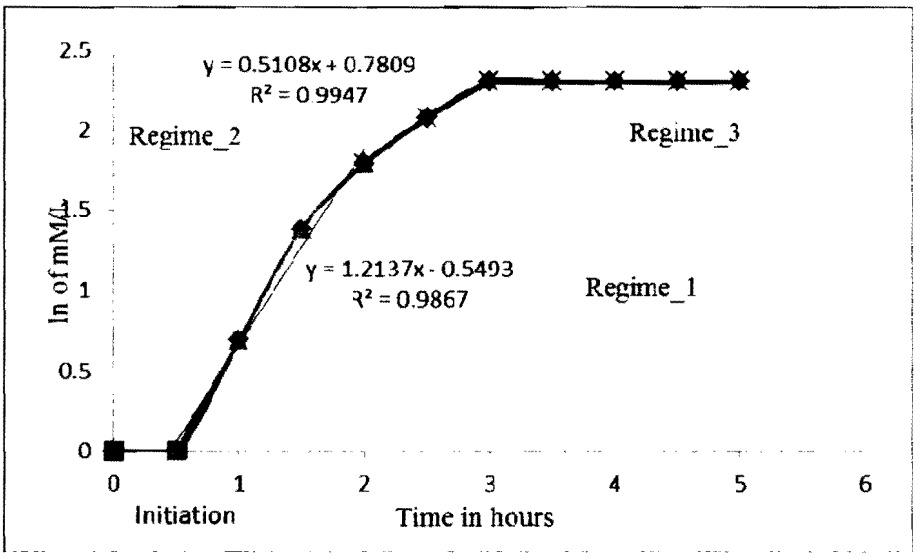

Figure 3-29. Rate of reaction for cyclohexanone.

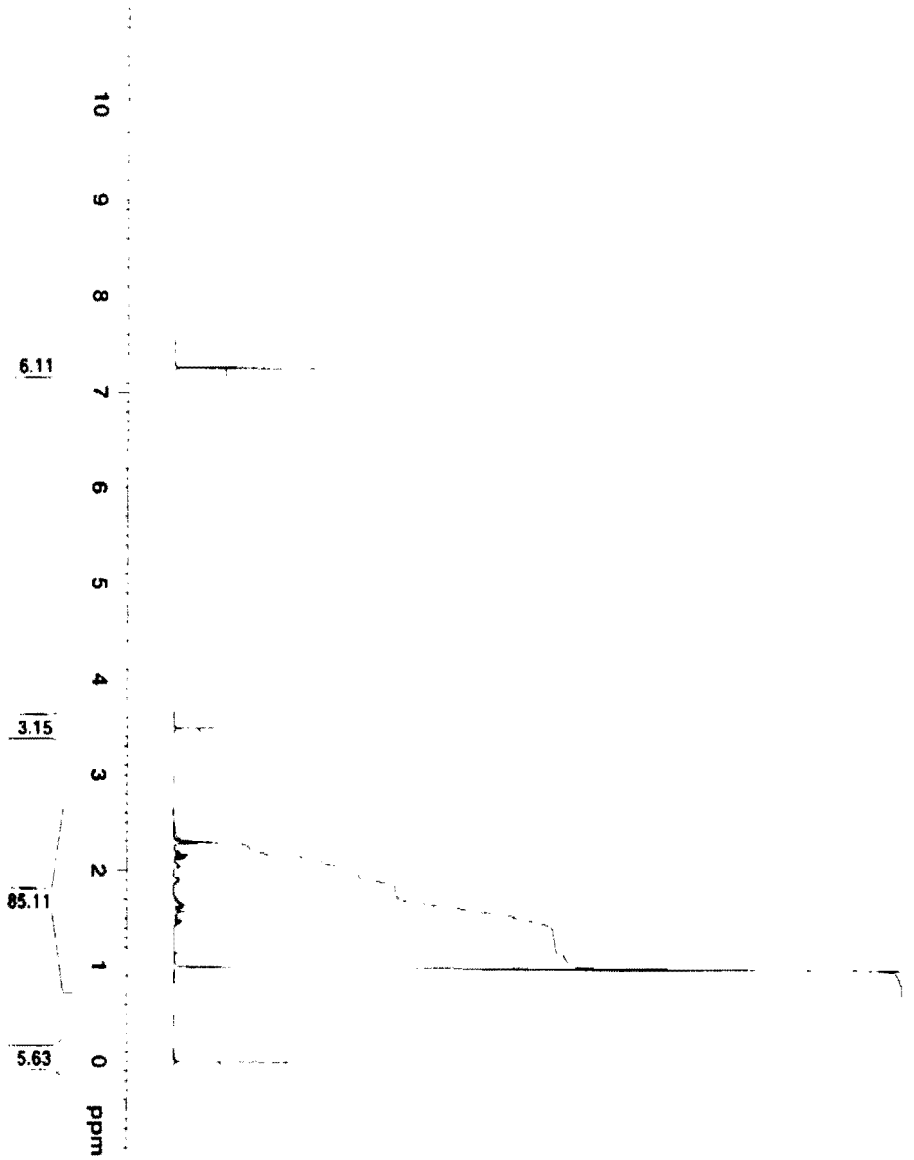

Figure 3-30. The ^{1}H NMR spectrum of crude cyclohexanone.

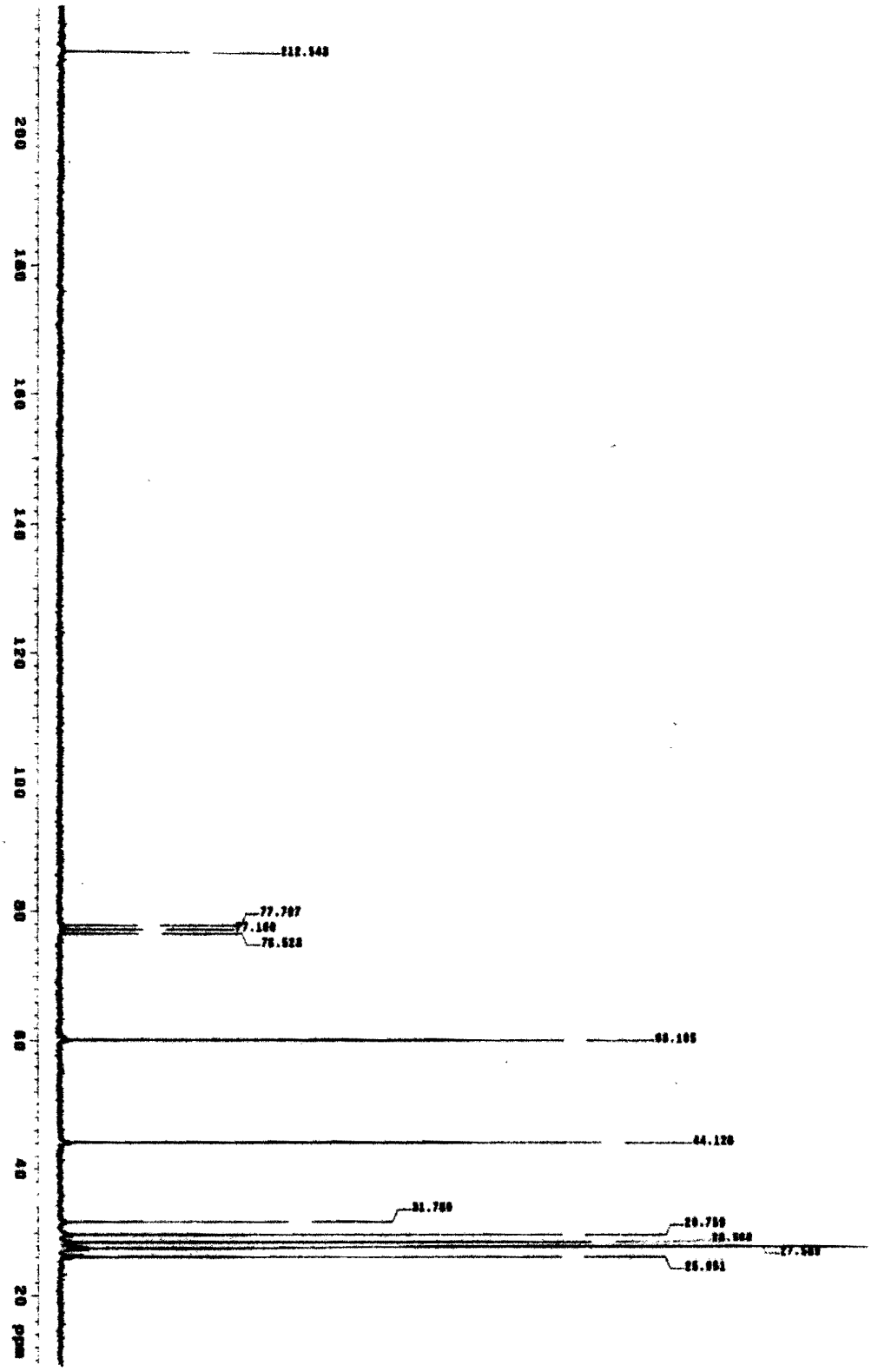

Figure 3-31. The ^{13}C NMR spectrum of crude cyclohexanone.

The crude cyclohexanone was analyzed by ^{1}H NMR and ^{13}C NMR to verify the complete conversion. The peak at 1 ppm by ^{1}H NMR proton from impurity and the peak at 27.8 ppm by ^{13}C NMR is due to carbon from unknown impurity were identified.

FlashIR analysis is used on purification of the crude reaction mixture. Since the isomerization reaction goes fully to completion, the cyclohexene-1-ol reactant is not seen during the separation. Fractions 3 and 4 show the presence of cyclohexanone as illustrated in Figure 3-30. The analysis of the fractions collected during FlashIR were further supported by off-line HPLC analysis (Figure 3-31).

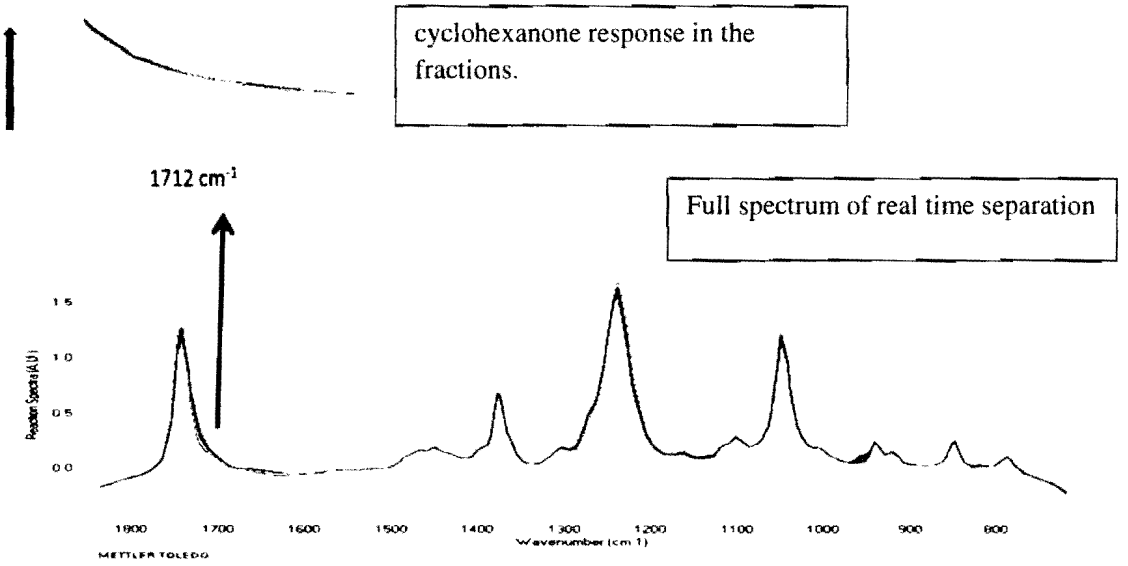

Figure 3-32. The full spectrum of real-time flash separation.

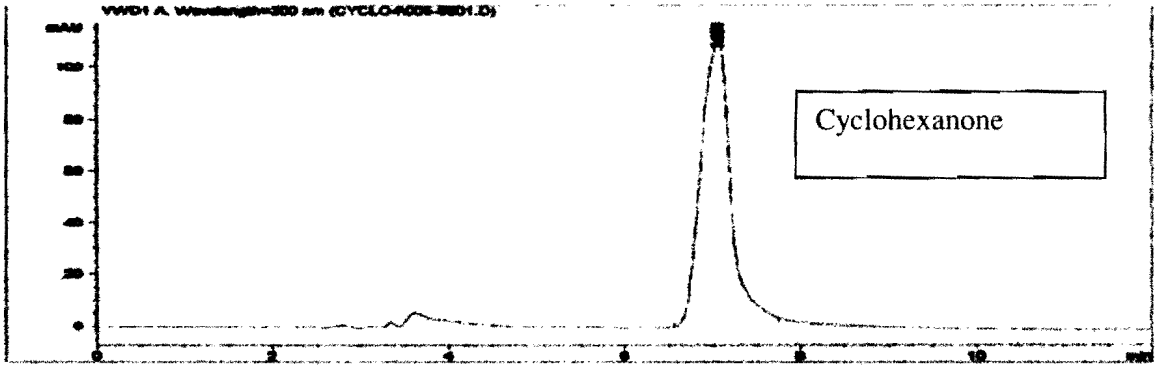

Figure 3-33. The HPLC analysis of fraction containing cyclohexanone.

The results are comparable since both curves are almost superimposed on each other indicating that the IR method is comparable with HPLC method (Figure 3-31).

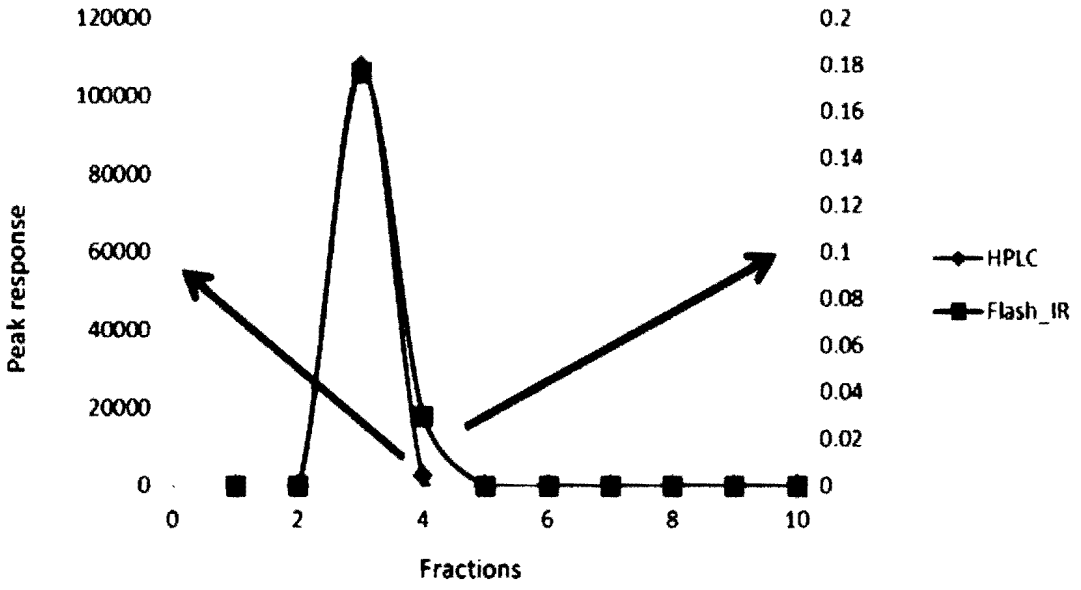

Figure 3-34. Comparison of the HPLC and FlashIR curve.

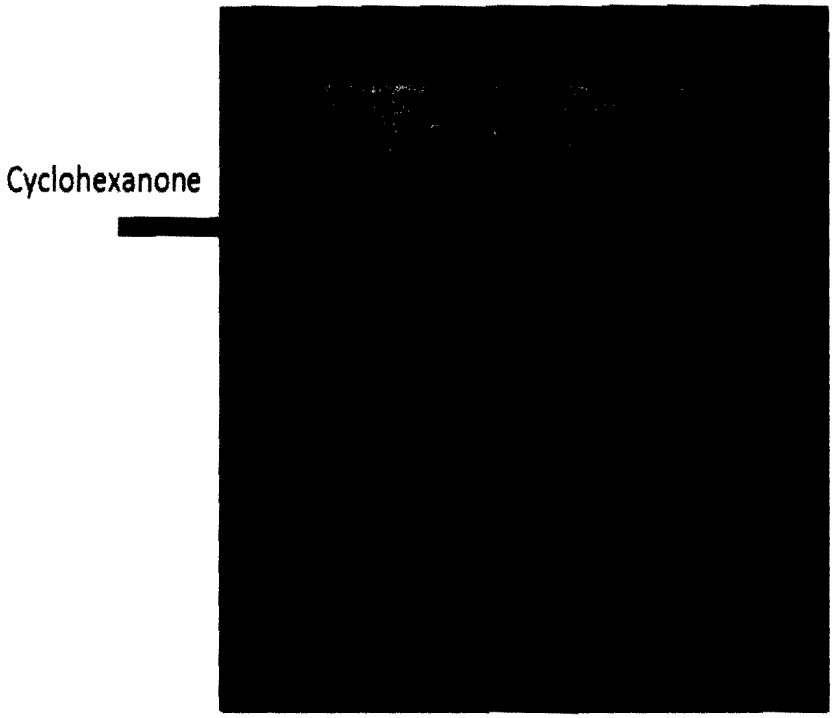

Figure 3-35.TLC separation of the fractions collected from flash chromatography.

The fractions collected during the FlashIR separation were also analyzed by thin layer chromatography. There is no spot observed in fractions 1 and 2. The spot due to cyclohexanone with matching R_f value compared with TLC analysis of the reaction mixture is observed in fractions 3 to 4 (Figure 3-32). The pure product is obtained by combining the fractions 3 to 4 and the solvents were removed using a rotary evaporator.

The isolated yield for the pure product is 0.85 g (85 %) and the purity of the product was confirmed by ^{1}H NMR as shown in the Figure 2-33 and ^{13}C NMR.

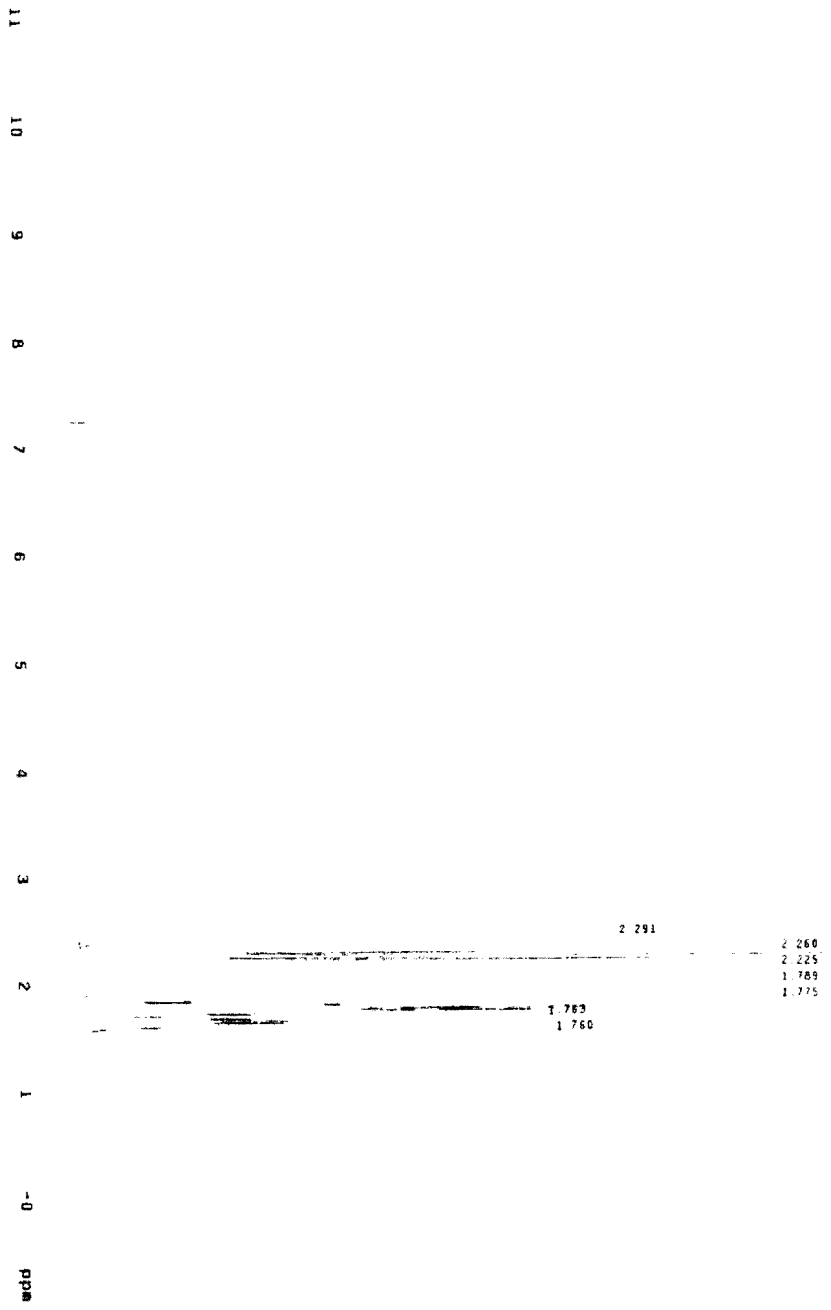

Figure 3-36.A. The ^{1}H NMR spectrum of purified cyclohexanone.

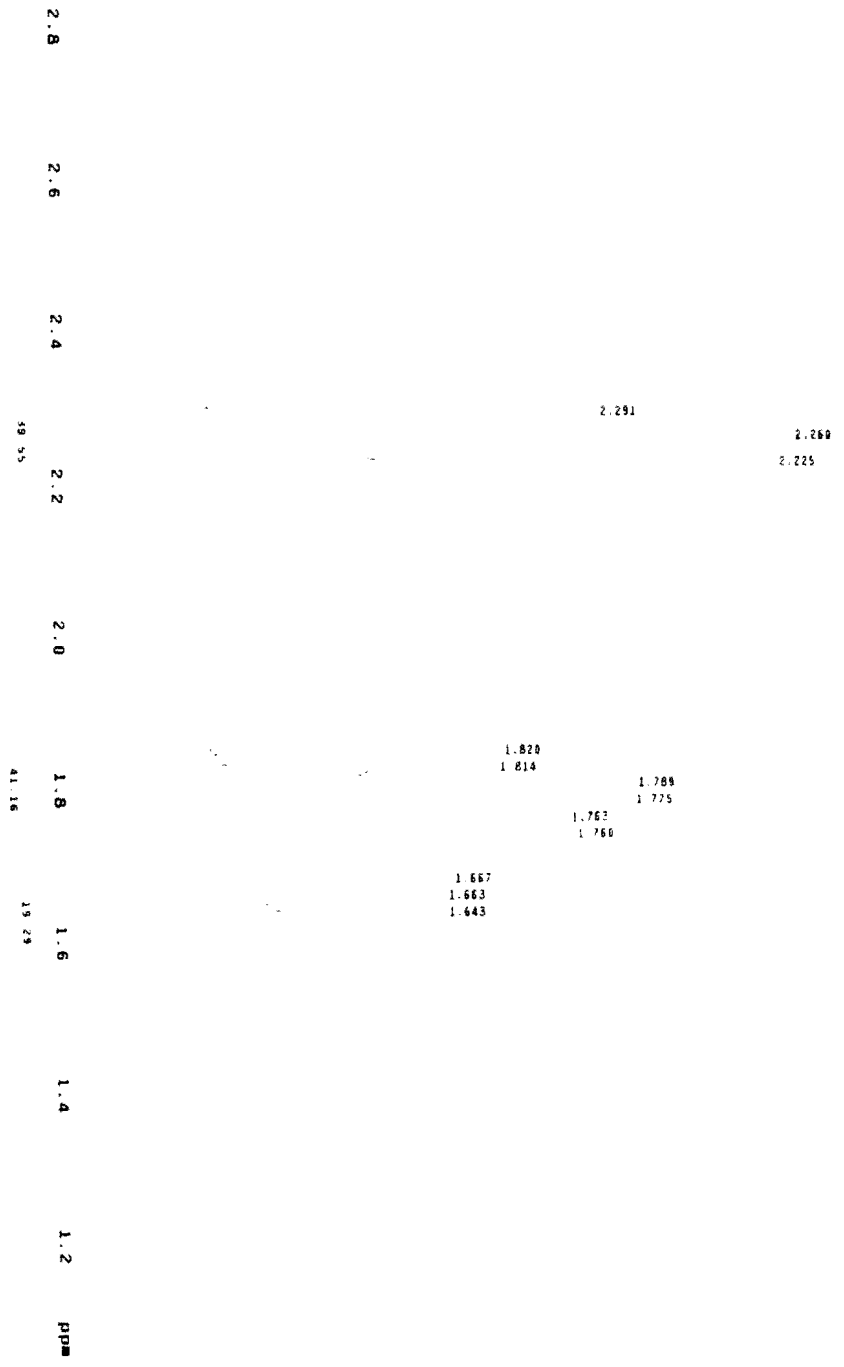

Figure 3-36.B. The ^{1}H NMR spectrum of purified cyclohexanone (expanded view).

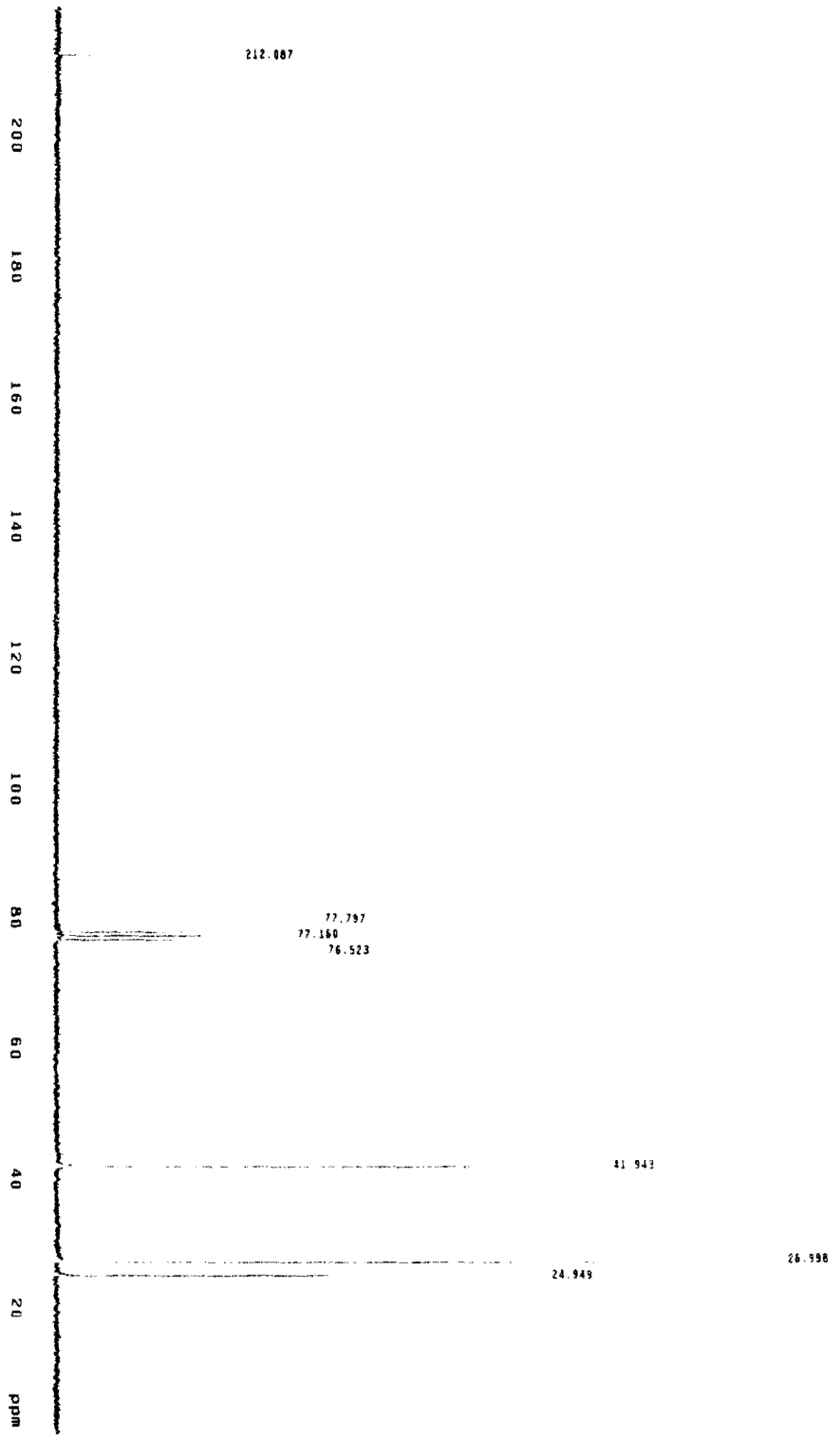

Figure 3-37. The ^{13}C NMR spectrum of purified cyclohexanone.

The ^{1}H NMR spectrum of cyclohexanone reveals a multiplet at 1.6 ppm indicating the protons on the cyclohexanone ring away from the oxygen atom. Another multiplet observed at 2.1 ppm was assigned to the protons present on both the carbon atoms near the carbonyl group. The peak at 3.5 ppm is also due to proton adjacent to the carbonyl group (Figure 3-36-A and B).

The ^{13}C NMR spectrum of cyclohexanone shows that the presence of C=O carbon due to peak at peak at 212.5 ppm. The peak at 44.1 ppm is due to the carbons adjacent to the carbonyl carbon. The peak at 25.9 ppm is due to the carbon parallel to the carbonyl function. The resultant spectrum is clean and impurity free. The total number of peaks (4) matches with the total number of carbons (4) (Figure 3-37).

3.6. Conclusion

A detailed study of three reactions was performed in which the reaction progress and the separation process were followed by IR spectroscopy. The reactions were the Williamson ether synthesis, the acetylation of cholesterol and the isomerization of cyclohexen-1-ol. The separations were confirmed by comparison with HPLC and TLC methods in order to validate the IR procedure. The experimental results obtained from real-time FlashIR separation is comparable as well as an orthogonal, detection technique to UV detection.

4.0 On-column Synthesis of Cyclohexanone by Isomerization of Cyclohexen-1-ol.

4.1. Introduction

Flow chemistry is a chemical reaction which runs in a continuously flowing stream rather than in batch production. In other words, pumps move fluids with reagents into a tube, and where tubes join one another, the fluids contact one another and a reaction takes place. Chemistry in flow provides exquisite control over reaction conditions, incorporates continuous separations and in-line recycling of reagents, and because reactor volumes are small compared to batch, this process significantly enhances safety. Scale-up to large production is achieved not with stepwise transitions to larger and larger vessels, but by knowledge based selection of the appropriate size, running multiple systems in parallel, and adjusting the time a system is in operation. Moreover, a much broader range of reaction conditions (temperature, pressure, and reaction time) and many classes of reactions that are impossible, hazardous or low-throughput in batch are safely and conveniently achieved in flow chemistry.[76] The chemical industry is constantly developing new technologies to increase the ease of syntheses. In the past five years, technologies such as microwaves and flow chemistry for small scale reactions have emerged and have been widely implemented in synthesis and other applications.

The parameters of the flow reactions can be kept constant making the reactions reproducible. Additionally, scaling up of the reaction requires no further work. The columns are packed with various catalyst used in flow chemistry. The most important advantage of flow chemistry is that the multistep reactions can be conducted in a single step, where as

[76] (a) *Handbook of Micro Reactors*, Eds.: Hessel, V.; Schouten, J. C.; Renken, A.; Wang, Y.; Yoshida, J., Wiley- VCH, Weinheim, **2009**; (b) Hessel, V.; Lcb, P.; Lcwe, H. in: *Microreactors in Organic Synthesis and Catalysis* (Ed.: T. Wirth), Wiley-VCH, Weinheim, **2008**, pp 211–275; (c) Whiteside, G. M. *Nature* **2006**, *442*, 368–373 (d) Geyer, K.; Codee, J. D. C.; Seeberger, P. H. *Chem. Eur. J.* **2006**, *12*, 8434-8439.

various steps are required to carry out multistep reaction in batch reactors as the intermediates have to be isolated in each step.

4.2. Experimental section

Our next aim within the same project is to explore flow chemistry coupled with real-time monitoring and separation. We used the known isomerization reaction which was carried out as a batch process and the background information collected was very helpful in designing the flow chemistry. To carry out the isomerization reaction of cyclohexen-1-ol to cyclohexanone by the mode of on column synthesis the column was prepared by tight packing of 5 wt % palladium-carbon (1.0 g) catalyst into an empty HPLC column (150 mm length and 4.6 mm diameter) by completely removing all the silica material from the column. Isopropanol (25 mL) containing cyclohexen-1-ol (3.0 g, 30 mmol) was circulated through the column in a continuous flow from a conical flask as shown in the Figure 4.1. The reaction is shown in Scheme 4-1.

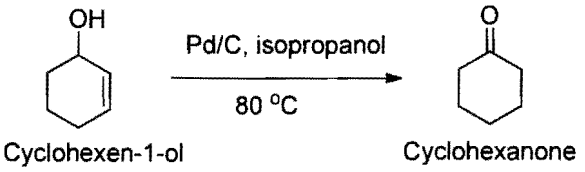

Scheme 4-1. The isomerization of cyclohexen-1-ol to cyclohexanone.

The temperature of the column was maintained at 80 °C by heating the column using an Eppendorf® column heater, Model 22851004. It is designed to accommodate single column up to 12.7 mm diameter and 300 mm length. The heater element consists of a 125 W heater adhered to a two-part oven aluminum heating block. The cyclohexen-1-ol was dissolved in measured quantity of isopropanol in a conical flask and pumped into the column packed with catalyst. The flow of substrate in isopropanol was maintained as 1.0 mL/min with the assistance of an HPLC pump. The flow cell shown in the Figure 2.4 which was used

in FlashIR system was used to monitor the flow reaction. The reaction was monitored by inserting the ReactIR probe into a flow cell. The reaction was monitored for about 9 h. The block diagram of the system is shown in the Figure 4-1.

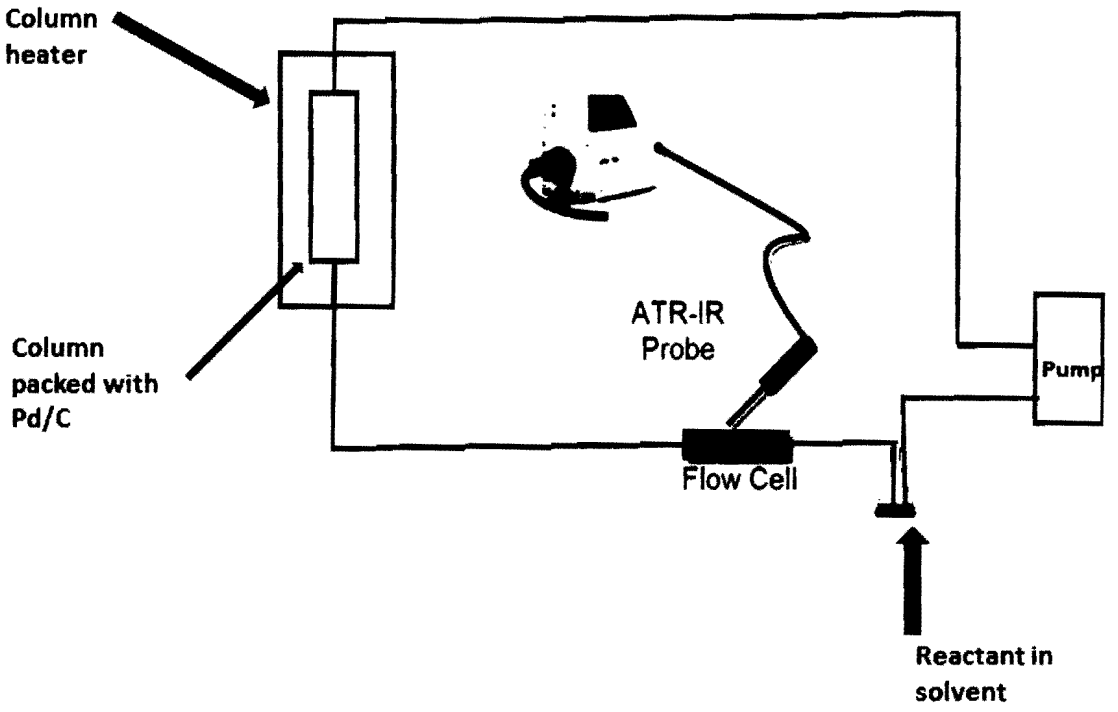

Figure 4-1. Schematic representation of on-column synthesis.

Since the same reaction was conducted as batch reaction the background information collected during real-time was very helpful in monitoring this flow chemistry as an on column reaction. The starting material, cyclohexen-1-ol, absorbs at 1660 cm^{-1} due to the stretching of the carbon-carbon double bond. The cyclohexanone product exhibits an absorption peak at 1710 cm^{-1} due to the stretching vibration of the carbonyl group. The peak response in those regions was monitored during the progress of the reaction.

By keeping the same set of conditions the flow reaction was repeated three times to understand the reproducibility of the reaction. In between the reactions, a 24 h time gap was given and the column packed with palladium and carbon catalyst was kept at room

temperature and remaining solvent. The percentage change in the peak area response was collected at 1660 cm^{-1} and 1710 cm^{-1} regions for cyclohexen-1-ol and cyclohexanone, respectively, and was used to build the reaction profile visualized in graphical format. The rate of reaction and the Turn-Over-Number (TON) of the catalyst were calculated. The rate of reaction was calculated by plotting the natural logarithm of molar concentration of cyclohexen-1-ol *vs.* time. The rate of reaction was obtained from the slope of the curve. The TON was calculated for the catalyst as the amount of reactant (moles) divided by the amount of catalyst (moles) times the % yield of product. The 1.0 g of 5% weight Pd/C with 50% wet was used and packed in the column and the moles of the catalyst was calculated as 0.00023 mM.

4.3. Results and discussion

The on-column synthesis of cyclohexanone from cyclohexene-1-ol as a flow reaction was conducted as described in the experimental section. Since the background information is was available from the batch process of the same reaction as described in the section 3.3 the monitoring of the flow reaction was obtained very conveniently. The reaction was conducted three times by keeping the same set of conditions.

4.3.1. First pass

The growing peak response due to the product at 1710 cm^{-1} wavenumber and the diminishing peak response at 1660 cm^{-1}due to the reactant undergoing isomerization was monitored. The real-time on column synthesis is visualized in the Figure 3-4.

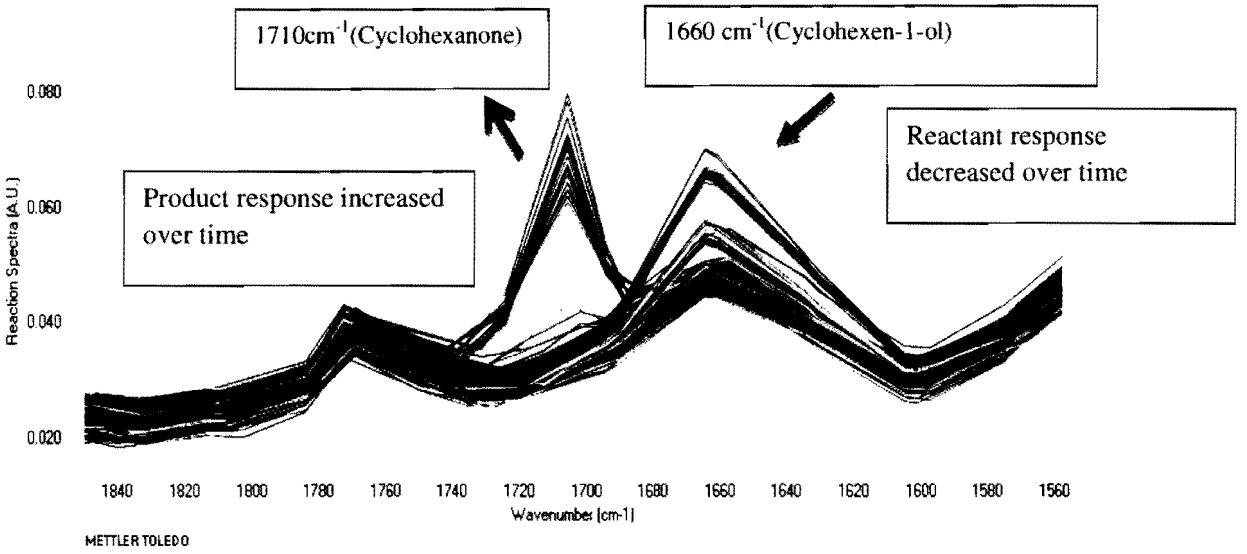

Figure 4-2. Flow Reaction spectra of isomerization of cyclohexen-1-ol to cyclohexanone (First pass)

TLC analysis was carried out using solvent system of ethyl acetate and hexane in the ratio of 90:10 which was found to be effective solvent system for identifying the reaction completion as well as for the optimal separation of isomerization products in the batch process. The visualization of the TLC spots was identified by keeping the developed TLC plates in iodine chamber. Two distinct spots from the reaction mixture and one matches with cyclohexen-1-ol indicates that the reaction is not completed and the reaction mixture has residual cyclohexen-1ol as shown in the Figure 4-3.

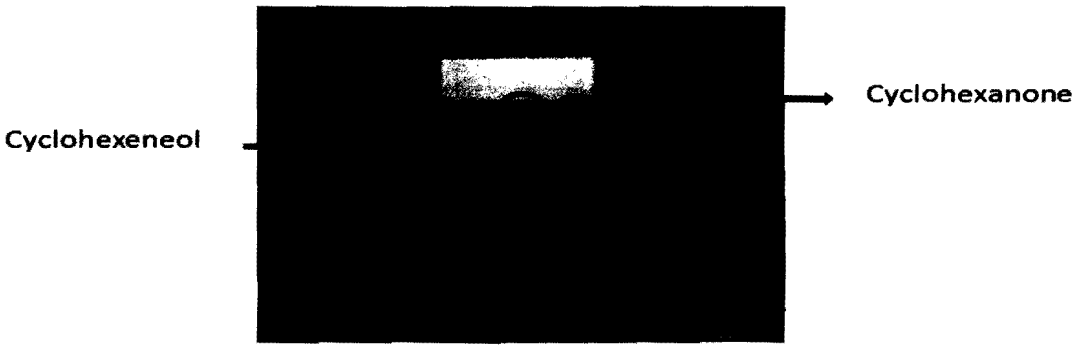

Figure 4-3. TLC analysis of reaction mixture (First pass).

The graphical representation is obtained by plotting percentage change in peak area response of the substrate and product was collected to visualize the reaction profile for the conversion of cyclohexen-1-ol to cyclohexanone is shown in Figure 4-4. The red curve indicates the decrease in the peak area response of cyclohexen-1-ol starts only after 3 h from the initial stage of the reaction indicating that there is an induction period for the reaction. Similarly the peak area response of cyclohexanone was only found to increase after 3 h as indicated by the blue curve. The reaction was monitored for 9 h since the isopropanol evaporates as the column was kept at 80 °C if the reaction was continued beyond 9 h to complete conversion.

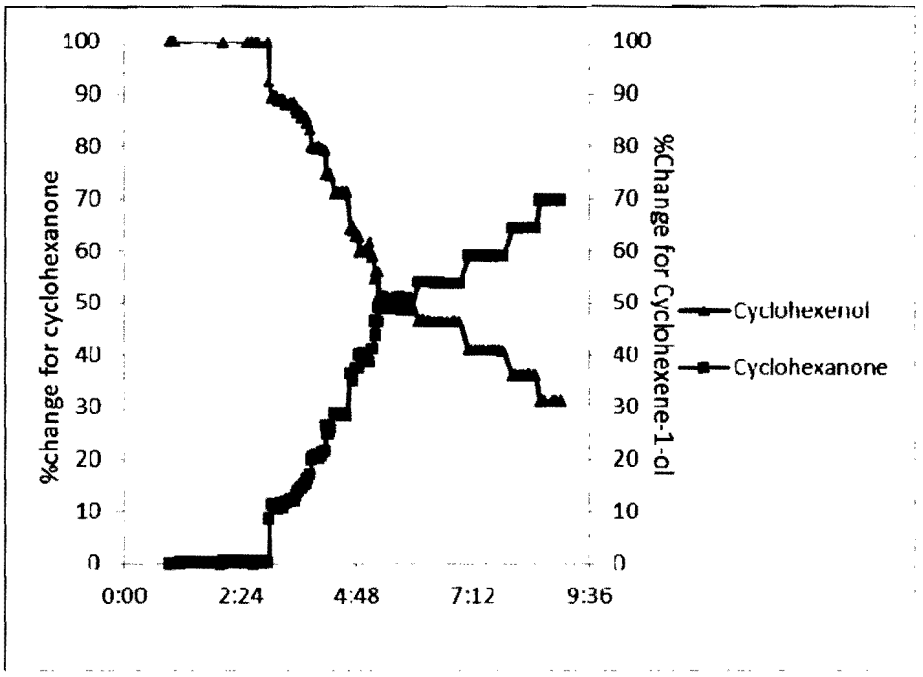

Figure 4-4. Graphical representation of reaction profile (First pass).

After completion of first flow reaction the solvents from reaction mixture was removed by rotary evaporator and purified by FlashIR. The isolated yield of cyclohexanone from the first pass reaction is 0.45 g (45%).

The rate of reaction was calculated plotting natural logarithm of concentration of the cyclohexanone concentration *vs.* time with the help of calibration curve as shown in Figure 3-29. The slope is considered as rate of reaction. as shown in the Figure 4-5. The initiation period is 0 to 3.5 hours. The regime_1 shows the faster convertion and slows down when it reaches regime_2.The rate formation of cyclohexanone is obtained as 0.69 mM/L per hour The rate of conversion is less than the batch process which was calculated at 1.21 mM/L per hour. The TON for the catalyst at the first pass flow reaction is 6000.

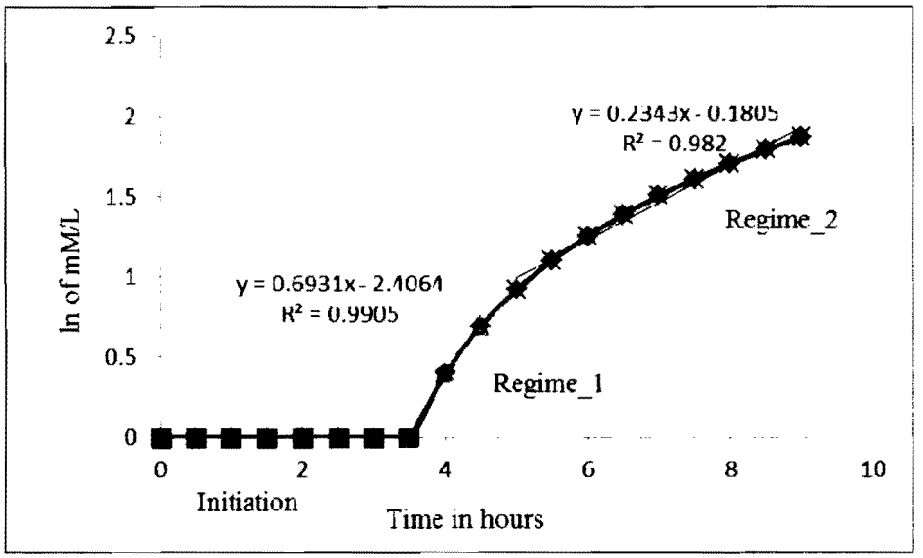

Figure 4-5. Rate of reaction (First pass).

4.3.2. Second pass

The same reaction was carried out with the same set-up and conditions to repeat the flow reaction for a second time in the same column. The growing peak response due to the product at 1710 cm^{-1} wavenumber and the diminishing peak response at 1660 cm^{-1} due to the reactant undergoing isomerization was monitored similar to the first pass reaction. The second pass real-time on-column synthesis is visualized in Figure 4-6.

It was observed that the height of the peaks at 1710 cm^{-1} and 1660 cm^{-1} were lower than the first pass as shown in Figure 4-6 indicates that the isomerization conversion was less than the first pass flow reaction.

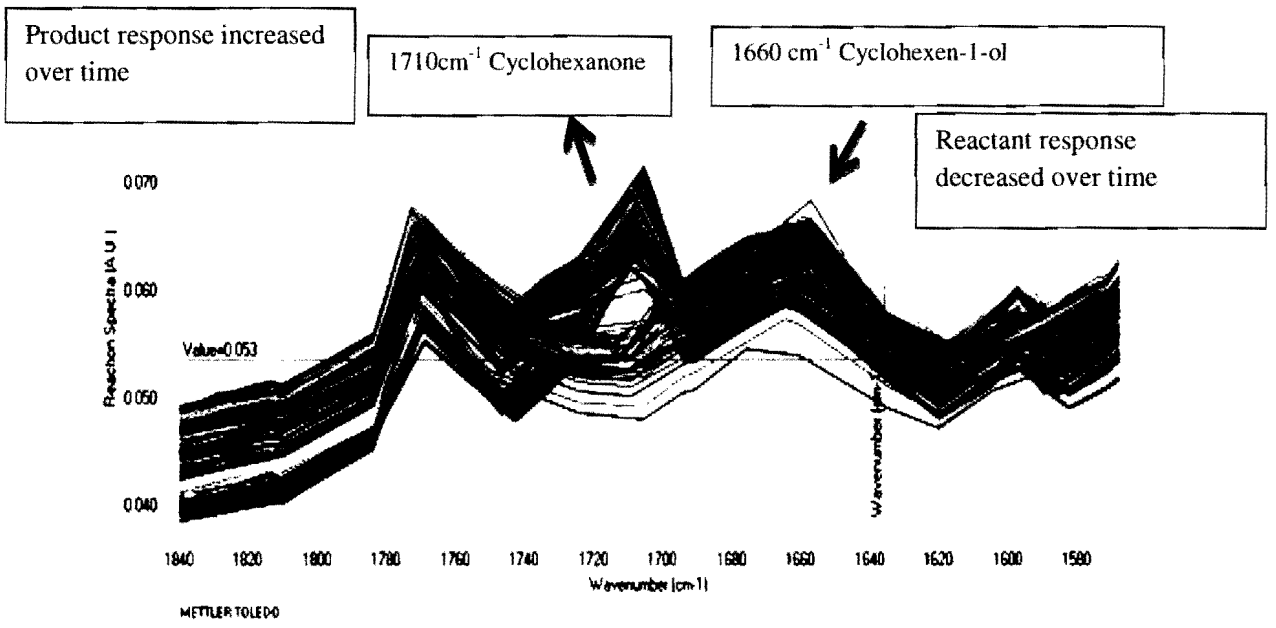

Figure 4-6. Flow Reaction spectra of isomerization of cyclohexen-1-ol to cyclohexanone (Second pass).

TLC analysis was carried out using solvent system of ethyl acetate and hexane in the ratio of 90:10 similar to the first pass reaction. Two distinct spots from the reaction mixture and one matches with cyclohexen-1-ol indicates that the reaction is not completed and the reaction mixture has residual cyclohexen-1-ol as shown in Figure 4-7.

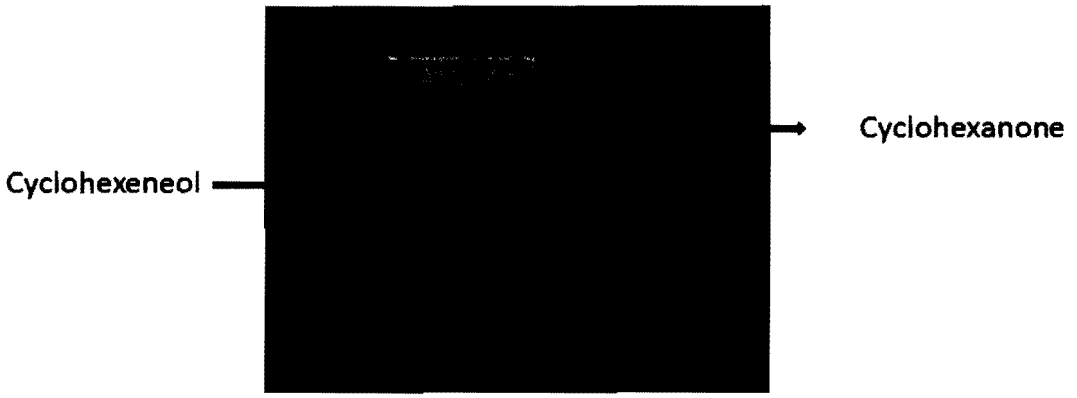

Figure 4-7. TLC analysis of reaction mixture (Second pass).

After completion of second flow reaction the solvents from the reaction mixture was removed by rotary evaporator and purified by FlashIR. The isolated yield of cyclohexanone from the second pass reaction is 0.39 g (39%).

The graphical representation is obtained by plotting percentage change in peak area response of the substrate and product from the reaction profile in the conversion of cyclohexen-1-ol to cyclohexanone is shown in Figure 4-8. The red curve indicates the decrease in the peak area response of cyclohexen-1-ol starts only after 3 h from the initial stage of the reaction indicating that there is an induction period for the reaction. Similarly the peak area response of cyclohexanone was only found to increase after 3 h as indicated by the blue curve. The reaction was monitored for 9 h.

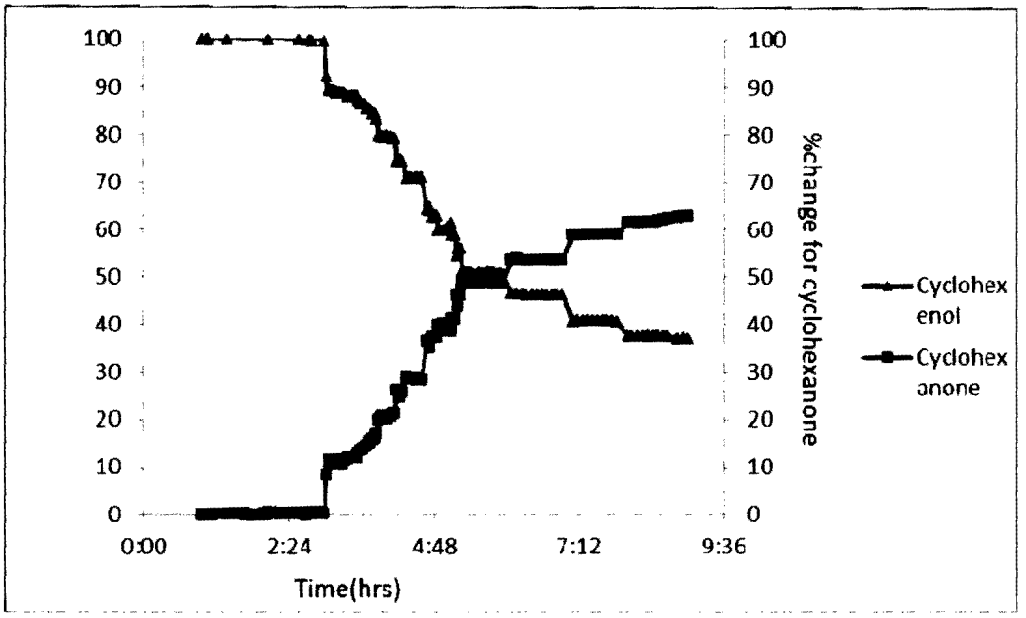

Figure 4-8. Graphical representation of the reaction profile (Second pass).

The rate of reaction was calculated from the graph (Figure 4-9) as explained in the first pass. The slope is considered as rate of reaction. The rate of formation of cyclohexanone is 0.55 mM/L per hour which is slower than the first pass (0.69 mM/L per hour). The TON for the catalyst at the first pass flow reaction is 5000.

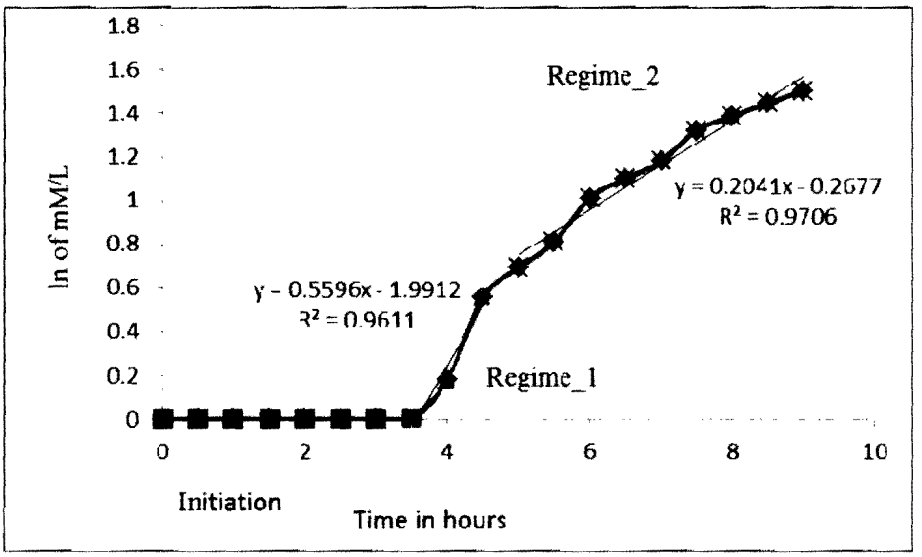

Figure 4-9. Rate of reaction (Second pass).

4.3.3. Third pass

The reaction was carried for the third time through the same column and a similar analysis was performed. It was observed that the reaction was sluggish and the signature peaks showed low response as shown in Figure 4-10.

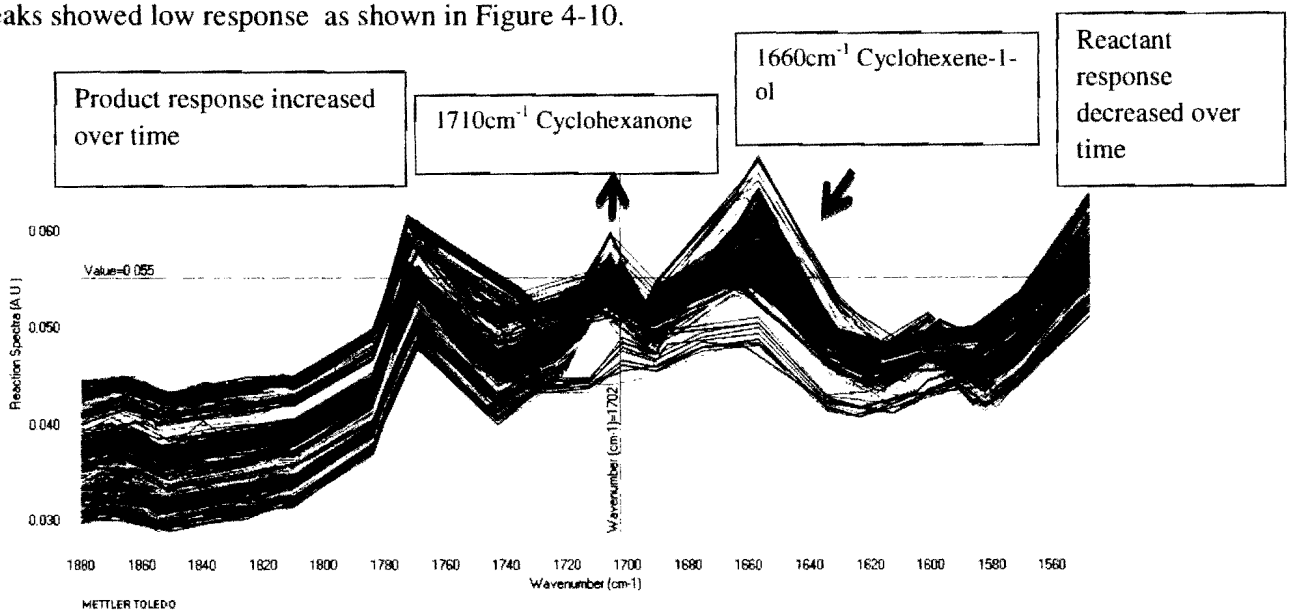

Figure 4-4. Flow Reaction spectra of isomerization of cyclohexen-1-ol to cyclohexanone (Third pass).

The TLC analysis as followed in first and second pass reaction shows that the reaction did not go to completion as shown in Figure 4-11.

Figure 4-5. TLC analysis of reaction mixture (Third pass).

After the completion of the third flow reaction the solvents from reaction mixture were removed using a rotary evaporator and purified by FlashIR. The isolated yield of cyclohexanone from the first pass reaction is 0.32 g (32%).

The visualization of reaction profile obtained by plotting the percentage change in peak area response of the reactant and product against time is shown in Figure 4-12.

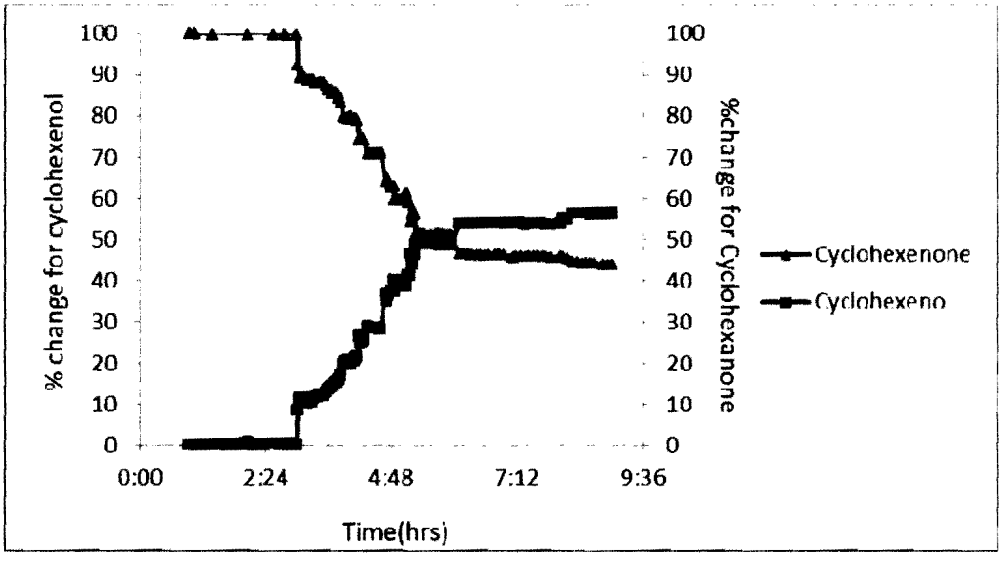

Figure 4-6. Graphical representation of the reaction profile (Third pass).

The rate of reaction was calculated plotting natural logiratham of percentage conversion *vs.* time in hours as shown in Figure 4-13. The slope is considered as rate of reaction. The rate of formation of cyclohexanone is 0.40 mM/L per hour which is slower than the first and second pass (0.69 and 0.55 mM/L per hour, respectively). The TON for the catalyst at the third pass is 4000.

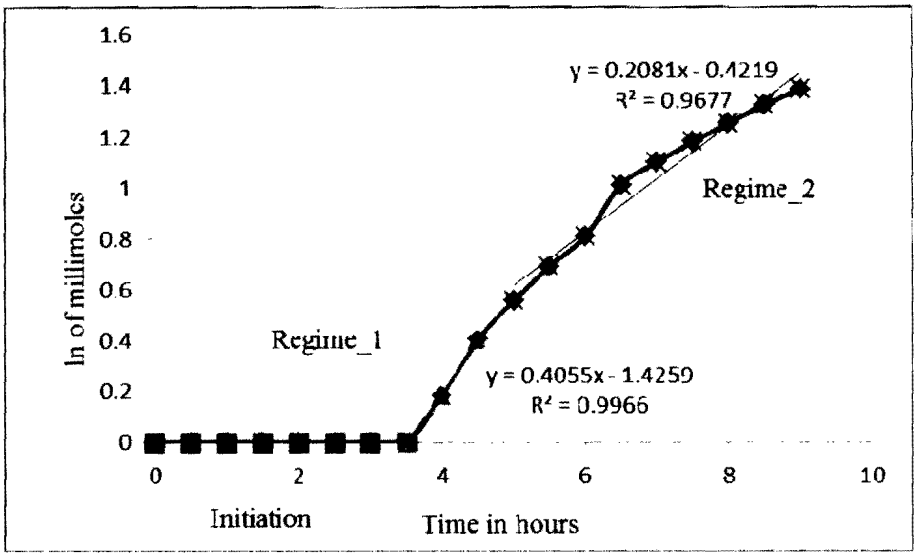

Figure 4-13. Rate of reaction (Third pass).

4.4. Conclusion

The reaction was repeated three times which produced different patterns of the results because the efficiency of the catalyst in the column decreased with repetitious use as shown by the analyzed spectra of the second and third experiments. The rate of formation is faster in the first pass (0.69 mM/L per hour) as compared to second (0.55mM/L per hour) and third passes (0.40 mM/L per hour) in the flow reaction. The overall flow reaction rate is slower as compared to the batch process (1.21mM/L per hour). The TON of the catalyst was higher in the first pass as compared to second and third pass.

5.0 A Rapid, Acetonitrile-free Method for Determination of Melamine in Infant Formula by HPLC.

5.1. Introduction

Melamine is a polar organic compound with a 1,3,5-triazine skeleton (Figure 5-1) which is commonly used for its fire retardant properties and is often combined with formaldehyde in the moulding of plastics. Recent recalls involving pet food and milk products contaminated with melamine (2,4,6-triamino-1,3,5-triazine) have created a concern about the safety of pet, dairy and snack foods. Melamine contamination has been reported in products such as milk, infant formula, frozen yogurt, pet food, biscuits, candy, and coffee drinks.[1] Melamine was previously considered a non-protein nitrogen (NPN) supplement for cattle feed; however, this use has been discontinued. A driving force for the adulteration of a food product with melamine is that its high nitrogen content (67%) increases the apparent protein content measured by Kjeldahl or Dumas methods[2] which are the standard protein analysis tests.

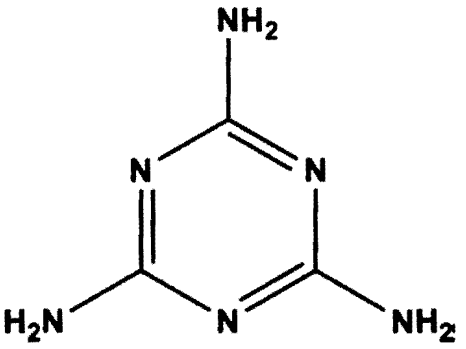

Figure 5-1 Structure of melamine

In 2007, pet food adulteration with melamine resulted in the illness and death of animals that consumed the contaminated product. A more recent incident of contamination of milk with melamine has resulted in numerous cases of renal complications in children and six

[1] World Health Organization, Melamine contamination event, China, **2008**, retrieved December 2, 2008, from http://www.who.int/foodsafety/fs management/infosan events/en/index.html.
[2] Newton,G. L.; Utley, P. R. *J. Anim. Sci.* **1978**, *47* , 1338–1344.

deaths have been attributed to consumption of tainted product.[3] Toxic effects associated with melamine consumption are usually associated with high doses and reported concentrations of melamine in contaminated samples ranged from 90 to 620 $\mu g\ mL^{-1}$.[4] The tolerable daily intake (TDI) of melamine is 0.63 mgkg−1 (0.63 μgmL^{-1}) body weight per day recommended by the US Food and Drug Administration (FDA) on 3 October 2008 (and updated 28 November) for food and food ingredients other than infant formula.[5] Additionally, it is thought that simultaneous ingestion of melamine and one of its analogues, cyanuric acid, may result in the formation of crystals in the kidney.[6] To ensure that the food supply is not affected by melamine-adulterated products, the FDA has taken proactive steps by increasing sampling and testing of imported milk-derived ingredients and finished products. The FDA has currently stated that a level of up to 2.5 gmL^{-1} of melamine and its analogues in foods (not including infant formula) does not raise public concern.[7]

In 2008, brands of infant formula produced and sold in the United States were found to contain low levels of melamine. Due to the serious health concerns associated with melamine consumption and the extensive scope of affected products, rapid and sensitive methods to detect melamine's presence are essential. This is especially important for infant formula because it is the major calorie and nutrient source for infants. The kidney function of infants is immature, and the product is consumed for an extended period of time. Recently, a

[3] (a) Chan, E. Y.; Griffiths, S. M.; Chan, C.W. Public-health risks of melamine in milk products, *Lancet* **2008**, 372, 1444–1445. (b) Filigenzi, M. S.; Puschner, B.; Aston, L. S.; Poppenga, R. H. *J. Agric. Food Chem.* **2008**, *56*, 7593.

[4] Zenobia, C. Y.; Chan, W. F. *Trends Food Sci. Technol.* **2009**, *20*, 366–373

[5] Dobson, R. L.; Motlagh, S.; Quijano, M.; Cambron, R. T.; Baker, T. R.; Pullen, A. M.; Regg, B. T.; Bigalow-Kern, A. S.; Vennard, T.; Fix, A.; Reimschuessel, R.; Overmann, G.; Shan,Y. and Daston, G. P. *Toxicol. Sci.* **2008**, *106*, 251–262.

[6] US Food and Drug Administration, Interim safety and risk assessment of melamine and its analogues in foods for humans, retrieved December 2, **2008**, from http://www.cfsan.fda.gov/~dms/melamra3.html.

[7] Wui, Y. N.; Zhao, Y. F.; Li, J. G. *Biomed. Environ. Sci.* **2009**, *22*, 95–99.

threshold of 1 $\mu gmL^{-1}$for melamine in infant formula was set by the FDA making the detection of low levels of melamine in infant formula very critical.

At the same time as the melamine crises, there was a coincidental global economic downturn that caused an overall reduction in the demand for acrylonitrile. The common HPLC solvent, acetonitrile, is obtained as a co-product in the production of acrylonitrile. Consequently, the pharmaceutical, food, environmental, and chemical industries are experiencing an unprecedented shortage in acetonitrile. This shortage has resulted in a sharp price increase which is projected to remain high even after the production returns to normal.[8] Acetonitrile is very important in the field of research as it is among the most commonly used organic solvents in reversed-phase liquid chromatography. This is mainly due to its miscibility with water, acceptable UV absorptivity and low viscosity. The ongoing acetonitrile shortage has forced chemists to either reduce their solvent usage by using shorter, narrower columns packed with small particles, or, replace acetonitrile with more readily available solvents such as methanol. To our knowledge, this is the first report of an acetonitrile-free liquid chromatography (LC) method for the determination of melamine.

The reported methods for quantitative determination of melamine include enzyme immunoassay (EIA), IR analysis, gas chromatography–mass spectrometry (GC–MS), liquid chromatography–mass spectrometry (LC–MS), and high performance liquid chromatography (HPLC) with UV detection.[9] Standard methods enacted by the Chinese government for determining melamine in raw milk and dairy products include HPLC–UV, LC–MS and GC–

[8] Yang, M.; Fazio, S.; Munch, D.; Drumm, P. *J. Chromatogr. A* **2005**, *124*. 1097.

[9] (a) Mauer, L. J.; Chernyshova, A. A.; Hiatt, A.; Deering, A.; Davis, R. *J. Agric.Food Chem.* **2009**, *57 (10)*, 3974–3980.(b) Filigenzi, M.S.; Tor, E. R.; Poppenga, R. H.; Aston, L. A.; Puschner, B. *Rapid commun. Mass Spectrom.* **2007**, *21 (24)*, 4027–4032. (c) Sancho, J. V.; Ibanez, M.; Grimalt, S.; Pozo, O. J.; Hernade, Z. F. *Anal. Chim. Acta* **2005**, *530*, 237–243.(d) Kim, B.; Perkins, L. B.; Bushway, R. J.; Nesbit, S.; Fan,T.; Sheridan, R.; Greene, V. *J. AOAC Int.* **2008**, *91 (2)*, 408–413.

MS methods. However, the high cost of operation and maintenance of GC/LC–MS systems as well as the labour intensive derivatization, limits their use in production facilities. The HPLC–UV method, therefore, is presently the most cost-effective choice for most analyses. Because of the need to monitor numerous batches of raw milk, another standard HPLC–UV method for rapidly determining melamine in raw milk was recently recommended which uses acetonitrile as an eluent. To date, there is no report of using methanol as an eluent in LC methods. Thus, the present work focuses in developing and validation of rapid analysis of melamine in both liquid and powder infant formula samples by HPLC–UV using methanol as an eluent.

5.1. Experimental Section

5.1.1. Chemicals and reagents

Melamine (99.0%) was obtained from Acros Organics, Morris Plains, NJ. TFA was purchased from Fluka, Sigma–Aldrich, St. Louis, MO. Methanol (HPLC grade) was obtained from Pharmaco-AAPER, CT. The infant milk products were purchased from a local food store. Water used for the mobile phase preparation and dilution was purified on a Millipore Q-Pod system.

5.1.2. Chromatographic equipment

The LC system consisted of a Hewlett-Packard (HP) 1050 series Quaternary Pump, 79853C VW UV detection, a 35900-C Interface and autosampler controlled by HP ChemStation (v. A.06.03[509]).

5.1.3. Chromatographic conditions

The chromatographic separation was accomplished on a Kromasil C18 analytical column (150 mm × 3.2 mm I.D., 5 μ particle size). The HPLC eluents were 0.10 % (pH 2.4) TFA/methanol (90:10) pumped at flow rate of 0.3 $mLmin^{-1}$ with an injection volume of 20

μL. The detection wavelength was set at 240 nm. The effect of TFA concentration on melamine retention time and peak shape was evaluated. At 0.050 (pH 2.8) and 0.10 % TFA, the retention time (3.7 min) was identical and peak shapes were sharp. However, at 1.0 % (pH 1.4) TFA, the retention time was longer (4.6 min) and the peak obtained was very broad.

5.2. Standards preparation

5.2.1. Diluent

A diluent of 50% aq. methanol (v/v) was prepared by mixing equal volumes of methanol and water.

5.2.2. Melamine stock solution

Accurately weighed melamine (100 mg) was dissolved by sonication for 30 min in a volumetric flask (100 mL) in 50 % aqueous methanol resulting in a melamine concentration of 1000 μgmL^{-1}.

5.2.3. Intermediate melamine stock solution.

This was prepared by diluting 5 mL of the melamine stock solution to 50 mL with 50 % aq. methanol to give a melamine concentration of 100 μgmL^{-1}.

5.2.4. Working melamine solution

This was prepared by diluting 5mL of the intermediate melamine stock solution to 50 mL with 50 % aq. methanol to give a melamine concentration of 10 μgmL^{-1}.

5.3. Sample preparation

5.3.1. Preparation of stock infant formula samples

In a volumetric flask (100 mL), liquid formula (10 mL) or dry powder (1 g) was added. The sample was spiked with 1000 μgmL^{-1} melamine stock solution (10 mL) followed by dilution with 50 % aq. methanol (50 mL) and sonicated for 30 min. After cooling to room

temperature, the volume of the volumetric flask was filled with 50 % aqueous methanol and mixed well to give a melamine concentration of 100 μgmL^{-1}.

5.3.2. Preparation of working infant formula samples

Samples for analysis including the above stock infant formula solution were centrifuged using a tabletop centrifuge (Clay Adams Compact II, #420225, 3200 rpm) and 5 mL of the supernatant was transferred to a volumetric flask (50 mL). The volume was filled with 50 % aqueous methanol with proper mixing. The sample was filtered through a 0.45 µm filter (Acrodisc, 25 mm, Nylon membrane). A recovery study on the filtrate indicated that the filter adsorbed melamine at the following levels: 22 % (for the initial 1 mL), 10 % (at 2 mL), < 1 % (at 3, 5 and 7 mL). Thus, the initial 3 mL of the filtrate was discarded and the remaining filtrate added to an HPLC vial for analysis.

5.4. Method validation

5.4.1. Linearity

Linearity test solutions were prepared from the stock melamine solution at five concentration levels ranging from 1.0 to 80 μgmL^{-1}. A calibration curve was obtained by plotting the peak area vs. concentration (Fig. 2). The % R.S.D. from five repeated injections at each concentration and % y-intercept bias was calculated. The LOD and LOQ of the method was estimated at a signal-to noise ratio of 3:1 and 10:1, respectively, by injecting a series of diluted solutions with known concentration. A precision study was also carried at the LOQ level by injecting six individual preparations and % R.S.D. of the peak area was calculated. A recovery study was performed in triplicate at the LOD and LOQ levels for powder and liquid samples. Samples spiked at the LOD level resulted in an average recovery of 75 ± 2 % and those spiked at the LOQ level resulted in an average recovery of 90 ± 1 %.

5.4.2. Accuracy

The accuracy of the method was evaluated at four-concentration levels of melamine (5, 10, 20 and 40 μgmL^{-1}) using 1 g of dry or 10 mL of liquid infant formula samples. The percentage recoveries reflect an average of six analyses at each concentration and are reported in Table 5-1.

Melamine added (μg)[a]	Recovered (μg)	% Recovery	% RSD
Powder			
5.05	5.07	100.4	1.5
10.05	10.17	101.2	0.8
20.60	20.02	97.2	2.9
40.85	40.80	99.9	1.0
Liquid			
5.05	5.10	101.0	1.0
10.04	10.14	101.0	0.8
20.03	19.86	99.2	1.5
40.36	40.70	100.8	0.4

[a]Analysis at each concentration performed in six times.

Table 5-1. Recovery results of melamine from dry infant formula.

5.4.3. Precision

Precision was measured as repeatability and reproducibility of dry and liquid infant formula samples. Using a sample processed according to Section 2.5.2 (check), the repeatability (intra-day) and reproducibility (inter-day) of the method was demonstrated by injections (in triplicate) of the sample on the initial day and three consecutive days. The recoveries ranged from 101.1 to 102.8 (0.8 % R.S.D.). In addition, the reproducibility of a sample processed (in triplicate) separately on day 0 and day 4 resulted in recoveries of 99.5 to 101.8 (0.8 % R.S.D.).

5.5. Results and discussion

Reversed-phase liquid chromatography is an excellent separation technique for ionizable molecules. Since melamine is a basic analyte (pKa = 5.0), under acidic conditions (pH < 3), the analyte is fully protonated in the mobile phase and residual silanol groups on the silica support of the column packing are also protonated. We have developed a simple analysis of infant formula spiked with melamine. The method uses a mobile phase mixture of trifluoroacetic acid (0.10 %, pH 2.4) and methanol. The method is advantageous as it avoids the use of expensive acetonitrile in the mobile phase.[10] The chromatogram indicates that there is no interference from the infant formula and the melamine signal is clearly distinguished at 3.7 min (Figure 5-3).

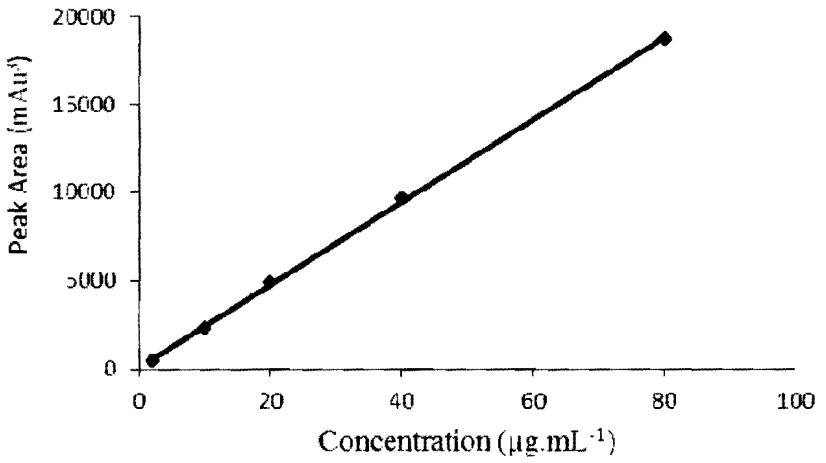

Figure 5-2. Linear relationship of melamine concentration vs. UV peak area.

Additionally, a linear calibration curve is depicted in Figure 5.2. Moreover, samples spiked with 5 – 40 gmL^{-1} of melamine show recoveries ranging from 97.2 to 101.2 with R.S.D.

[10] Cai, B.; Li, J. *Anal. Chim. Acta.* **1999**, *399*, 249–258.

values ranging from 0.4 % to 2.9 % indicating that the method is accurate over this concentration range (Table 5-1).

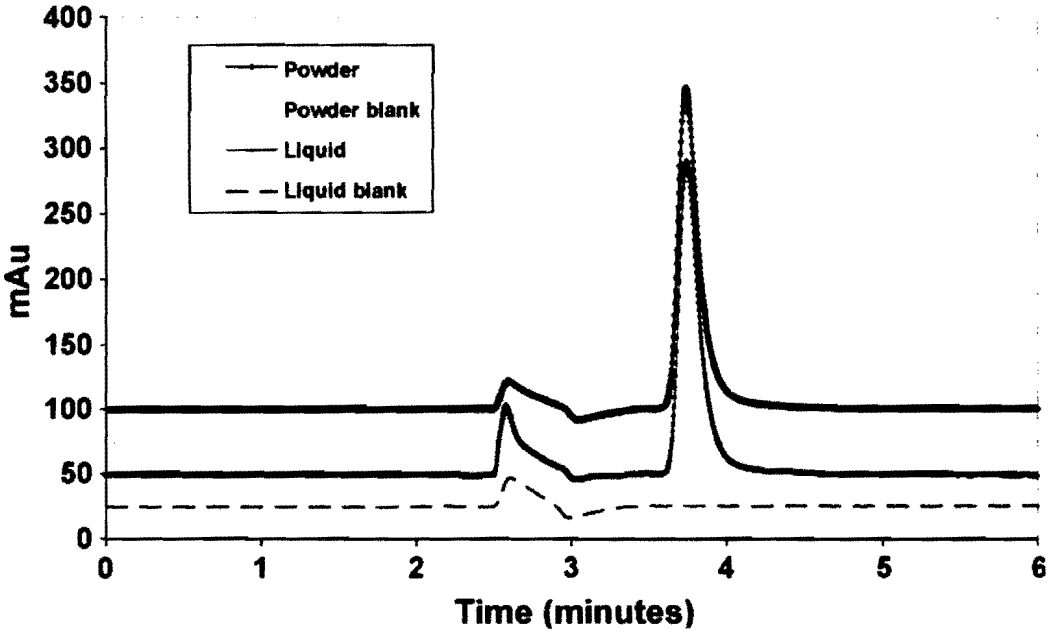

Figure 5-3. Chromatogram of infant formula with and without melamine spiking.

This method involves relatively simple sample processing consisting of dilution with 50 % aqueous methanol, centrifugation, dilution, filtration and analysis. The HPLC chromatogram is complete in 6 min.

5.5.1. Linearity

A linear calibration plot (Figure 5-1) is obtained over the calibration range of 1.0 – 80 gmL^{-1} with a correlation coefficient (r) of 0.999. The percentage R.S.D. values of the repeated injections are less than 2 % within each concentration and the y-intercept bias is less than 2 %.

5.5.2. Limit of detection (LOD) and limit of quantification (LOQ)

The LOD was determined to be 0.1 μgmL^{-1} and the LOQ was determined to be 0.2 μgmL^{-1}. The percentage R.S.D. of the precision study carried at the LOQ level was within 5

%. An exact comparison to conditions in acetonitrile solvent was not performed. However, Sunet *et al.*[11] found lower LOD and LOQ values (0.018 and 0.060 μgmL^{-1}, respectively) using solid phase micro extraction and sodium heptanesulfonate (10 mM in/acetonitrile).

5.5.3. Accuracy

The percentage recovery of melamine in milk samples ranged from 97.2 % to 101.2 % (Table 1). The method indicated reliable recovery.

5.5.4. Precision

The method shows good repeatability (intra-day) and reproducibility (inter-day) for processed samples as indicated by recoveries of 101.1 – 102.8 % (0.8 % R.S.D.). In addition, the reproducibility of a sample separately processed (in triplicate) on day 0 and day 4 resulted in recoveries of 99.5 – 101.8 (0.8 % R.S.D.).

[11] Sun, H.; Wang, L.; Ai, L.; Liang, S.; Wu, H. *Food Control* **2010**, *21 (5)*, 686–691.

6. Conclusion

This paper describes a simple method to determine the melamine contamination in infant formula samples using isocratic, reverse phase HPLC. This method is advantageous because the mobile phase is acetonitrile-free and the analysis time of ~6min per sample is reasonably rapid. The separation was performed on a Kromasil C18 column (150 mm × 3.2 mm I.D., 5 μm particle size) at room temperature with a mobile phase of 0.1 % TFA/methanol (90:10), a flow rate of 0.3 $mLmin^{-1}$ and detection at 240 nm. Starting with an analyte concentration of 10 μgmL^{-1}, a linear response ($r > 0.999$) was observed for samples ranging from 10 % to 400 % of this concentration. The method provides recoveries of 97.2 – 101.2 % in the concentration range of 5 – 40 μgmL^{-1}. Intra- and inter-day reproducibility's are less than 1.0 % R.S.D. The LOD and LOQ are 0.1 μgmL^{-1} and 0.2 μgmL^{-1}, respectively. This analytical method provides excellent sensitivity, reproducibility, accuracy and precision for the detection of melamine in infant formula.

7. Research conclusions

The application of the *in-situ* attenuated total reflection infrared technique for the investigation of a detection tool for flash chromatographic analysis has been emphasized in this research. The purification procedure for most of the synthetic reactions is mainly based on flash chromatography. A variety of detecting tools such as UV light, refractive index measurement and HPLC have been combined with flash column with an aim to detect the eluted compounds in the column. This technology reduces further purification process mainly conducted with the help of TLC. In this dissertation, a new technique of *in-situ* attenuated total reflection-infrared spectroscopy (ATR-IR) has been developed as a detection tool to monitor the flash chromatographic analysis. Furthermore, the system has been tested and proved for on-column synthesis monitoring capability of monitoring real-time transformations during the reactions. We conducted the etherification, acetylation and isomerization as traditional batch reactions followed by flash separation which was monitored by IR detection. Additionally, an on-column synthesis procedure was developed by monitoring the isomerisation of cyclohexen-1-ol to cyclohexanone by IR.

In the second part of the thesis, a sensitive and validated RP–HPLC method for the determination of melamine residue in infant milk was developed. The proposed method is sensitive, reliable and accurate which can permit the detection of melamine residues at levels as low as 0.1 μg/mL. The method can be used for the routine determination of melamine residue in different liquid milk samples.

8.0. Appendix

Raw data and model calculation for Williamson ether synthesis and Separation

Table-8.1. Reaction monitoring for Williamson ether synthesis at 1250 cm^{-1} for BTBE and at 750 cm^{-1} for BnBr.

BTBE				BnBr		
Time	Peak area	Difference	%Change	Peak area	Difference	%Change
0:57	0.019195	0	0	0.7037079	0.44794309	100
0:58	0.019196	1.745E-06	0	0.704045	0.44828019	100
1:00	0.019212	1.706E-05	0	0.7037079	0.44794309	100
1:02	0.019228	3.359E-05	0	0.703045	0.44728019	100
1:04	0.019229	3.42E-05	0	0.7055902	0.44982539	100
1:06	0.019244	4.967E-05	0	0.7051547	0.44938989	100
1:08	0.019263	6.823E-05	0	0.7041974	0.44843259	100
1:10	0.019589	0.000394	0	0.7058708	0.45010599	100
1:12	0.019731	0.0005366	0	0.705157	0.44939219	100
1:14	0.019673	0.0004785	0	0.7050119	0.44924709	100
1:17	0.019662	0.0004677	0	0.7041155	0.44835069	100
1:18	0.019637	0.0004419	0	0.704041	0.44827619	100
1:21	0.019624	0.0004291	0	0.70382832	0.44806351	100
1:23	0.019587	0.0003925	0	0.70316481	0.4474457	100
1:24	0.019581	0.0003866	0	0.70509605	0.44933124	100
1:27	0.019559	0.0003641	0	0.70538035	0.44961554	100
1:28	0.019529	0.0003339	0	0.70587184	0.45010703	100
1:30	0.019512	0.0003174	0	0.7055019	0.44973709	100
1:33	0.019479	0.0002843	0	0.70509394	0.44932913	100
1:34	0.019468	0.000273	0	0.70517532	0.44941051	100
1:37	0.019457	0.0002617	0	0.70533267	0.44956786	100
1:38	0.019436	0.0002416	0	0.70496595	0.44920114	100
1:41	0.019421	0.0002263	0	0.70398502	0.44822021	100

1:42	0.019418	0.0002235	0	0.70496235	0.44919754	100
1:45	0.019393	0.0001981	0	0.70493484	0.44917003	100
1:46	0.019378	0.0001829	0	0.70593058	0.45016577	100
1:48	0.019383	0.0001882	0	0.70487295	0.44910814	100
1:50	0.019365	0.0001706	0	0.70490945	0.44914464	100
1:52	0.019358	0.0001634	0	0.70493597	0.44917116	100
1:54	0.019344	0.0001488	0	0.70394251	0.4481777	100
1:56	0.01933	0.0001355	0	0.70487146	0.44910665	100
1:59	0.019924	0.0007295	0	0.70490627	0.44914146	100
2:00	0.019306	0.0001114	0	0.70384872	0.44808391	100
2:03	0.051047	0.0318526	10	0.65882969	0.40306488	90
2:04	0.052821	0.033626	11	0.65594072	0.40017591	89
2:06	0.052947	0.0337525	11	0.65566335	0.39989854	89
2:08	0.053015	0.0338199	11	0.65642569	0.40066088	89
2:10	0.053589	0.0343941	11	0.65566284	0.39989803	89
2:13	0.053857	0.0346624	11	0.65535636	0.39959155	89
2:14	0.054361	0.0351666	11	0.65609338	0.40032857	89
2:16	0.054445	0.0352503	11	0.65550052	0.39973571	89
2:18	0.054501	0.0353064	11	0.6558844	0.40011959	89
2:20	0.055208	0.0360135	11	0.63939914	0.38363433	86
2:23	0.056209	0.0370141	12	0.63511858	0.37935377	85
2:24	0.056011	0.0368167	12	0.63527128	0.37950647	85
2:26	0.057002	0.0378075	12	0.63815161	0.3823868	85
2:28	0.06092	0.041725	13	0.62798306	0.37221825	83
2:30	0.06178	0.0425851	14	0.6250947	0.36932989	82
2:32	0.061757	0.0425618	14	0.62185214	0.36608733	82
2:34	0.067807	0.0486127	15	0.61651552	0.36075071	81
2:36	0.069564	0.0503697	16	0.61477255	0.35900774	80
2:39	0.070427	0.0512325	16	0.6136825	0.35791769	80
2:40	0.072354	0.0531591	17	0.60714533	0.35138052	78
2:43	0.073357	0.0541623	17	0.60716893	0.35140412	78
2:44	0.075216	0.0560213	18	0.59949783	0.34373302	77

2:47	0.077359	0.0581643	18	0.59922245	0.34345764	77
2:48	0.07913	0.0599354	19	0.59419465	0.33842984	76
2:51	0.086154	0.0669595	21	0.58511794	0.32935313	74
2:52	0.088069	0.0688739	22	0.57742293	0.32165812	72
2:55	0.090131	0.0709361	23	0.57520321	0.3194384	71
2:57	0.095969	0.0767742	24	0.56605712	0.31029231	69
2:59	0.096789	0.0775946	25	0.56015155	0.30438674	68
3:00	0.109156	0.0899613	29	0.53925961	0.2834948	63
3:03	0.112089	0.0928946	29	0.53890952	0.28314471	63
3:04	0.120766	0.1015709	32	0.52120572	0.26544091	59
3:06	0.125791	0.1065957	34	0.50887609	0.25311128	57
3:08	0.127833	0.1086381	34	0.50899507	0.25323026	57
3:10	0.127864	0.1086692	34	0.50913416	0.25336935	57
3:12	0.127709	0.1085143	34	0.50905626	0.25329145	57
3:14	0.130725	0.1115303	35	0.50422953	0.24846472	55
3:16	0.130796	0.1116014	35	0.50378532	0.24802051	55
3:18	0.13077	0.1115752	35	0.50337288	0.24760807	55
3:21	0.135743	0.1165484	37	0.49261957	0.23685476	53
3:23	0.136631	0.1174359	37	0.49271332	0.23694851	53
3:25	0.140689	0.1214941	39	0.48152046	0.22575565	50
3:26	0.142791	0.1235967	39	0.48285034	0.22708553	51
3:29	0.15076	0.1315652	42	0.46741374	0.21164893	47
3:31	0.1558	0.1366048	43	0.45888949	0.20312468	45
3:33	0.170801	0.1516063	48	0.4343911	0.17862629	40
3:34	0.170805	0.1516103	48	0.43385704	0.17809223	40
3:36	0.170763	0.1515684	48	0.43270494	0.17694013	40
3:39	0.170844	0.1516488	48	0.43397563	0.17821082	40
3:40	0.170783	0.1515879	48	0.43275274	0.17698793	40
3:43	0.170517	0.151322	48	0.43071005	0.17494524	39
3:45	0.170552	0.1513571	48	0.43172559	0.17596078	39
3:46	0.170573	0.1513786	48	0.43076161	0.1749968	39
3:48	0.170523	0.151328	48	0.4317331	0.17596829	39

3:50	0.170361	0.1511665	48	0.43272163	0.17695682	40
3:52	0.170392	0.1511969	48	0.43175612	0.17599131	39
3:54	0.170257	0.1510626	48	0.43272963	0.17696482	40
3:56	0.17187	0.1526752	48	0.43272757	0.17696276	40
3:59	0.17187	0.1526757	48	0.43176158	0.17599677	39
4:02	0.181948	0.1627528	52	0.409733	0.15396819	34
4:04	0.181945	0.1627502	52	0.40968525	0.15392044	34
4:06	0.182118	0.1629234	52	0.40903708	0.15327227	34
4:08	0.182283	0.1630887	52	0.40807045	0.15230564	34
4:10	0.18229	0.1630948	52	0.40855902	0.15279421	34
4:12	0.182444	0.1632495	52	0.40761547	0.15185066	34
4:14	0.18263	0.1634351	52	0.40781974	0.15205493	34
4:16	0.185887	0.1666924	53	0.40508708	0.14932227	33
4:20	0.187314	0.1681188	53	0.4062157	0.15045089	34
4:22	0.186733	0.1675378	53	0.40540119	0.14963638	33
4:26	0.186624	0.1674293	53	0.40671155	0.15094674	34
4:28	0.186366	0.1671713	53	0.4070041	0.15123929	34
4:30	0.186239	0.1670442	53	0.40608283	0.15031802	34
4:32	0.185872	0.1666774	53	0.40701648	0.15125167	34
4:34	0.185813	0.1666184	53	0.40606047	0.15029566	34
4:36	0.185589	0.166394	53	0.40538035	0.14961554	33
4:40	0.186286	0.1670914	53	0.40687184	0.15110703	34
4:42	0.187122	0.1679268	53	0.4055019	0.14973709	33
4:44	0.185791	0.166596	53	0.40609394	0.15032913	34
4:46	0.189678	0.1704829	54	0.40097532	0.14521051	32
4:48	0.189565	0.1703702	54	0.4013267	0.14556189	32
4:50	0.189364	0.170169	54	0.40096595	0.14520114	32
4:52	0.18921	0.1700155	54	0.40098502	0.14522021	32
4:54	0.189183	0.1699883	54	0.40096235	0.14519754	32
4:56	0.189929	0.1707343	54	0.40093484	0.14517003	32
5:00	0.189776	0.1705813	54	0.40093058	0.14516577	32
5:02	0.19383	0.1746351	55	0.3922946	0.13652979	30

5:04	0.193654	0.1744591	55	0.39509447	0.13932966	31
5:06	0.193582	0.1743868	55	0.39535972	0.13959491	31
5:08	0.193436	0.174241	55	0.39442512	0.13866031	31
5:10	0.203302	0.1841073	58	0.37871463	0.12294982	27
5:12	0.203243	0.1840479	58	0.37806268	0.12229787	27
5:14	0.203062	0.183867	58	0.37848718	0.12272237	27
5:16	0.203047	0.1838526	58	0.37882969	0.12306488	27
5:18	0.202821	0.183626	58	0.37794072	0.12217591	27
5:20	0.202847	0.1836525	58	0.37866335	0.12289854	27
5:22	0.202715	0.1835199	58	0.37842569	0.12266088	27
5:24	0.202589	0.1833941	58	0.37866284	0.12289803	27
5:26	0.202457	0.1832624	58	0.37759564	0.12183083	27
5:28	0.202361	0.1831666	58	0.37609338	0.12032857	27
5:30	0.202245	0.1830503	58	0.37550052	0.11973571	27
5:32	0.202201	0.1830064	58	0.3778844	0.12211959	27
5:34	0.202208	0.1830135	58	0.37639914	0.12063433	27
5:36	0.202089	0.182894	58	0.37611858	0.12035377	27
5:38	0.202011	0.1828167	58	0.37827128	0.12250647	27
5:40	0.202002	0.1828075	58	0.37815161	0.1223868	27
5:42	0.20192	0.182725	58	0.37798306	0.12221825	27
5:44	0.20178	0.1825851	58	0.37794702	0.12218221	27
5:46	0.201707	0.1825118	58	0.37785214	0.12208733	27
5:48	0.201807	0.1826127	58	0.37751552	0.12175071	27
5:50	0.201564	0.1823697	58	0.37577255	0.12000774	27
5:52	0.201427	0.1822325	58	0.37676825	0.12100344	27
5:54	0.201354	0.1821591	58	0.37714533	0.12138052	27
5:56	0.201357	0.1821623	58	0.37616893	0.12040412	27
6:05	0.221216	0.2020213	64	0.34049783	0.08473302	19
6:10	0.221359	0.2021643	64	0.34122245	0.08545764	19
6:15	0.22113	0.2019354	64	0.34019465	0.08442984	19
6:20	0.221154	0.2019595	64	0.34111794	0.08535313	19
6:25	0.221069	0.2018739	64	0.34042293	0.08465812	19

6:30	0.221131	0.2019361	64	0.34120321	0.0854384	19
6:35	0.220969	0.2017742	64	0.34205712	0.08629231	19
6:40	0.220789	0.2015946	64	0.34115155	0.08538674	19
6:45	0.220916	0.2017209	64	0.34225961	0.0864948	19
6:50	0.220894	0.2016991	64	0.34290952	0.08714471	19
6:55	0.220766	0.2015709	64	0.34120572	0.08544091	19
7:06	0.240791	0.2215957	70	0.34319572	0.08743091	20
7:10	0.240833	0.2216381	70	0.34125572	0.08549091	19
7:15	0.240864	0.2216692	70	0.34135572	0.08559091	19
7:20	0.240709	0.2215143	70	0.34120572	0.08544091	19
7:25	0.240725	0.2215303	70	0.34112572	0.08536091	19
7:30	0.240796	0.2216014	70	0.34114572	0.08538091	19
7:35	0.24077	0.2215752	70	0.34116572	0.08540091	19
7:40	0.240743	0.2215484	70	0.34119572	0.08543091	19
7:45	0.240631	0.2214359	70	0.34121572	0.08545091	19
7:50	0.240689	0.2214941	70	0.34111572	0.08535091	19
8:00	0.260791	0.2415967	77	0.34133572	0.08557091	19
8:05	0.26076	0.2415652	77	0.34166572	0.08590091	19
8:10	0.2608	0.2416048	77	0.34188572	0.08612091	19
8:15	0.260801	0.2416063	77	0.34133572	0.08557091	19
8:20	0.260805	0.2416103	77	0.34122572	0.08546091	19
8:25	0.260763	0.2415684	77	0.34113572	0.08537091	19
8:30	0.260844	0.2416488	77	0.34120523	0.08544042	19
8:35	0.280783	0.2615879	83	0.34121573	0.08545092	19
8:40	0.280517	0.261322	83	0.34122572	0.08546091	19
8:50	0.280552	0.2613571	83	0.34111572	0.08535091	19
8:55	0.280573	0.2613786	83	0.33741374	0.08164893	18

9:00	0.280523	0.261328	83	0.33751374	0.08174893	18
9:05	0.300361	0.2811665	89	0.33731374	0.08154893	18
9:10	0.300392	0.2811969	89	0.33755374	0.08178893	18
9:15	0.300257	0.2810626	89	0.33712374	0.08135893	18
9:20	0.30263	0.2834351	90	0.33733374	0.08156893	18
9:25	0.305887	0.2866924	91	0.33744374	0.08167893	12
9:30	0.307314	0.2881188	91	0.33788374	0.08211893	18
9:35	0.306733	0.2875378	91	0.33733374	0.08156893	18
9:40	0.32624	0.3070456	97	0.30722374	0.05145893	11
9:45	0.326366	0.3071713	97	0.30712374	0.05135893	11
9:50	0.326239	0.3070442	97	0.30713374	0.05136893	11
9:55	0.335872	0.3166774	100	0.30743374	0.05166893	12
9:59	0.335813	0.3166184	100	0.30733374	0.05156893	12
10:05	0.335589	0.316394	100	0.30722374	0.05145893	11
10:10	0.335286	0.3160914	100	0.30734374	0.05157893	12
10:15	0.335122	0.3159268	100	0.30732374	0.05155893	12
10:20	0.334791	0.315596	100	0.30735374	0.05158893	12
10:25	0.334878	0.3156829	100	0.30715374	0.05138893	11
10:30	0.334965	0.3157702	100	0.30723373	0.05146892	11
10:40	0.334504	0.315309	100	0.30732372	0.05155891	12
10:45	0.335514	0.3163188	100	0.30746371	0.0516989	12
10:50	0.334524	0.315329	100	0.30722379	0.05145898	11
10:55	0.334534	0.315339	100	0.30712377	0.05135896	11
11:00	0.334544	0.315349	100	0.30766371	0.0518989	12
11:05	0.334554	0.315359	100	0.30734375	0.05157894	12
11:10	0.334564	0.315369	100	0.30724371	0.0514789	11

11:15	0.334574	0.315379	100	0.30755371	0.0517889	12
11:20	0.334359	0.315164	100	0.30788372	0.05211891	12
11:25	0.334594	0.315399	100	0.30733376	0.05156895	12
11:30	0.334604	0.315409	100	0.30722371	0.0514589	11
11:35	0.334614	0.315419	100	0.30714377	0.05137896	11
11:40	0.334624	0.315429	100	0.30733376	0.05156895	12
11:45	0.334634	0.315439	100	0.30755372	0.05178891	12
11:50	0.334365	0.31517	100	0.30734371	0.0515789	12
11:55	0.334366	0.315171	100	0.30742372	0.05165891	12
12:00	0.334367	0.315172	100	0.30723373	0.05146892	11
12:10	0.334368	0.315173	100	0.30722371	0.0514589	11
12:15	0.334369	0.315174	100	0.30733375	0.05156894	12
12:20	0.33437	0.315175	100	0.30721372	0.05144891	11
12:25	0.334371	0.315176	100	0.30711372	0.05134891	11
12:30	0.334372	0.315177	100	0.30722373	0.05145892	11
12:35	0.334373	0.315178	100	0.30779379	0.05202898	12
12:40	0.334374	0.315179	100	0.30743372	0.05166891	12
12:45	0.334374	0.315179	100	0.30733372	0.05156891	12
12:50	0.334376	0.315181	100	0.30722373	0.05145892	11
12:55	0.334377	0.315182	100	0.30733372	0.05156891	12
13:00	0.334378	0.315183	100	0.30721371	0.0514489	11
13:05	0.334379	0.315184	100	0.30732372	0.05155891	12
13:10	0.33438	0.315185	100	0.30733372	0.05156891	12
13:15	0.334381	0.315186	100	0.30788373	0.05211892	12
13:20	0.334382	0.315187	100	0.30755372	0.05178891	12
13:25	0.334383	0.315188	100	0.30733374	0.05156893	12

13:30	0.334384	0.315189	100	0.30741371	0.0516489	12
13:35	0.334385	0.31519	100	0.30722373	0.05145892	11
13:40	0.334386	0.315191	100	0.30732377	0.05155896	12
13:45	0.334387	0.315192	100	0.30777376	0.05200895	12
13:50	0.334388	0.315193	100	0.30755378	0.05178897	12
13:55	0.334389	0.315194	100	0.30712372	0.05135891	11
14:05	0.33439	0.315195	100	0.30722371	0.0514589	11
14:10	0.334391	0.315196	100	0.30733372	0.05156891	12
14:15	0.334392	0.315197	100	0.30733374	0.05156893	12
14:20	0.334393	0.315198	100	0.30734373	0.05157892	12
14:25	0.334394	0.315199	100	0.30777373	0.05200892	12
14:30	0.334944	0.315749	100	0.30713372	0.05136891	11
14:35	0.334396	0.315201	100	0.30722373	0.05145892	11
14:40	0.334397	0.315202	100	0.30745373	0.05168892	12
14:45	0.334974	0.315779	100	0.30766371	0.0518989	12
14:50	0.334984	0.315789	100	0.30723372	0.05146891	11
14:55	0.3344	0.315205	100	0.30765372	0.05188891	12
15:05	0.334464	0.315269	100	0.25576481	0.0518891	12

Formula:

Peak area difference = Peak area minus peak area at the end for reactant and at the beginning for product

$$\% \text{ change for the reactant} = \frac{Peak\ area\ difference}{Peak\ area\ at\ the\ end} X\ 100$$

Table 8-2. Raw data for the FlashIR separation of benzyl tert-butyl ether.

Time	Peak area	Fractions
0:00:52	0.000001	
0:02:53	0.000001	
0:04:52	0.000001	F1
0:06:52	0.000001	
0:08:52	0.000001	
0:10:53	0.000001	F2
0:12:52	0.000001	
0:14:52	0.000001	
0:16:52	0.000001	F3
0:18:53	0.000001	
0:20:53	0.000001	
0:23:07	0.000001	F4
0:24:53	0.000001	
0:26:53	0.000001	
0:30:37	0.000001	F5
0:31:30	0.022967	
0:32:53	0.022967	
0:34:52	0.022967	F6
0:39:15	0.026047	
0:40:07	0.026047	
0:41:00	0.026047	F7
0:42:53	0.260529	
0:44:53	0.260529	
0:46:52	0.260529	F8
0:48:53	0.036245	
0:50:52	0.036245	
0:55:19	0.036245	F9
0:57:09	0.033092	
0:58:02	0.033092	
0:58:54	0.033092	F10

1:02:15	0.026464	
1:03:28	0.026464	
1:06:33	0.026464	F11
1:07:26	0.026464	
1:08:53	0.026464	
1:10:52	0.026464	F12
1:13:43	0.010248	
1:14:53	0.010248	
1:17:19	0.010248	F13
1:18:54	0.008449	
1:21:30	0.00845	F14

Table 8-3. Raw data for comparison of FlashIR and HPLC separation.

Fractions	HPLC Peak area	FlashIR Peak area (average of each fractions from Table 6-2)
1	0	0
2	0	0
3	0	0
4	0	0
5	0	0
6	1783	0.022967
7	16681	0.026047
8	101048	0.260529
9	7180	0.036245
10	5658	0.033092
11	5032	0.026464
12	4377	0.026464
13	3257	0.010248
14	2768	0.00845